Doctor Thesis

Functional studies of human nucleolar proteins, fibrillarin and nucleophosmin

(ヒト核小体タンパク質、フィブリラリンとヌクレオフォスミンの機能解析)

Mohammed Abdullahel Amin

Department of Biotechnology

Osaka University

Japan

September, 2008

Doctor Thesis

Functional studies of human nucleolar proteins, fibrillarin and nucleophosmin

A dissertation submitted to Osaka University in partial fulfillment of the requirements for the degree of doctor of engineering in Biotechnology

Mohammed Abdullahel Amin

Department of Biotechnology

Osaka University

Japan

September, 2008

Contents

Major Abbreviations

BCIP	5-bromo-4-chloroindol-3-yl phosphate
BrdU	5-bromo-2-deoxyuridine
CO_2	Carbon Dioxide
DIC	Differential Interference Contrast
EDTA	Ethylene Diamine Tetraacetic Acid
FBL	Fibrillarin
FBS	Fetal Bovine Serum
FCM	Flow Cytometry
GFP	Green Fluorescent Protein
HEK293T	Human Embryonic Kidney-293T
kDa	Kilo Dalton
NBT	Nitro Blue Tetrazolium
NCL	Nucleolin
NE	Nuclear Envelop
NHDF	Normal Human Dermal Fibroblast
NPM	Nucleophosmin
nM	Nano molar
PBS	Phosphate Buffer Saline
PFA	Para-formaldehyde
PNB	Pre-nucleolar body
RNAi	RNA interference
siRNA	Small interfering RNA
TRITC	Tetramethyl Rhodamine Isothiocyanate
μg	Micro gram
μm	Micro miter

TO MY BELOVED

PARENTS & TEACHERS

Chapter 1

General Introduction

1.1 Overview of Nucleolus

The nucleolus is the most active and dynamic nuclear sub-domain that is formed at the end of mitosis around the tandemly repeated clusters of ribosomal DNA (rDNA) gene and result in a subnuclear compartment that locally concentrates the transcription and processing machineries that are responsible for generating ribosome subunits. Nucleolus plays a prominent role in the organization of various components of the nucleus. The primary function of the nucleolus is as the site of ribosome biogenesis in eukaryotic cells (Hadjiolov, 1985). The nucleolus organizes the various components of nucleus and considered to be plurifunctional (Pederson, 1998). Nucleolus plays important roles in the regulation of numerous cellular processes including cell cycle regulation, apoptosis, telomerase production, RNA processing monitoring and response to cellular stress, gene silencing, and ribonulceoprotein complex formation (Hernandez-Verdun et al., 2002; Olson et al., 2005; Mayer and Grummt, 2005; Lo et al., 2006). Thus a fully active nucleolus is not only essential for ribosome production, but also for control of cell survival and cell proliferation (Carmo-Fonseca et al., 2000). It also regulates numerous cellular processes, promoting a broadened view of the potential functions of nucleolar proteins (Maggi and Weber, 2005).

When viewed by thin-section electron microscopy, the nucleus from most higher eukaryotes is composed of three structurally distinguished constituents: fibrillar centers

(FCs), dense fibrillar components (DFCs), and granular components (GCs) (Fig. 1) (Busch and Smetana, 1970; Hadjiolov, 1985). The structure of the interphase nucleolus is organized around the tandemly repeated genes for pre-ribisomal RNA (also called rDNA).

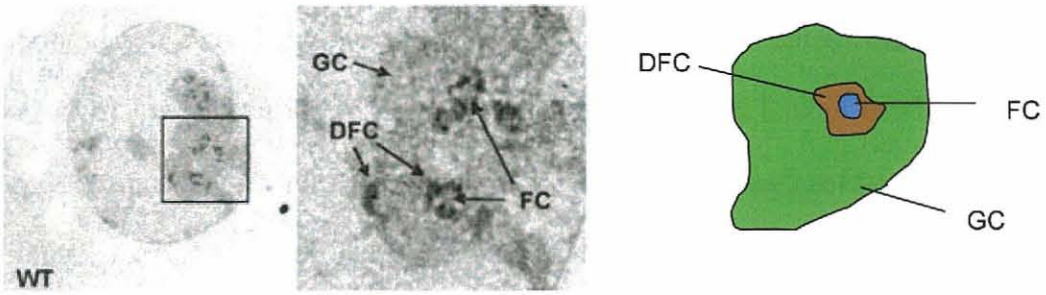

Fig. 1.1 Ultrastructural analysis of the nucleolar compartment after uranyl-EDTA-lead staining of ribonucleoproteins, showing the classical pattern of nucleolar organization in fibrillar centers (FC), dense fibrillar components (DFC) and granular components (GC) in HeLa cells (Espada et al., 2007).

Transcription of these genes generated two structures that are found in all nucleoli: the dense fibrillar component (DFC) and the granular component (GC). The third component, the fibrillar center (FC), is usually observed in the nucleoli of most metazoans but is generally not found in lower eukaryotes. When present, the FC is surrounded by the DFC, which in turn is surrounded by the GC, which fills out the peripheral parts of the nucleolus.

1.2 Formation of nucleolus in telophase

Nucleolus disintegrates early in mitosis, and the nucleolar components are distributed to various parts of the cell. The transcriptional apparatus remains attached to the nucleolar organizing regions (NORs) on chromosomes, whereas the processing complexes adhere to the chromosome periphery or are dispersed in the cell. Large particles called nucleolus-derived focus (NDF) are assembled from the processing complexes in anaphase. During telophase prenucleolar bodies (PNBs) are fromed from the processing complexes, which are derived from two sources. The first is from the periphery of chromosomes, which are in the process of decondensing. The dispersing chromosomes are positioned around inside surface of the nuclear envelope. The second source is the NDF, which dissociate into small particles that are eventually imported into nuclei. The PNBs eventually establish the daughter nucleolus (Fig. 1.2).

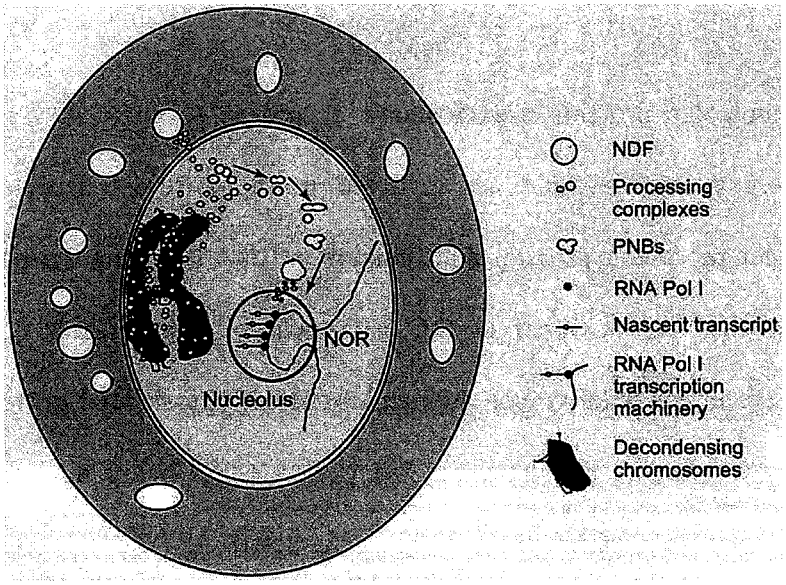

Fig. 1.2 Proposed model for the formation of nucleolus in telophse (Olson et al., 2000).

1.3 Nucleolar Proteins

Purification and mass-spectrometric identification of nucleolar proteins have led to the identification of more than 200 plant proteins and over 700 human proteins that stably co-purify with isolated nucleoli (Andersen et al., 2002, 2005; Pendle et al., 2005; Scherl et al., 2002). The results of nucleolar proteome analysis for human are shown in Fig. 1.3.

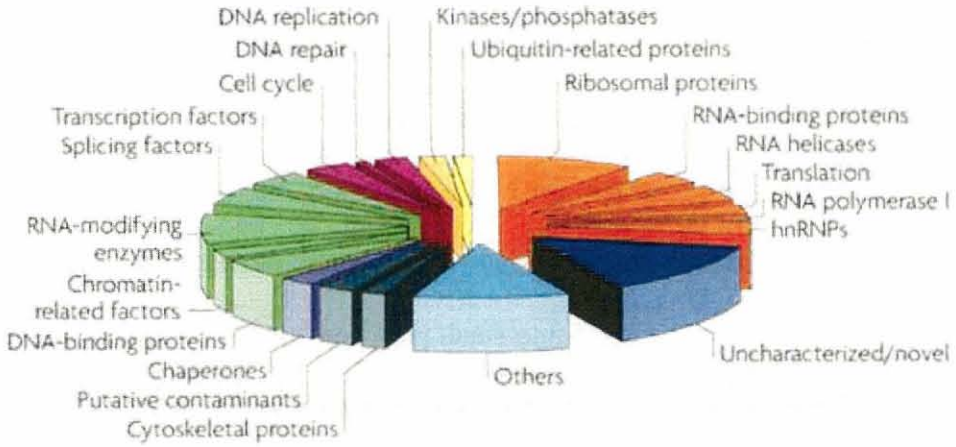

Fig. 1.3 726 human nucleolar proteins are clustered according to their molecular functions. Orange represents proteins that are involved in the different aspects of ribosome biogenesis. Green represents proteins that function in RNA Pol II transcription. Pink represents proteins that are involved in the cell cycle or DNA repair. Grey represents proteins that are either putative contaminants or know cytoskeletal proteins. Light blue represents other proteins that have not been reported as being nuclear or nucleolar. Dark blue represents proteins previously uncharacterized (Biosvert et al., 2007).

The plurifunctional activity of nucleolus can be achieved by the transient localization of the several hundred proteins within the nucleolar structure (Coute et al., 2006). In addition, several well-known nucleolar proteins seem to have multiple functions. Amongst them, the abundant nucleolar proteins fibrillarin (FBL), nculeolin (NCL/C23) and nucleophosmin (NPM/B23) have been the subject of numerous studies.

1.4 Mitosis and nucleolar proteins

When cells enter mitosis nucleolar proteins are dispersed in prophase and nucleolar signals move to the peripheral region of chromosome and are again accumulated in newly formed nucleoli at the end of mitosis. The perichormosomal layer, which covers the chromosomes except in centromeric regions, includes nuclear and nucleolar proteins (such as NCL, ki-67, NPM, FBL, etc.) as well as ribonucleoproteins (Hernandez-Verdun and Gautier, 1994). There are evidences that nucleolar proteins serve as means of transport for various proteins at the chromosome periphery during mitosis (Azum-Gelade et al., 1994; Dundr et al., 1997) and are involved in chromosome organization (Takagi et al., 1999; Kametaka et al., 2002; Scholzen et al., 2002). A previous study with highly purified human metaphase chromosome showed that FBL and NPM belong to the class of chromosome peripheral proteins (Fig 1.4), which indicate that these proteins would have functional importance in chromosome organization and/ or mitotic progression. Moreover, previously we reported that nucleolin has a role in mitotic progression (Ma et al., 2007).

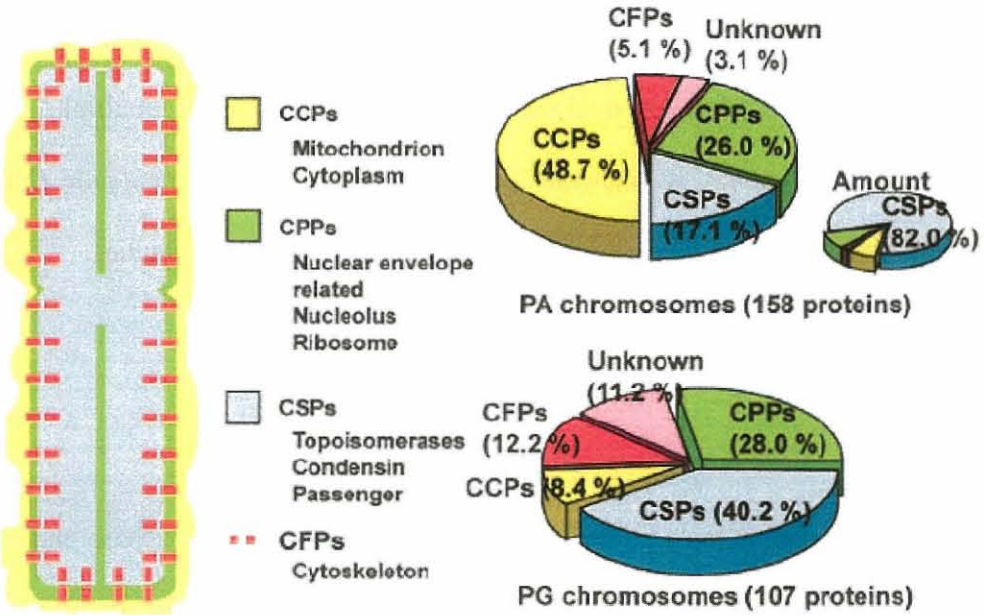

Fig. 1.4 A schematic representation of the metaphase chromosome from the constituent protein perspective. Proteins have been newly classified into 4 groups: CCPs (Chromosome coating proteins), CPPs (Chromosome peripheral proteins), CSPs (Chromosome structural proteins) and CFPs (chromosome fibrous proteins) (Uchiyama et al., 2005).

1.5 Fibrillarin and nucleophosmin

Fibrillarin (FBL) is an abundant small nucleolar protein in eukaryotes. FBL was originally identified in *Physarum polycephalum* by Christensen et al. (1977), termed FBL by Ochs et al. (1985). Human fibrillarin, a ~36-kDa protein, contains an amino-terminal domain that is rich in glycine and arginine residues (termed the GAR domain), a central RNA-binding domain comprising an RNP-2-like consensus sequence, and C-terminal α-

helical domain (Aris and Blobel, 1991). FBL has been highly conserved throughout evolution, for instance human FBL is 67% identical to its yeast homolog (named Nop1p) and 81% identical to the Xenopus protein (Aris and Blobel, 1991, Henriquez et al., 1990). FBL plays an important role in pre-rRNA processing and modification, ribosome assembly (Tollervey, et al., 1993) and is essential for mouse embryonic development (Newton et al., 2003).

Nucleophismin (NPM) also known as B23, NO38 and numatrin, is an acidic nucleolar protein of MW 35-40 kDa. NPM exists in two heavily phosphorylated splicing variants, NPM1 and NPM1.2 (B23.1 and B23.1, respectively), which form multimers (Chang and Olson, 1989; Umekawa et al., 1993). NPM1 is mostly nucleolar, while NPM1.2 is present both in cytoplasm and nucleoplasm (Wang et al., 1993; Okuwaki et al., 2002). The main function of NPM is ribosome biogenesis (Savkur and Olson 1998). Other functions of NPM are protein chaperoning, centrosome duplication (Okuwaki et al., 2001; Okuda et al., 2000). NPM continuously shuttles between cytoplasm and nucleus (Borer et al., 1989). NPM is required for the development of mouse embryo (Grisendi et al, 2005). NPM is thus considered as a mulitifunctional protein. Although various functions of FBL and NPM have been reported as mentioned above; however, the function of FBL during cell cycle and the role of NPM on mitotic chromosomes have not yet been reported.

1.6 Objective of this study

Previous study by proteome analyses of highly purified human metaphase chromosomes showed that FBL and NPM are chromosome peripheral proteins (Uchiyama et al., 2005). However their functional significances on chromosome structure and function are still unknown. In this study, the functional analyses of the two major nucleolar proteins, FBL and NPM were performed by a combination of RNA interference (RNAi) method, fluorescence or 3-D microscopy and live cell imaging which will be described in the following chapters. The Chapter 2 will describe the functional analyses of FBL in the cell cycle of HeLa cells. The Chapter 3 will describe the function of NPM on mitotic chromosomes of HeLa cells. The Chapter 4 will describe the role of NPM in the maintenance of nucleolar as well as nuclear structure in HeLa cells. Finally, the Chapter 5 will summarize the major findings obtained in the present study and mention the conclusions in the view of functional importance of FBL and NPM in cell cycle progression, and the therapeutic importance of NPM in cancer treatments.

Chapter 2

Functional analyses of a nucleolar protein, fibrillarin in HeLa cells

2.1 Introduction

FBL is a key small nucleolar protein in eukaryotes, which has an important role in pre-rRNA processing during ribosomal biogenesis. Electron microscopic and immunocytochemical studies showed that FBL also plays a role in nucleolar assembly by packaging prenuclear bodies (PNBs) (Fomproix et al., 1989). The yeast FBL named *NOP1* (*nucleolar protein 1*) is essential for cell viability (Schimmang et al., 1989). The human or *Xenopus* fibrillarin can functionally replace *NOP1* (Jansen et al., 1991). Knockout of FBL in mice leads to embryonic lethality at the early stage of development (Newton et al., 2003), suggesting that FBL would play an essential role in cell growth. In addition, FBL has methyl transferase activity, which can methylate 2′-O-ribose of rRNA (Wang et al., 2000).

Although there are a plenty of evidences for abnormal nuclear morphology after siRNA depletion of nuclear or related proteins i.e., lamin B and LAP2 (Kimura et al., 2003), emerin (Manilal et al., 1996), Lem2 (Ulbert et al., 2006a), FACE1 protease (Gruber et al., 2004), however there is only one report about nucleolar protein, SENP5 (Bacco et al., 2006).

Although several functions of FBL are known, its function during the cell cycle is still unknown. In this chapter, the dynamic localization of FBL during the cell cycle of HeLa cells was illustrated. The novel functions of FBL by using a combination of immunofluorescence microscopy and RNAi technique have been studied. The depletion of FBL has no effect on the nucleolar structure. However, FBL depletion leads to abnormal nuclear morphologies. Moreover, FBL depletion results in the reduction of the

cellular growth and modest accumulation of cells with 4*n* DNA content. The results in this study suggest that FBL would play a critical role for the maintenance of nuclear shape and cellular growth.

2.2 Materials and methods

2.2.1 Cell Culture and strains

HeLa cells were cultured in growth medium, DMEM (Gibco BRL) with 5% fetal calf serum (Equitech-Bio), penicillin (100 U/ml) and streptomycin (0.1 μg/ml) at 37°C in a humidified incubator with 5% CO_2. A stable cell line expressing GFP-histoneH1.2 was constructed as previously described (Higashi et al., 2007).

2.2.2 siRNA (small interference RNA) transfection

In this study, we designed two siRNA duplexes to knock down fibrillarin: fib1: 5′-UGGAGGACACUUUGUGAUUUU-3′ and fib2: 5′-GUCUUCAUUUGUCGAGGAAtt-3′. siRNA duplexes were transfected into HeLa cells plated on ploy-L-lysine coated microscope cover glass in 24-well plates using Lipofectamine^{TM} 2000 (Invitrogen). The final concentration of siRNA used in each transfection was 150 nM. The control transfection with siRNA against the GL2 luciferase gene (5′-CGUACGCGGAAUACUU CGAtt-3′) was performed as mock experiments.

2.2.3 Western blot analysis of cell extracts

The protein extracts were prepared with SDS sample buffer from transfected HeLa cells. Western blotting was performed as standard methods. The primary antibodies used were: a rabbit polyclonal anti-fibrillarin (ab5821, Abcam; dilution 1:250), a mouse monoclonal anti-nucleolin (sc-8031, Santa Cruz Biotechnology; dilution 1:250), a goat polyclonal anti-lamin A/C (sc-6215, Santa Cruz Biotechnology; dilution 1:100), a goat polyclonal

anti-B23 (sc-6013, Santa Cruz Biotechnology; dilution 1:100), and a mouse monoclonal anti-α-tubulin (Calbiochem; dilution 1:250). Secondary antibodies conjugated to alkaline phosphatase (anti-mouse from Leinco Technologies; anti-rabbit and goat from Vector Laboratories) were used for immunoreactions, which were finally detected by NBT (Ntiro Blue Tetrazolium/BCIP (5-bromo-4-chloroindol-3-yl phosphate) solution (Roche) in AP buffer (100 mM Tris-HCl pH 9.5, 100 mM NaCl, and 1 mM $MgCl_2$).

2.2.4 Immunofluorescence microscopy

Immunofluorescence staining was performed as standard methods. In most cases, HeLa cells grown on poly-L-lysine coated microscope cover glass (Fisherbrand®, Fisher Scientific) were fixed with 4% (w/v) para-formaldehyde in PBS for 10 min at 37°C. For some experiments cells were fixed for 10 min in methanol at –20°C. The same antibodies were used for immunofluorescence. For the detection of primary antibodies the following secondary antibodies were used: Alexa Flour® 488-conjugated goat anti-mouse, and anti-rabbit and rabbit anti-goat antibodies (Invitrogen, USA), TRICT-conjugated goat anti-rabbit antibodies (Zymed Laboratories, USA). DNA was labeled with Hoechst 33342 (Sigma). After immunostaining, specimens were mounted on glass slides with Vectashield mounting medium (Vector Laboratories, Inc. Burlingame, CA). Samples were examined with an epifluorescence microscope (Carl Zeiss, Oberkochen, Germany) equipped with a cooled charged-coupled device (CCD) camera (Cool-SNAP™ HQ^2, Photometrics Image Point, Tuscon, AZ) 72 h after transfection at 40X as well as 100X magnification. Image processing was performed with the following software: IPLab (Visitron systems, Germany) and Adobe Photoshop version 7.0 (Adobe Systems, USA).

For quantification of abnormal nuclear morphology ~150-300 HeLa cell nuclei were examined in three independent experiments and results were expressed graphically as the average percentage of the total nuclei observed.

2.2.5 Live cell imaging

After 72 h of siRNA transfection into the cell line HeLa GFP-histoneH1.2, the transfected cells were incubated in the observation medium for 1h at 37°C in a humidified incubator with 5% CO_2. For cell fate analysis, cells were observed under an inverted microscope (Olympus 1X81 SIF-3, Japan) with an environmental chamber maintained at 37°C with 5% CO_2. Living images were recorded at every 10 min over a time period of 8-10 h using 40X oil objective lens and a CCD camera (Photometrics). Images were analyzed with the following software: Metamorph (Universal Imaging, Downington, PA) and WCIF Image J program (http://www.uhnresearch.ca/facilities/wcif/fdownload.html).

2.2.6 Flow Cytometry (FCM) analysis

Cells were treated with trypsin/EDTA and washed twice in ice cold PBS before fixing them in 70% ethanol overnight at –20 ^{0}C. Cells were washed twice with PBS and incubated in staining solution (20 μg/ml propidium iodide, 20 μg/ml Rnase, 0.1% Triton X-100in PBS) for 1 h at 37 ^{0}C. Cells were analyzed in a FCM machine (EPICS® ALTRA™ Beckman Coulter, USA).

2.3 Results and discussion

2.3.1 Dynamic Localization of FBL throughout the cell cycle

Although there are several reports about FBL localization in different cell lines such as CHO cells (Azum-Gelade et al., 1994) and PtK_1 cells (Medina et al., 1995), in the present study the dynamic localization of FBL throughout the cell cycle of fixed HeLa cells was firstly reported by immunostaining with anti-fibrillarin (Fig. 2.3.1A). During interphase, FBL is prominently found in nucleoli mainly in fibrillar centers (FCs) and dense fibrillar components (DFCs) as well as in the Cajal bodies (CBs). CBs are small nuclear organelles with a number of nuclear functions. CBs have been observed in a variety of animal and plant nuclei. CBs frequently localize to the nucleolar periphery or within the nucleoli (Gall et al., 2000; Dundr et al., 2004). They are involved in modification of small nuclear RNAs and small nuclear RNPs (Gall et al., 2000). CBs disappear from prophase nuclei and reappear in late G_1 after resumption of transcription in the daughter nuclei (Gall et al., 2003). In prophase, when nucleolus is dispersed, FBL is dispersed to the chromosomal periphery and remains there until anaphase. This chromosomal localization is supported by previous proteome analyses using highly purified metaphase chromosomes of HeLa cells (Uchiyama et al., 2005). At the end of mitosis during telophase, FBL is considerably accumulated in PNBs, which eventually form new nucleolus. This considerable accumulation thus supports the notion that nucleolus is formed by the recruitment of pre-rRNA processing factors followed by fusion of prepackaged PNBs into nucleolus (Savino et al., 1999; Dousset et al., 2000). In

early G_1 phase, FBL is found to localize in condensed chromatin of nuclei (Fig. 2.3.1B), which is consistent with the previous study with PtK1 cell (Fomproix et al., 1989). Thus FBL may also play a role in nuclear function.

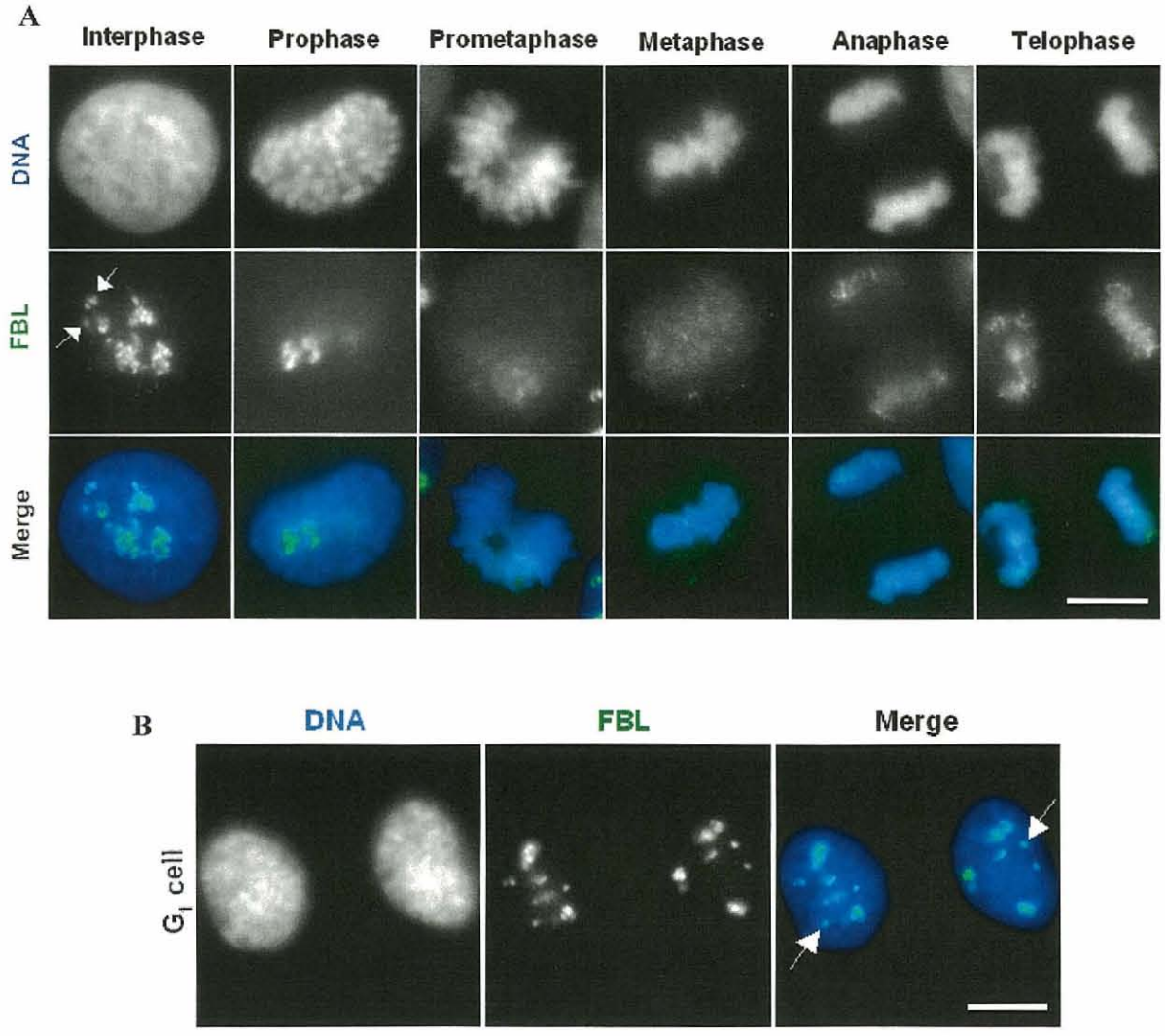

Fig. 2.3.1 Dynamic localization of FBL throughout the cell cycle. (A) Para-formalidehyde-fixed HeLa cells were stained by mouse anti-FBL antibody. DNA was counter-stained by Hoechst 33342. The green and blue signals represent FBL and DNA,

respectively. The arrows indicate the Cajal bodies. Scale bar = 5 μm. (B) G_1 cell stained with FBL (green) and DNA (blue). Scale bar = 5 μm. Arrows indicate localization of FBL at condensed chromatin in nuclei (arrow indication).

In addition to immunostaining, we confirmed FBL localization in HeLa cells transiently expressing Dendra2-FBL (Fig. 2.3.1C) as similar as that obtained from HeLa cells expressing GFP-FBL (Angelier et al., 2005; Leung et al., 2004) and immunostaining data herein.

C

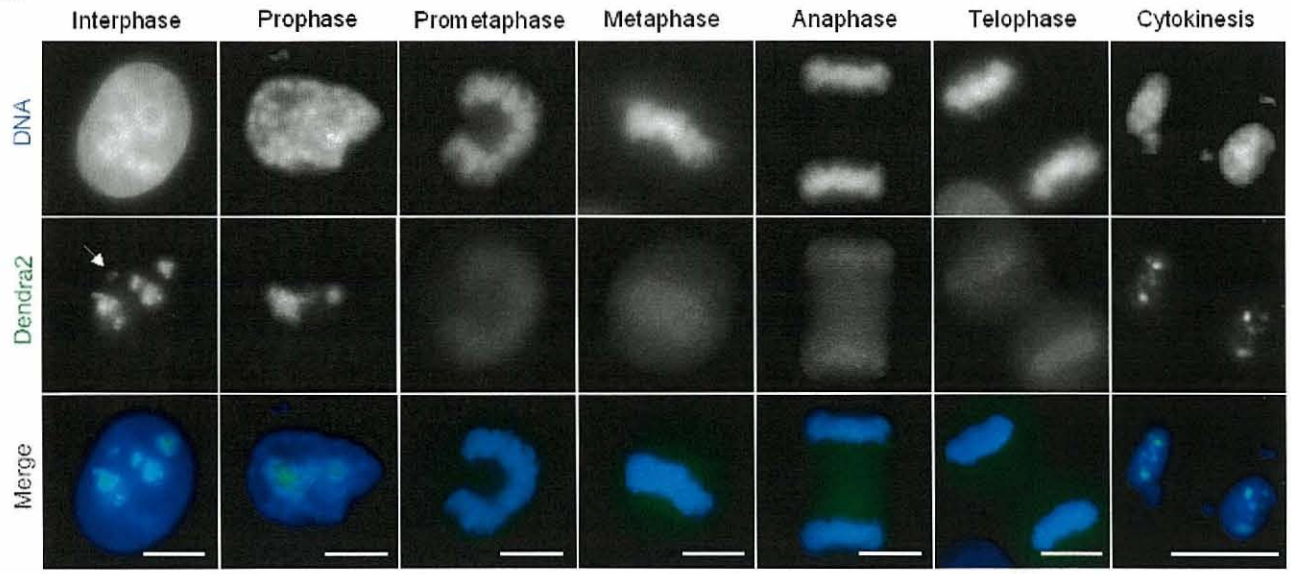

Fig. 2.3.1C Localization of FBL detected by transient expression of Dendra2-fused FBL protein in HeLa cells. The green and blue signals represent Dendra2 and DNA, respectively. Scale bars = 5 μm.

2.3.2 Depletion of FBL has almost no effect on nucleolar structure in HeLa cells

To obtain insights into the function of FBL during cell cycle progression, two different siRNAs of distinct targeting parts of FBL mRNA were designed to specifically deplete FBL in HeLa cells. Western blot analyses revealed that the FBL expression level was efficiently depleted (to more than 70%) in HeLa cells by both FBL siRNAs (Fig. 2.3.2A), whereas expression of α-tubulin was not affected. The depletion of FBL did not affect both the expression levels and localization of major nucleolar proteins, NCL and NPM (Figs. 2.3.2B-D).

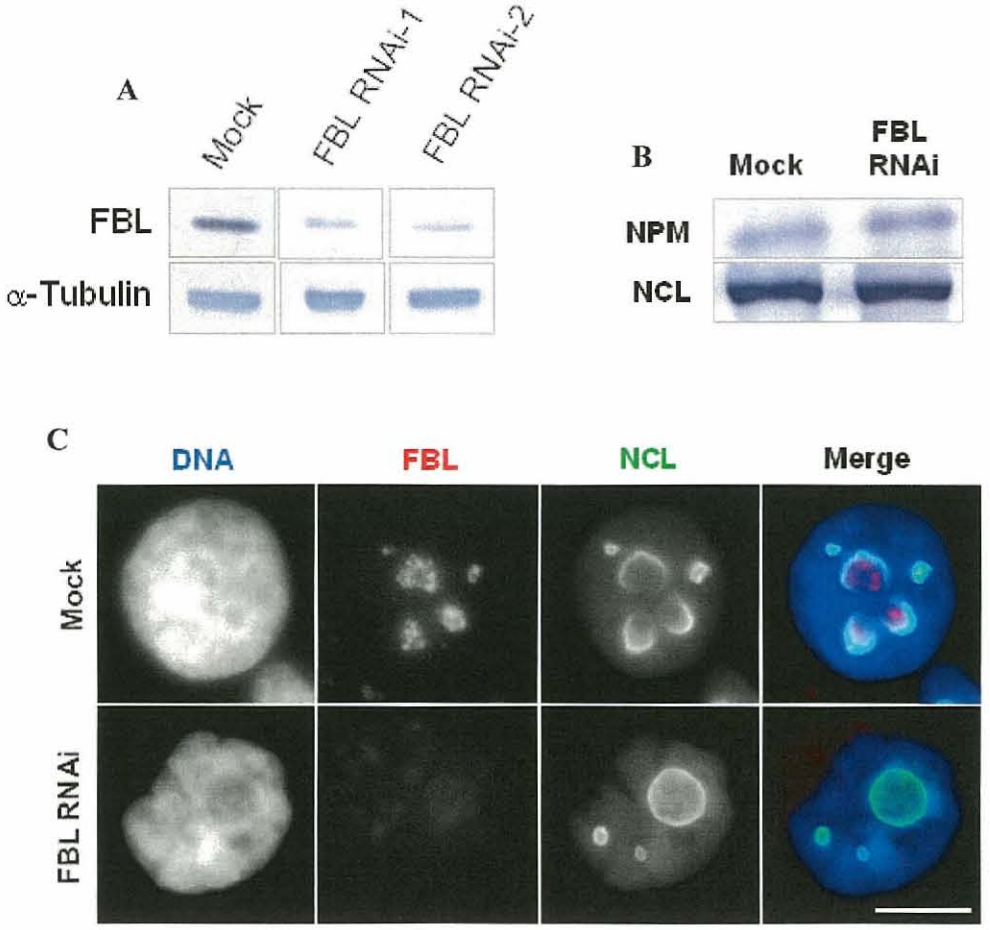

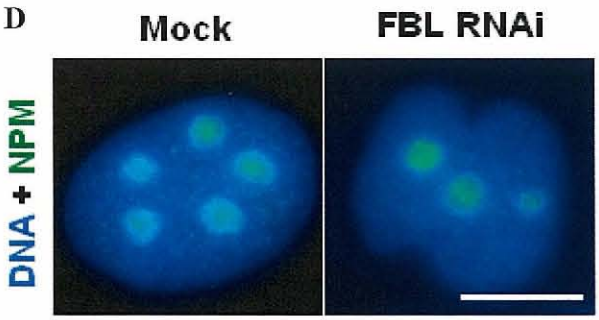

Fig. 2.3.2 Depletion of FBL has almost no effect on nucleolar structure. (A) Western blot analysis of HeLa cells treated with siRNAs corresponding to luciferase (mock) and FBL. The level of FBL was significantly reduced at 72 h post-transfection with siRNAs. Western blot analysis of α-tubulin served as loading control. Scale bar = 5 μm. (B) Proteins extracted from mock and FBL siRNAs-treated cells were Western blotted for nucleolar proteins, NPM and NCL. (C) Immunostaining of both mock (top panels) and FBL (bottom pannels) siRNAs-treated cells at 72 h pot-transfection for NCL (green), FBL (red), and DNA (blue). Nucleolar signals for FBL disappeared by FBL RNAi. Scale bar = 5 μm. (D) Immunostaining of mock and FBL-depleted cells for NPM (green). DNA (blue) was counter-stained with Hoechst 33342. Scale bar = 5 μm.

Moreover, a previous study showed that NCL depletion caused a defect in FBL localization and nucleolar structure (Ma et al., 2007); however, no changes in the localization as well as levels of other major nucleolar proteins such as NCL and NPM were obtained in FBL-depleted cells (Figs. 2.3.2B-D). Thus FBL depletion did not affect the localization of nucleolar proteins as well as nucleolar structure in a way similar to NCL depletion, suggesting that FBL would have no effect on the nucleolar structure, which is paradox to the previous study with PtK_1 cells (Fomproix et al., 1989).

2.3.3 Depletion of FBL causes abnormal nuclear shape in HeLa cells

In general, HeLa cells contain a regularly shaped nucleus with smooth edge border in an equatorial confocal section, whereas cells after FBL depletion showed aberrant nuclear morphologies (Fig. 2.3.3A). Approx. 30-45 % of cells had malformed structures at 72 h post-transfection with FBL-siRNA (Fig. 2.3.3B). The number of cells with abnormal nuclei was more than 6-fold higher in FBL-siRNA treated cells as compared with mock treated cells. FBL depletion caused accumulation of cells with a wide range of nuclear morphology defects such as irregular, ruffled, lobulated/dumpbell and severe. On the other hand, knock down of NCL, did not show any abnormal nuclear morphology (Ma et al., 2007), which will further support a specific role for FBL in cell proliferation described below.

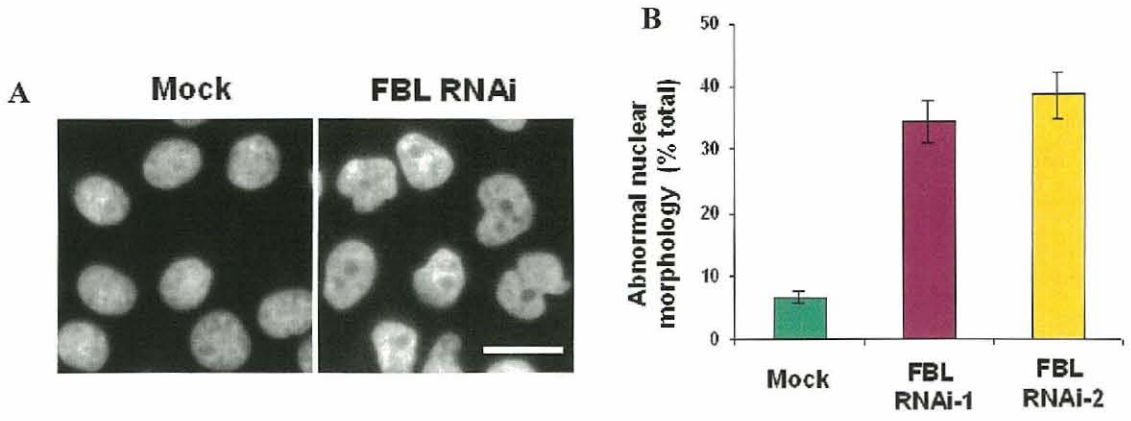

Fig. 2.3.3 FBL is required for normal nuclear shape. (A) FBL-depleted cells showing abnormal nuclear morphology. Scale bar = 10 μm. (B) The percentages of aberrant nuclei after FBL depletion. At 72 h post-tranfection of FBL siRNA over 30% abnormal nuclei were observed.

Usually abnormal nucleus could result from a defect in post-mitotic nuclear envelope (NE) assembly (Foisner et al., 1993; Ulbert et al., 2006b). To test weather malformed nuclei of FBL-depleted cells was due to mislocalization or co-depletion of NE proteins, immunofluorescence and Western blot analysis were performed for major NE protein lamin A/C. Both the localization and the level of lamin A/C were remained unaffected in FBL-depleted cells (Fig. 2.3.3C,D) indicating that FBL depletion has no effect on NE assembly.

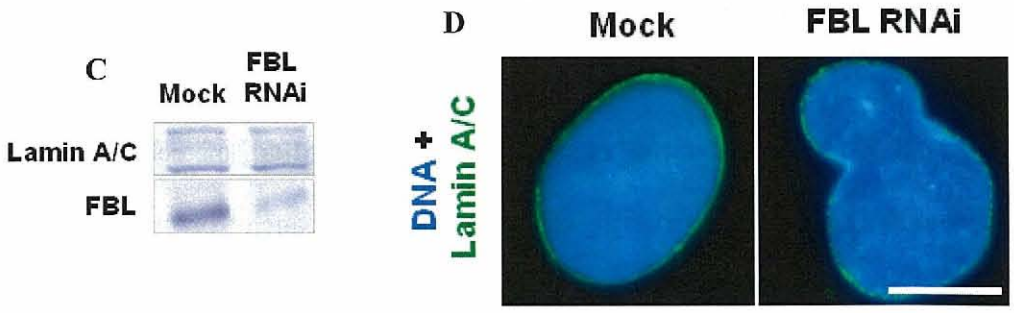

Fig. 2.3.3 FBL depletion has no effect on NE assembly. (C) Western blot indicating the levels of nuclear envelop protein lamin A/C at 72 h post-transfection of mock and FBL siRNAs. (D) Mock and FBL-depleted cells were immunostained for NE protein lamin A/C (green) and DNA (blue). Scale bar = 5μm.

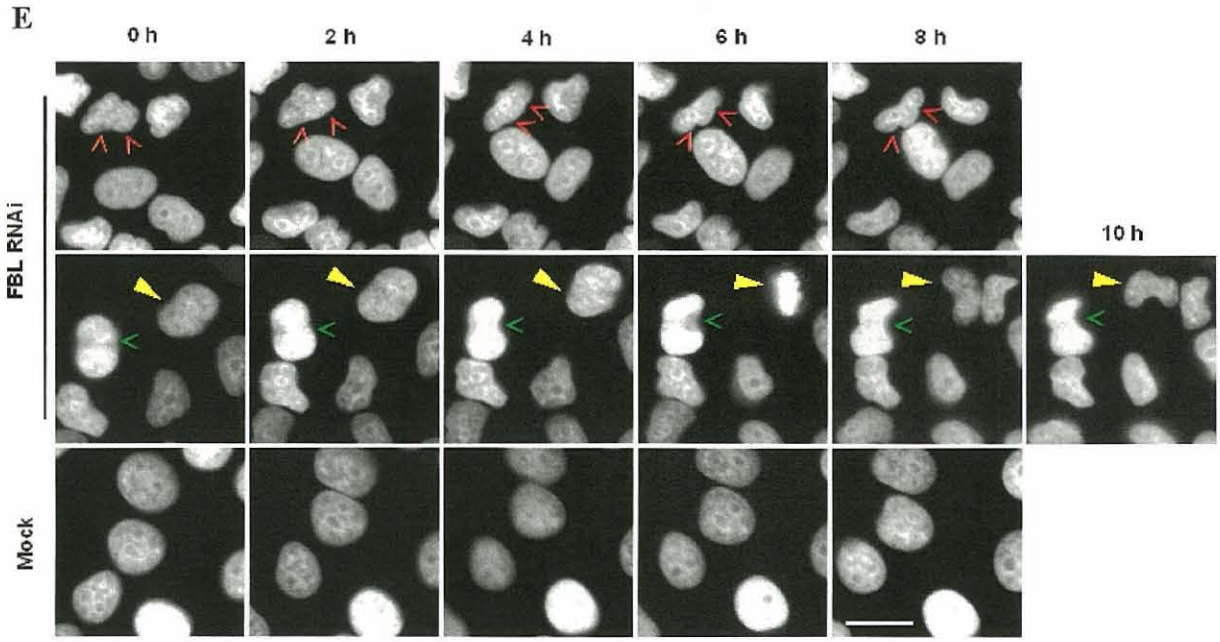

Fig. 2.3.3E Nuclear shape change by live recording of cells expressing GFP-histoneH1.2. Cells were transfected with FBL (top panels) or mock (bottom pannels) siRNAs and recorded after 72 h for an additional 8-10 h. The arrowheads (red and green) indicate changes in NE morphology. Cell indicated by the yellow arrowhead passes through mitotic cycle. Scale bar = 10 μm.

Next the onset of change of nuclear architecture was observed by recoding live image of HeLa GFP-histoneH1.2 cells to check whether abnormalities came from mitotic defect. Live images were acquired after 72 h transfection for additional 8-10 h. Mock treated cells were usually found to divide and produce normal nuclei (Fig. 2.3.3E), whereas approx. 30 % of FBL-depleted cells showed the abnormal nuclear shape. During the course of our recordings, the change of nuclear morphology was clearly observed (Fig. 2.3.3E, arrowheads). The occurrence of nuclear abnormality would take two courses: (a)

pre-mitotic and (b) post-mitotic. During pre-mitotic course cells, which might or might not be previously divided, were found to change in their nuclear structure without entering mitosis during our observation period. Besides this, cells also produced abnormal nuclei after passing through a normal mitosis, considering as post-mitotic course. Moreover, approx. 7% of cells with an abnormal nucleus could not divide and finally died which is consistent with the growth curves (Fig. 2.3.4A). It can thus be concluded that nuclear abnormality in FBL-depleted cells appeared independently of mitotic defect as well as post-mitotic nucleolar and nuclear reassembly.

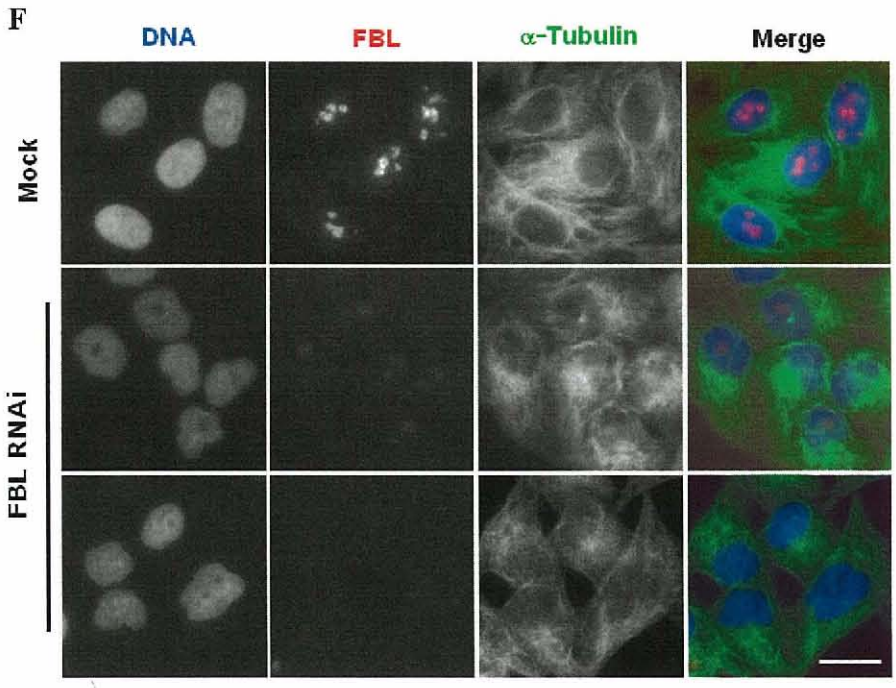

Fig. 2.3.3F FBL depletion does not affect the cytoskeletal structure. Immunostaining of both mock and FBL-depleted cells with FBL (red) and α-tubulin (green). DNA was counter-stained with Hoechst 33342 (blue). Scale bar = 10 μm.

Normally, the nuclear shape is also influenced by the cytoskeletal structure (Ulbert et al., 2006a and references therein). Immunofluorescence experiments showed that the cytoskeletal elements such as α-tubulin were not affected by the depletion of FBL (Fig. 2.3.3F). Nucleolar proteins act as binding sites for chromosomal passenger proteins necessary to the early process of nuclear assembly (Hernandez-Versun et al., 1994) and remain on chromosomal surfaces for nuclear reformation in daughter cells (Yasuda et al., 1990). FBL is believed to play a role in the nuclear matrix (Ochs et al., 1991). Yeast depleted of *NOP1* (yeast FBL) can be complemented by human FBL, which results in the modifications of nuclear morphology (Jansen et al., 1991). Together with these reports, results of the present study suggest that FBL is critically involved in maintaining the structural integrity of the nucleus.

2.3.4 FBL is required for proliferation of HeLa cells

Next to examine the proliferation ability of FBL-depleted cells, the number of both mock and FBL-depleted cells were counted. Mock treated cells grow normally, whereas FBL-depleted cells proliferate with decreased growth rate (Fig. 2.3.4A). The activation of p53 (a key cell-cycle checkpoint protein involved in tumor suppression and premature aging) has been linked to cell-cycle arrest, apoptosis and the impairment of nucleolar function (Rubbi et al., 2003). Interestingly, Western blot analysis showed that p53 expression level remained unchanged in FBL-depleted cells (Fig. 2.3.4B). Moreover, expression of PCNA (a proliferative marker) and NPM still remained high level following FBL depletion (Fig. 2.3.2B and 2.3.4B). These results suggest that cells

continue to proliferate even in the absence of FBL with a reduced rate. The retained proliferative activity may be driven by the residual FBL, perhaps cells lacking FBL can continue to proliferate. This result support the notion that a novel control mechanism of cell cycle progression in HeLa cells involving a nucleolar protein may function through known tumor suppressor genes in late S and G_2 (Tsai et al., 2002).

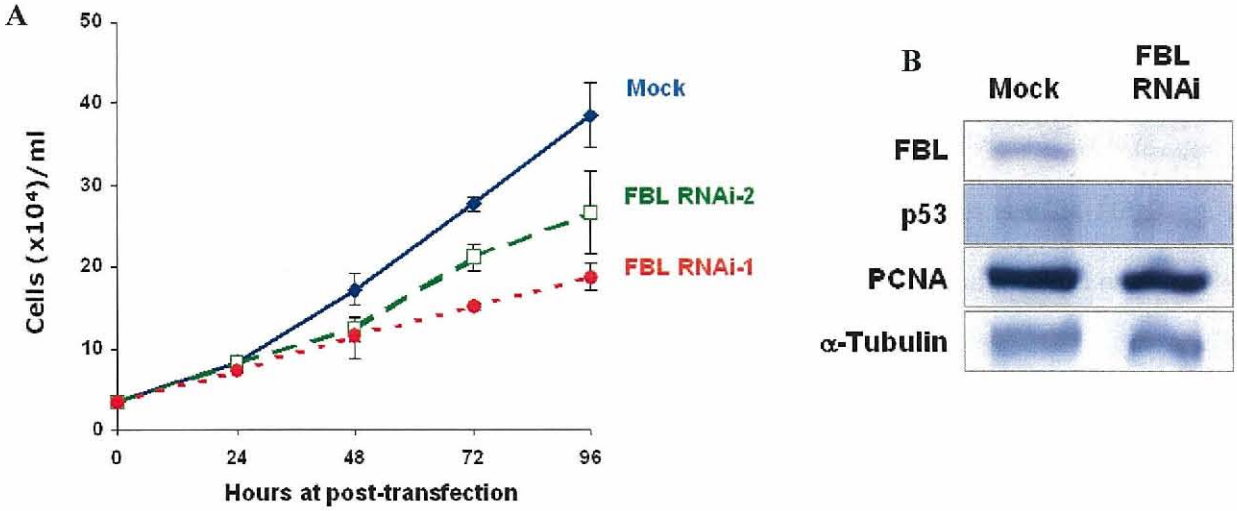

Fig. 2.3.4 FBL depletion leads to proliferation inhibition of HeLa cells. (A) HeLa cells were treated with two different siRNAs against FBL (dashed lines) or luciferase (solid line) and cell numbers were counted at the time points indicated. The error bar is produced from 3 independent experiments. (B) Western blot analyses for cell cycle checkpoint protein p53 and proliferative marker PCNA of both mock and FBL siRNAs-treated cell extracts.

To characterize the inhibition of cell growth by FBL depletion, cell cycle progression was analyzed by flow cytometry (FCM). As show in Fig. 2.3.4C mock

treatment did not affect the cell cycle profile, whereas FBL depletion caused a moderate accumulation of cells with 4*n* DNA content (an increase from 9.32 ± 0.34% to 14.5 ± 0.92% of cells analyzed, n=3) at 72 h post-transfection. The accumulation of 4*n* DNA content cells could be due to delay at the G_2-M transition, which further supports the abnormal nuclear morphology as well as decreased cellular growth. We could not find any inhibition of DNA synthesis assessed by BrdU incorporation assay (data not shown), which is consistent with the unchanged p53 expression in FBL depleted cells as DNA synthesis is dependent on a post-mitotic checkpoint pathway involving p53 (Yang et al., 2004). These results suggest that decreased cell growth after FBL depletion might result from a cessation of the cell division cycle rather from the direct effect on DNA synthesis.

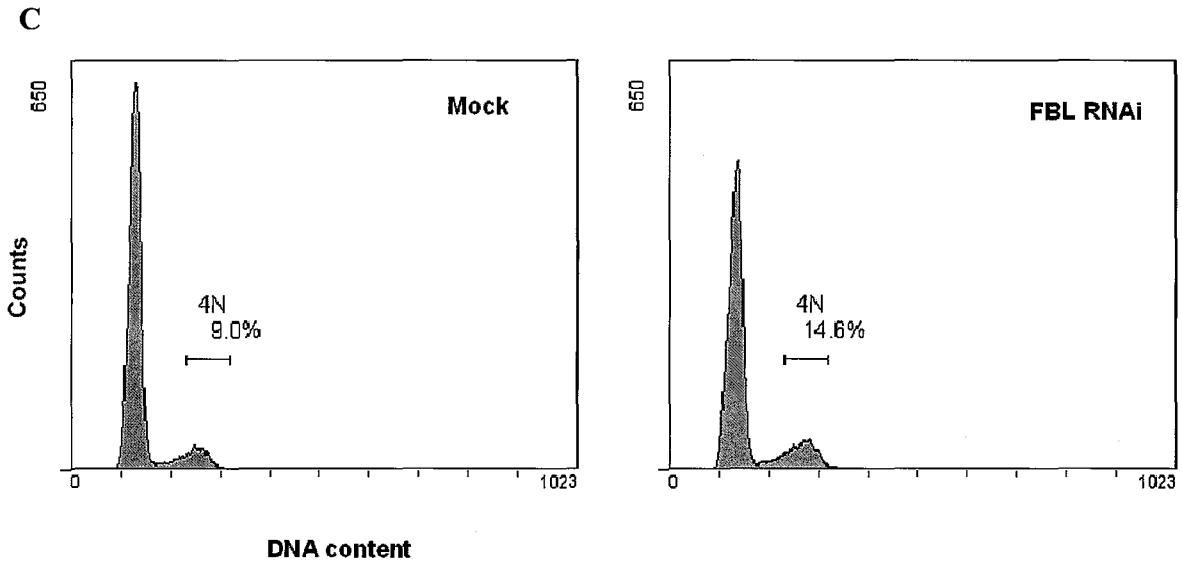

Fig. 2.3.4C Cell cycle profiles of control and FBL-depleted cells were investigated by FCM. The bars indicate the G_2/M phase and percentages of cells in that phase are indicated.

For further support of the cellular growth inhibition live cell imaging using HeLa cells stable expressing GFP-Histone1.2-fused protein was performed. Live recoding showed that FBL depletion causes a delay in the mitotic progression, whereas mock-treated cells finish the mitosis within 60 min (Fig. 2.3.4D). Some cells underwent apoptosis, which is consistent with the growth curve (Fig. 2.3.4A).

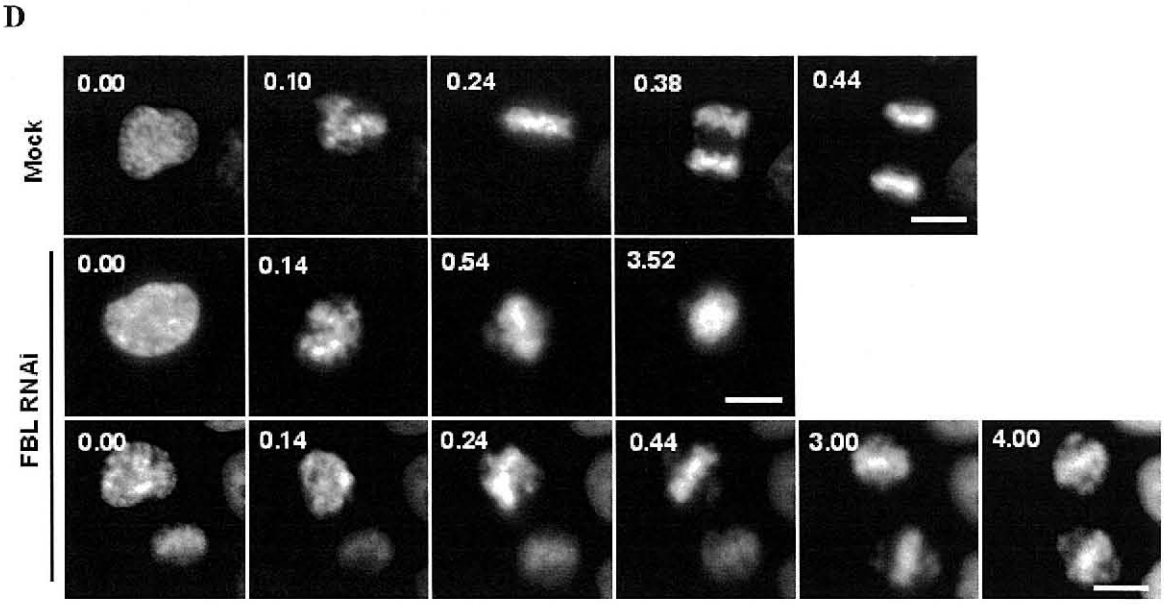

Fig. 2.3.4D Mitotic progression is delayed in fibrillarin-depleted cells. Mock and FBL siRNAs-treated HeLa cells stably expressing GFP-H1.2 were used for live cell imaging at 65 h post-transfection. Images were collected at every 10 min intervals until more than 8 h. Scale bars = 5 μm.

2.4 Summary

FBL and its interacting proteins such as SMN, CBs were found to be essential for early mouse embryo development (Schrank et al., 1997; Tucker et al., 2001). Moreover nucleolar proteins have a role in regulating cell proliferation and growth by controlling ribosome biosynthesis and p53 functions (Du et al., 2002; Michael et al., 2002). In agreement with these findings, the current study suggests that FBL would be involved in cellular growth.

FBL is localized throughout the cell cycle of HeLa cells. During interphase mainly in nucleolus and during mitosis at the peripheral region of chromosome. Although FBL is a nucleolar protein, its depletion has almost no effects on the nucleolar structure. Depletion of FBL leads to abnormalities in the nuclear shape, which was not due to defects in the localization of nuclear envelope protein lamin A/C and defects in cytoskeletal elements. Depletion of FBL causes inhibition of cells proliferation, which was judged by the growth curve, moderate accumulation of G_2/M cells and mitotic delay. Thus FBL is required for normal nuclear morphology to sustain the cellular growth and can be considered as multifunctional protein in HeLa cells.

Chapter 3

Functional analyses of a nucleolar protein, nucleophosmin on mitotic chromosomes in HeLa cells

3.1 Introduction

Nulceolar proteins bind to the chromosome peripheral surface during mitosis and become incorporated into the newly formed nucleoli at the end of telophase (Azum-Gelade et al., 1994; Dundr et al., 2004). Ki-67 is involved in the formation of higher order chromosomes structures (Kametaka et al., 2002). In Chapter 2, it has been shown that FBL has roles in the maintenance of nuclear shape and cellular growth and another study reported that nucleolin is required for chromosome congression and spindle formation during mitosis (Ma et al., 2007). Other observations suggest that FBL, NCL, NPM and Ki-67 act as promoters in cell proliferation (Chapter 2; Schluter et al., 1993; Derenzini et al., 1995; Mehes and Pajor, 1995). Therefore, nucleolar proteins have roles not only in mitosis but also in cell proliferation and thus regulate numerous cellular processes, suggesting a broadened view of their potential functions (Maggi and Weber, 2005).

NPM (nulceolphosmin/B23), a multifunctional nucleolar protein, is involved in many cellular activities, including ribosomal biogenesis, protein chaperoning, and centrosome duplication (Okuwaki et al., 2002; Okuwaki et al., 2001; Okuda et al., 2000). NPM appears to be involved in different aspects of DNA metabolism and chromatin regulation (Frehlick et al., 2007). NPM has a role in embryonic development (Grisendi et al., 2005). NPM has been reported as an oncogenenic (Grisendi et al., 2005, 2006) and, controversially, as a tumor suppressor protein (Colombo et al., 2002; Kurki et al., 2004). However, the role of NPM on mitotic chromosomes is still unknown. In this chapter, it was shown that depletion of NPM by RNAi (RNA interference) causes defects in cell

division followed by an arrest of DNA synthesis due to activation of p53-dependent checkpoint response in HeLa cells. Depletion of NPM leads to mitotic arrest due to spindle checkpoint activation. The mitotic cells arrested by NPM depletion have defects in chromosome congression, proper mitotic spindle and centrosome formation, as well as defects in kinetochore-microtubule attachments. Loss of NPM thus causes severe mitotic defects and delayed mitotic progression. These findings indicate that NPM is essential for mitotic progression and cell proliferation.

3.2 Materials and methods

3.2.1 Cell culture and synchronization

HeLa cells were cultured in growth medium, Dulbecco's modified Eagle's medium (DMEM; Gibco BRL) with 5% fetal bovine serum (Equitech-Bio, Inc) and penicillin-streptomycine (100 U ml^{-1} and 100 μg ml^{-1} respectively; Nacalai Tesque, Inc., Kyoto Japan), at 37°C in a humidified incubator with 5% CO_2. Cells were treated with 2.5 mM thymidine (Sigma) for 16 h, washed and released into fresh medium for 8 h, and then treated with thymidine for another 16 h to obtain cells uniformly blocked at the G_1/S boundary. At 8-10 h after release from second thymidine block, cells were harvested for further analysis.

3.2.2 siRNA (small interference RNA) transfection and rescue assay

Double-stranded siRNA sequence (synthesized by HSS Co Ltd. Hokkaido in Japan) siRNA sequences 5′-AGAUGAUGAUGAUGAUGAUTT-3′ and 5′-UACGGACUCACC UUGCUUGTT-3′ were used to knockdown human NPM and Mad2, respectively. As mock, siRNA sequence 5′-CGUACGCGGAAUACUUCGATT-3′ specific for GL2 luciferase gene was used. Transfection of siRNA was performed according to the manufacturer's instructions (Invitrogen). For the rescue assay, we constructed an RNAi-refractory GFP-NPM vector (NPMr). Three silent mutations were introduced into the GFP-NPM vector by changing nucleotide sequence 671-682 of NPM to GA*C*GATGA*C*GA*C* (underlined nucleotides in italics indicate silent mutations). Site-directed mutagenesis was performed by PCR and confirmed by sequencing. RNAi-

refractory construct was transfected to 1 d-old cell culture with FuGENE6 (Roche) before ~6 h of siRNA transfection. Cells were harvested at 24 h post-transfection for further experiments.

3.2.3 Antibody reagents

Antibodies used in this study were as follows: mouse monoclonals anti-α-tubulin (Calbiochem), anti-fibrillarin (Abcam), anti-nucleolin (Abcam), anti-BubR1 (BD Transduction Laboratories), anti-Bub1 (Chemicon) and anti-BrdU (Amersham BioSciences) at 1:50~100, and anti-nucleophosmin (Santa Cruz) at 1:1,000; and rabbit polyclonal anti-p53 (Santa Cruz) at 1:100~200 and human monoclonal anti-centromere autoimmune serum (CREST) at 1:1,000. Secondary antibodies conjugated to Alexa Fluor 488, Alexa Fluor 594 (Invitrogen) and TRITC (Sigma) were used for signal detection.

3.2.4 Indirect immunofluorescence microscopy

HeLa cells grown on cover slips were fixed with 4% (w/v) para-formaldehyde at 37°C or methanol at –20°C, and incubated with primary antibodies. Standard methods for immunofluorescence staining were used. DNA was stained with Hoechst 33342 (Sigma).

For the analysis of microtubule stability, culture media were changed with ice-cold media and cells were incubated on ice for 10 min, followed by fixation and permeabilization at room temperature using PBS.

All images were acquired as *Z*-stacks with 0.2-μm spacing using a x100, 1.3 NA oil objective on an IX-70 microscope (Olympus) and processed by iterative constrained deconvolution (SoftWorx, Applied Precision Instruments). Images were cropped, sized and placed using Adobe Photoshop CS version 8.0 (Adobe Systems, San Jose, CA).

For BrdU assay, cells were incubated for 1 h with BrdU cell proliferation kit (dilution 1:1000, Amersham Biosciences) before being fixed and permeabilized. After washing, cells were treated with 2 M HCl for 20 min at room temperature followed by neutralization with two volumes of 0.1 M sodium borate (pH 8.5). After three washes with PBS-Tween 0.1%, BrdU was detected by immunostaining.

3.2.5 Live-cell imaging

HeLa cells stably expressing GFP-histoneH1.2 grown in 35 mm ploy-L-lysine coated glass-bottomed dishes were transfected with siRNA. The medium was changed to a CO_2-independent medium (GIBCO BRL) supplemented with 10% FBS 1 hr before imaging. After 21 h of siRNA transfection, sequences of GFP images were acquired every 6 min for 8 to 18 h using a 40x, 1.4 NA oil objective on an inverted fluoresecence microscope (IX-81, Olympus) equipped with a Z-motor and CCD camera (Photometrics). Experiments were performed in a chamber maintained at 37°C with a humidified atmosphere of 5% CO_2 in air. Metamorph software (Universal Imaging, Downington, PA) and WCIF Image J Program were used for acquisition and analysis.

3.3 Results and discussion

3.3.1 NPM is required for normal growth and survival of HeLa cells

To analyze the function of NPM in the cell cycle of HeLa cells, endogenous NPM was depleted by RNAi. Western blotting revealed that NPM expression levels were significantly depleted (to more than 80 %), whereas expression levels of other nucleolar proteins (such as fibrillarin and nucleolin) and α-tubulin was not affected (Fig. 3.3.1A). Mock treated cells had regular morphology and proliferated normally (Fig. 3.3.1B upper panel, D), whereas NPM-depleted cells underwent remarkable morphological changes, including dynamic change in nuclear structure and tetraploid micronuclei formation (Fig. 3.3.1B,C), and lost proliferation ability (Fig. 3.3.1D). Proliferation assay showed that NPM depletion of NPM led to decreased DNA synthesis as evidenced by diminished BrdU incorporation for both 24- and 48- h siRNA post-transfection (Fig. 3.3.1E). The decreased DNA synthesis possibly occurs secondarily from cessation of cell division rather than as a direct effect on DNA replication. To test this hypothesis, the p53 pathway was being checked. Immunostaining showed that NPM depletion induced activation of p53 and its downstream target p21 (Fig. 3.3.1F, G and data not shown) and suppressed HPV18 E6, which promotes degradation of p53, as a consequence (Fig. 3.3.1H). Moreover, p53 levels induced by NPM depletion were suppressed by co-depletion of p53, which largely restored DNA synthesis (Fig. 3.3.1E, I) but failed to restore proliferation, and morphological and mitotic defects in the absence of NPM, whereas single depletion of p53 had no effect (data not shown and Fig. 3.3.1G). Thus, p53 was required for the

inhibition of DNA synthesis caused by depletion of NPM. Absence of the p53-p21 pathway would exacerbate the cell-division defects caused by NPM depletion by allowing DNA endoreduplication without completion of mitosis. The morphological changes were accompanied by a gradual decrease of G_2 cells and a concomitant increase of G_1 cells ($BrdU^-$, cyclin B_1^- cells) (Fig. 3.3.1E, J). Taken together these results indicate that the proliferative inhibition HeLa cells caused by NPM depletion is due to the activation of a p53-dependent checkpoint response.

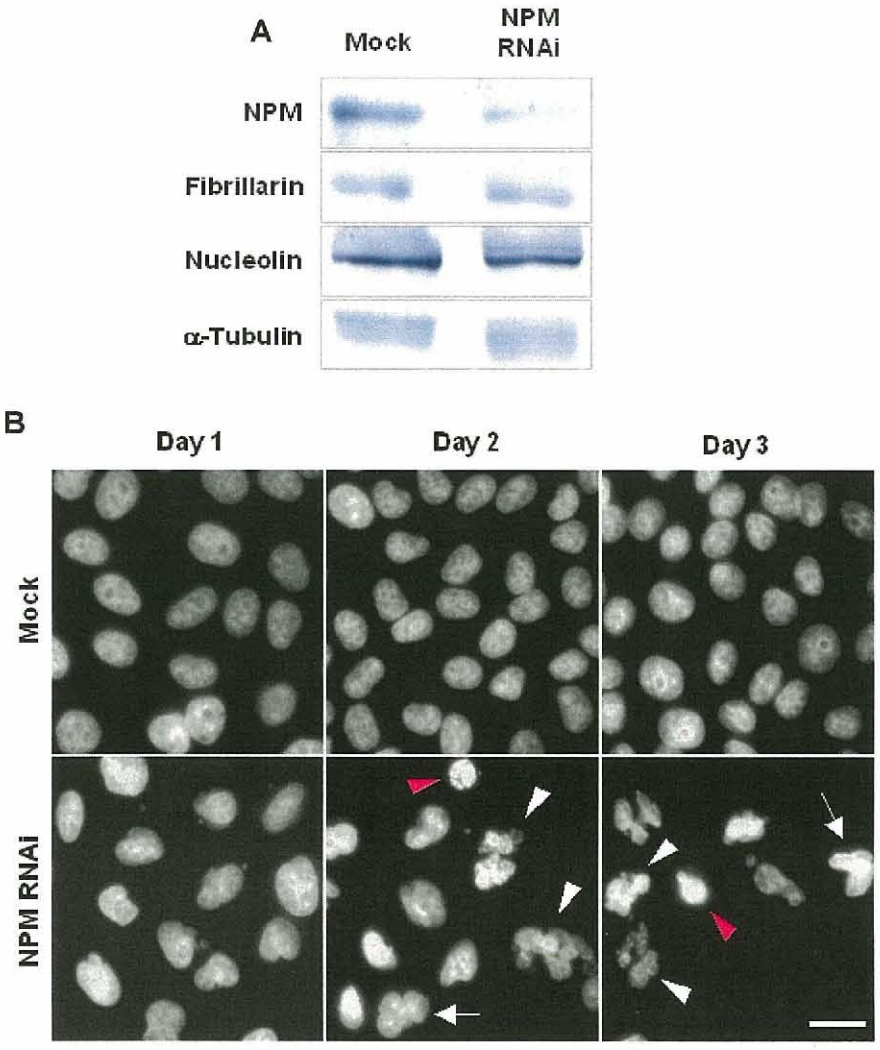

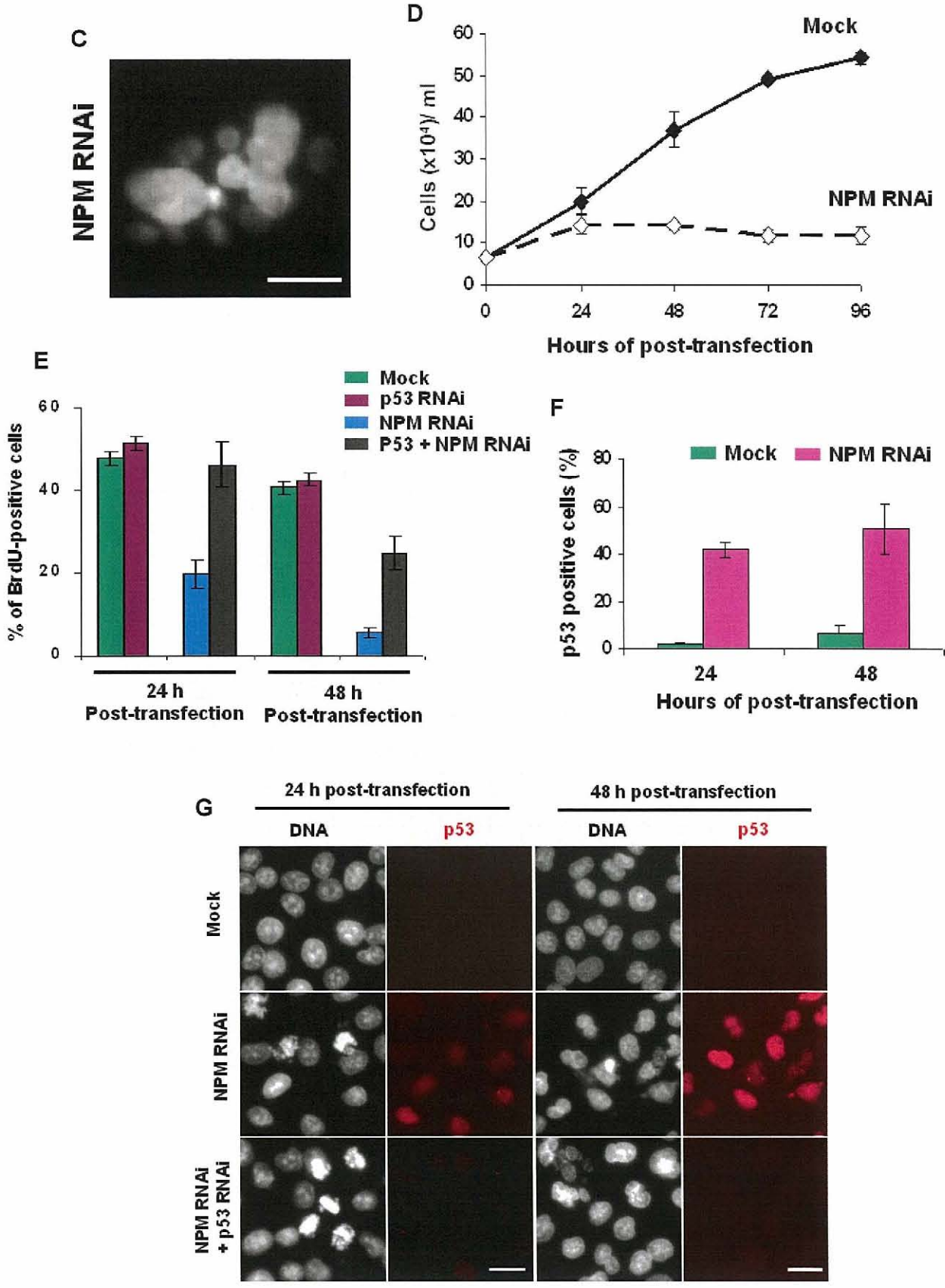
C
NPM RNAi
D
Mock
NPM RNAi
Cells (x10⁴)/ ml
Hours of post-transfection
E
Mock
p53 RNAi
NPM RNAi
P53 + NPM RNAi
% of BrdU-positive cells
24 h Post-transfection
48 h Post-transfection
F
Mock
NPM RNAi
p53 positive cells (%)
Hours of post-transfection
G
24 h post-transfection
48 h post-transfection
DNA
p53
Mock
NPM RNAi
NPM RNAi + p53 RNAi

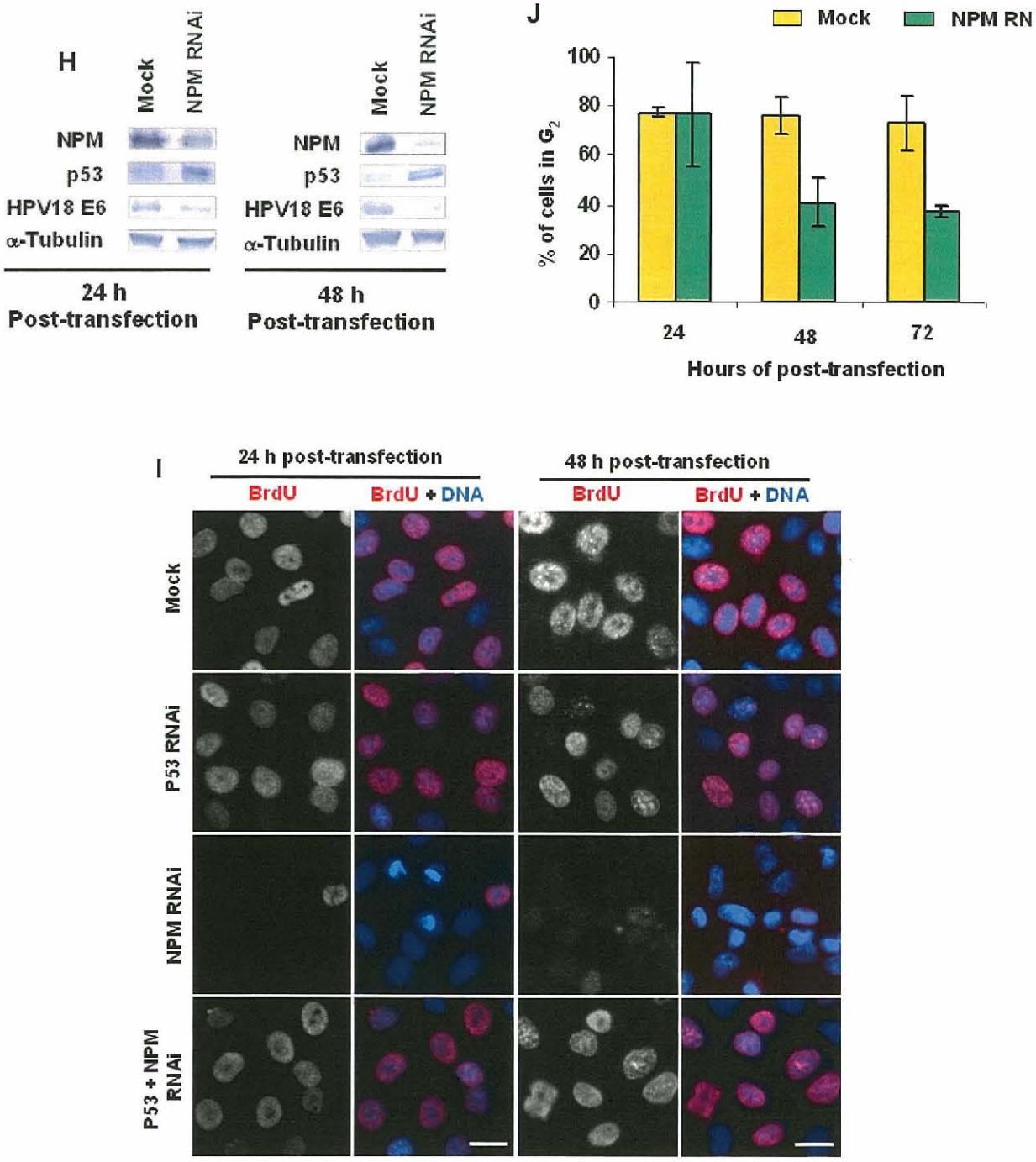

Fig. 3.3.1 Depletion of NPM causes proliferative arrest of HeLa Cells. (A) Western blotting with mock and NPM –depleted cells at 24 h post-transfection. NPM was down-

regulated ~80% by its respective siRNA. The expression levels of fibrillarin and nucleolin were unaffected by NPM RNAi. Immunoblotting of α-tubulin served as loading controls. (B) Representative morphological features of mock and NPM-depleted cells at various times. Scale bar = 5 μm. Arrows indicate abnormal nuclear shape with the white arrowheads indicating micronucleated cells and the red arrowheads indicating apoptotic cells. Apoptotic cells were detected by staining with trypan blue 0.4 %, GIBCO BRL). (C) Cell containing multiple micronuclei. Scale bar = 5 μm. (D) Growth curves of mock and NPM siRNAs-treated cells until 4 d pot-transfection. Error bars represent the mean ± s. d. of three independent experiments. (E) BrdU-positive percentages at 24- and 48- h post-transfection of mock, NPM, p53 and both p53 and NPM siRNAs. Data are the mean ± s. d. of triplicate cell counts (n= 500-1,000). (F) Percentages of cells expressing p53 at 24- and 48- h post-transfection for mock and NPM siRNAs. 300-1000 cells per sample were counted; data are the mean ± s. d. percentages. (G) Immunostaining of mock and NPM, both NPM and p53 siRNAs-treated cells with p53 at 24- and 48- h post-transfection. Red and blue signals for p53 and DNA, respectively. Scale bars = 10 μm. (H) Western blotting for p53 and HPV18 E6 using extracts of mock and NPM-depleted cells at 24- and 48-h post-transfection. The loading control was α-tubulin. (I) Immunostaining of mock, NPM, and both NPM and p53 siRNAs-treated cells for BrdU incorporation at 24- and 48- h post-transfection. Red and blue signals for BrdU and DNA, respectively. Scale bars = 10 μm. (J) NPM-depletion impairs cell cycle progression. HeLa cells were treated with mock and NPM siRNA sequences for 24 h, 48 h and 72 h, followed by fixation and immunostaining with anti- cyclin B_1, followed by counter staining with Hoechst 33342. The number of cells in G_2 (identified based on their high

cytoplasmic levels of cyclin B_1) decreased after NMP depletion with time. At least 550 cells per sample, obtained from independent experiments, were scored and the results were expressed in percentages (mean ± standard deviation, *P* 0.02 and 0.01 for 48 h and 72 h samples).

3.3.2 Depletion of NPM leads to mitotic arrest with aberrant chromosomes

Since NPM is localized at the perichormosomal region (Okuwaki et al., 2002; Sandeep et al., 2006) and identified at the peripheral region of highly purified human metaphase chromosome (Uchiyama et al., 2005), its function on mitotic chromosomes was examined. Depletion of NPM caused accumulation of prometaphase and metaphase cells two-fold higher compared to that of mock treatment (Fig. 3.3.2A). This was accompanied by an increased mitotic index (6-fold to 7-fold) in NPM-depleted cells relative to that of mock treated cells (Fig. 3.3.2B). Mitotic arrest by NPM depletion was abrogated by co-depletion of spindle checkpoint protein Mad2 with siRNA (Fig. 3.3.2B,C). Furthermore the ratio of BubR1- and Bub1-positive cells in the mitotic populations was higher in NPM-depleted cells than mock treated cells (Fig. 3.3.2D). Notably, they accumulated at kinetochores of uncongressed chromosomes in NPM-depleted cells, to a similar extent as found with unattached kinetochores in mock treated cells during prometaphase when spindle checkpoint activity is robust (Fig. 3.3.2E). These results indicate that depletion of NPM causes mitotic arrest due to the activation of spindle assembly checkpoint proteins. To rule out potential off-target effects (Echeverri et al., 2006) rescue assays were performed, which showed that mitotic arrest was

markedly recovered by introducing GFP-tagged NPM-siRNA resistant (NPMr) plasmid as revealed by the decrease of mitotic index (Fig. 3.3.2B,F). Moreover, the amount of mitotic cells 48 h decreased to only 1.74%, which was even lower than that of mock treated cells (Fig. 3.3.2B). This tendency is consistent with gradual escape of mitotic arrest and procession to G_1 state.

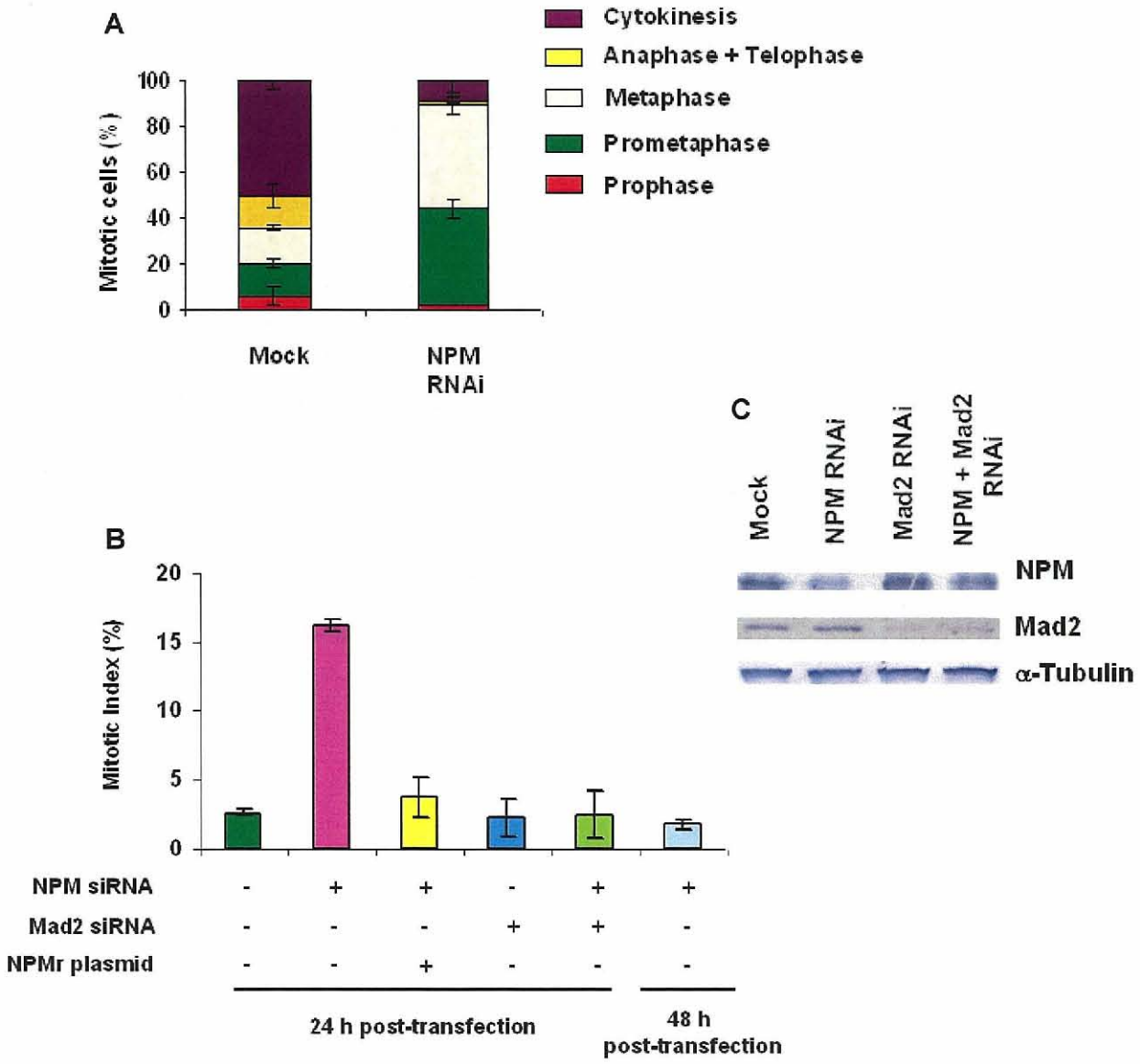

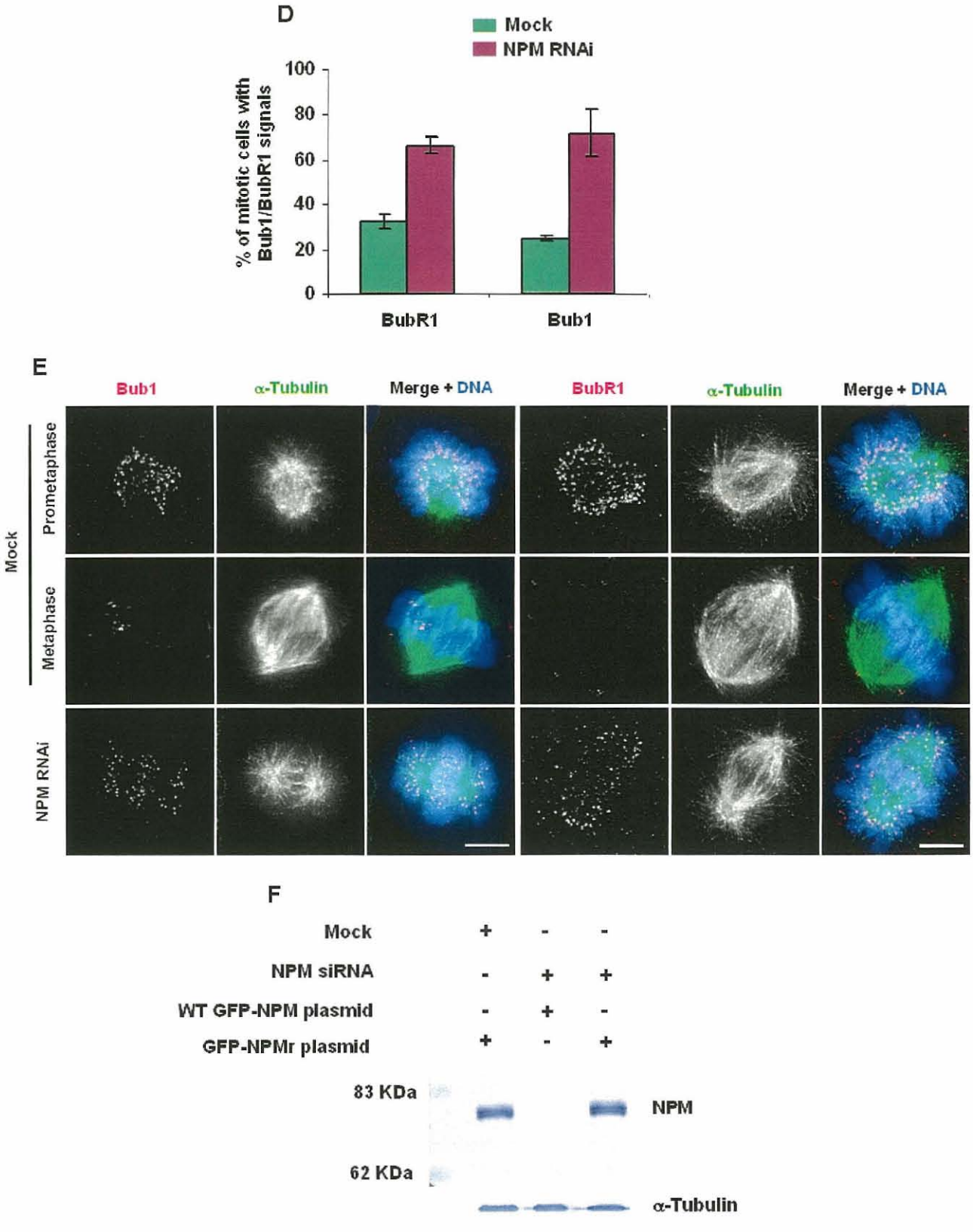
D
Mock
NPM RNAi
% of mitotic cells with Bub1/BubR1 signals
100
80
60
40
20
0
BubR1
Bub1
E
Bub1
α-Tubulin
Merge + DNA
BubR1
α-Tubulin
Merge + DNA
Mock
Prometaphase
Metaphase
NPM RNAi
F
Mock + - -
NPM siRNA - + +
WT GFP-NPM plasmid - + -
GFP-NPMr plasmid + - +
83 KDa
NPM
62 KDa
α-Tubulin

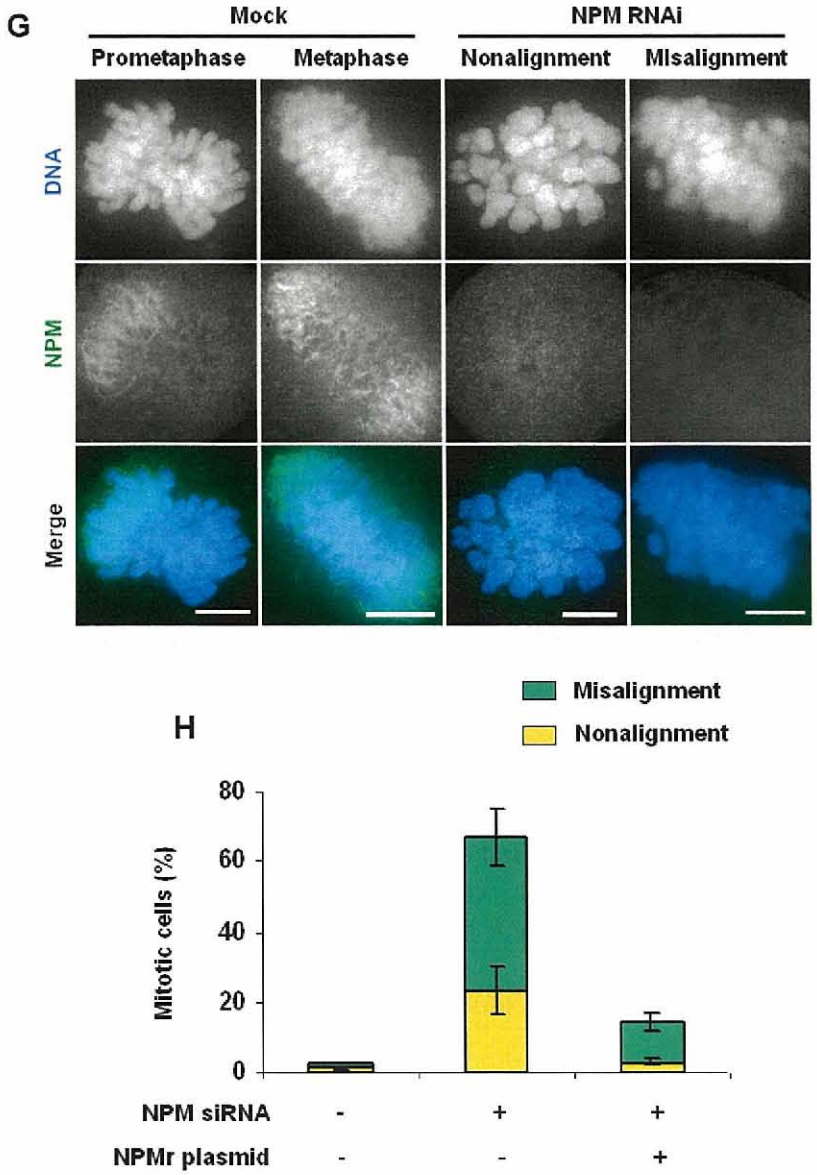

Fig. 3.3.2. NPM depletion leads to mitotic arrest due to spindle checkpoint activation and aberrant chromosomes in HeLa cells. (A) The percentages of mitotic phases were determined at 24 h post-transfection with mock and NPM siRNAs by staining with α-tubulin and DNA. Data are the mean ± s. d. of at least triplicate cell counts (n= at least 200). (B) Mitotic indices of mock, NPM-depleted, Mad2-depleted and both NPM- and Mad2-depleted cells at 24 h post-transfection and of NPM depleted cells at 48 h post-

transfection. Expression of NPMr plasmid results in significant reduction of mitotic index in NPM-depleted cells. The mitotic index was calculated from the number of cells immunostained with anti-α-tubulin and DNA. Data are the mean ± s. d. of triplicate cell counts (n=350~1000). (C) Specific depletion of NPM and/or Mad2 was confirmed by Western blot analysis. (D) The ratio of BubR1– and Bub1-positive cells in mitotic populations in mock and NPM-depleted cells. Data are the mean ± s. d. of triplicate cell counts (n >100). (E) Immunostaining of both mock and NPM siRNAs-treated cells at 24 h post-transfection for Bub1 / BubR1 (red), α-tubulin (green) and DNA (blue). Scale bars = 5 μm. (F) Western blot analysis for GFP-tagged NPM siRNA resistant (NPMr) plasmid at 24 h post-transfection of mock and NPM siRNAs. (G) Commonly observed mitotic defects in NPM-depleted cells. Green and blue signals are for NPM and DNA, respectively. Scale bars = 5 μm. (H) Percentages of mitotic cells with nonaligned or misaligned chromosomes were scored from three independent experiments (mean ± standard deviation, n=100). Aberrant chromosomes were recovered by the rescue assay.

Mitotic cells arrested by NPM depletion mostly showed two types of defects: approx. 20 % of nonaligned (defined as more than 10 chromosomes were not aligned at the metaphase plate or scattered throughout the cytoplasm) and approx. 40 % of misaligned (defined as 1 to 10 chromosomes were not aligned at the metaphase plate). IN contrast the majority of the mock chromosomes were aligned (Fig. 3.3.2G,H). The mitotic defects were significantly recovered by the rescue assay (Fig. 3.3.2H). These results indicate that NPM plays an important role in proper congression of mitotic chromosomes.

3.3.3 NPM is required for mitotic spindle formation

Failure of proper chromosome alignment is due to the defects in the mitotic spindles and/or kinetochore-microtubule attachment (Ishii et al., 2007). Immunofluorescence experiments showed that NPM-depleted cells had two types of abnormalities in mitotic spindles: disorganized (~26%) and multi-polar (~9%) spindles with fragmented centrosomes whereas almost all mock treated cells had normal bipolar mitotic spindles (Figs. 3.3.3A,B). These phenotypes were consistent with those of NPM-null mouse embryonic fibroblasts (Grisendi et al., 2005). No increase in abnormal mitotic spindles was observed in the rescue assay (data not shown).

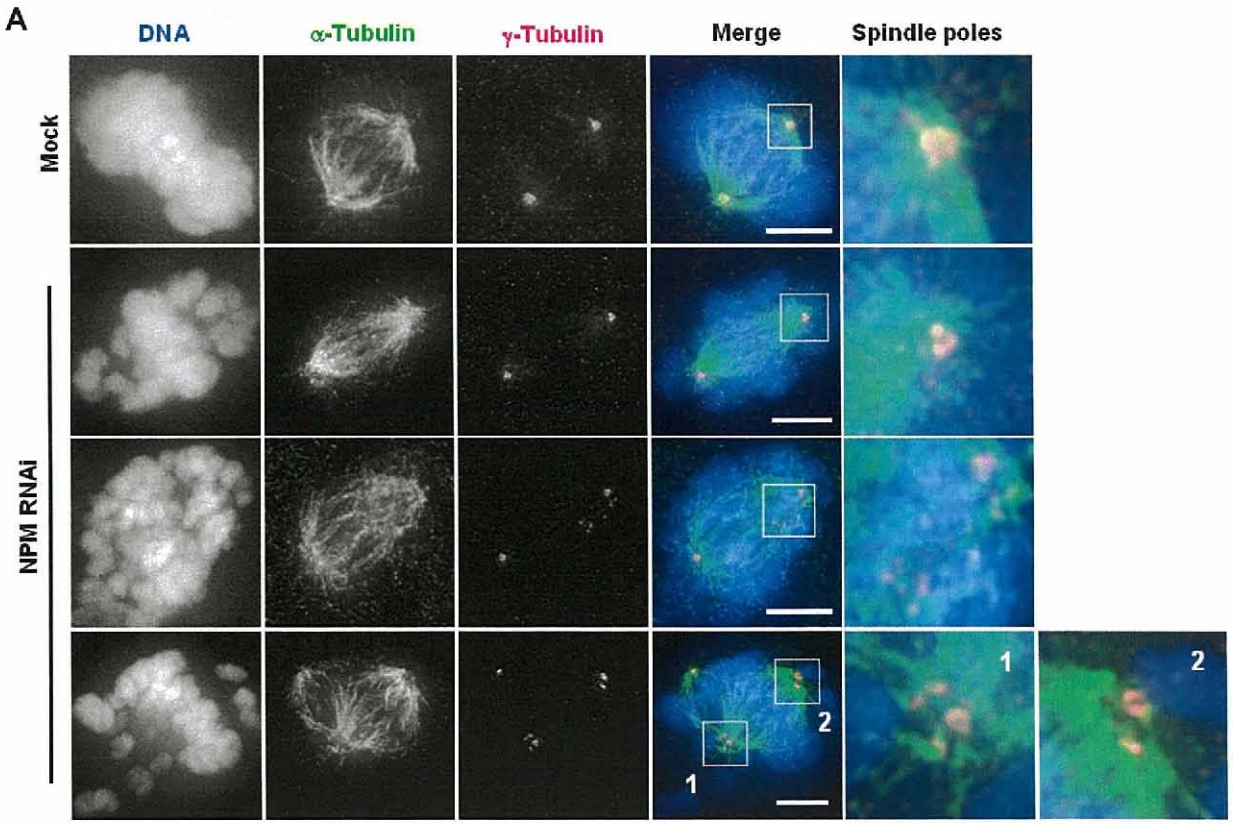

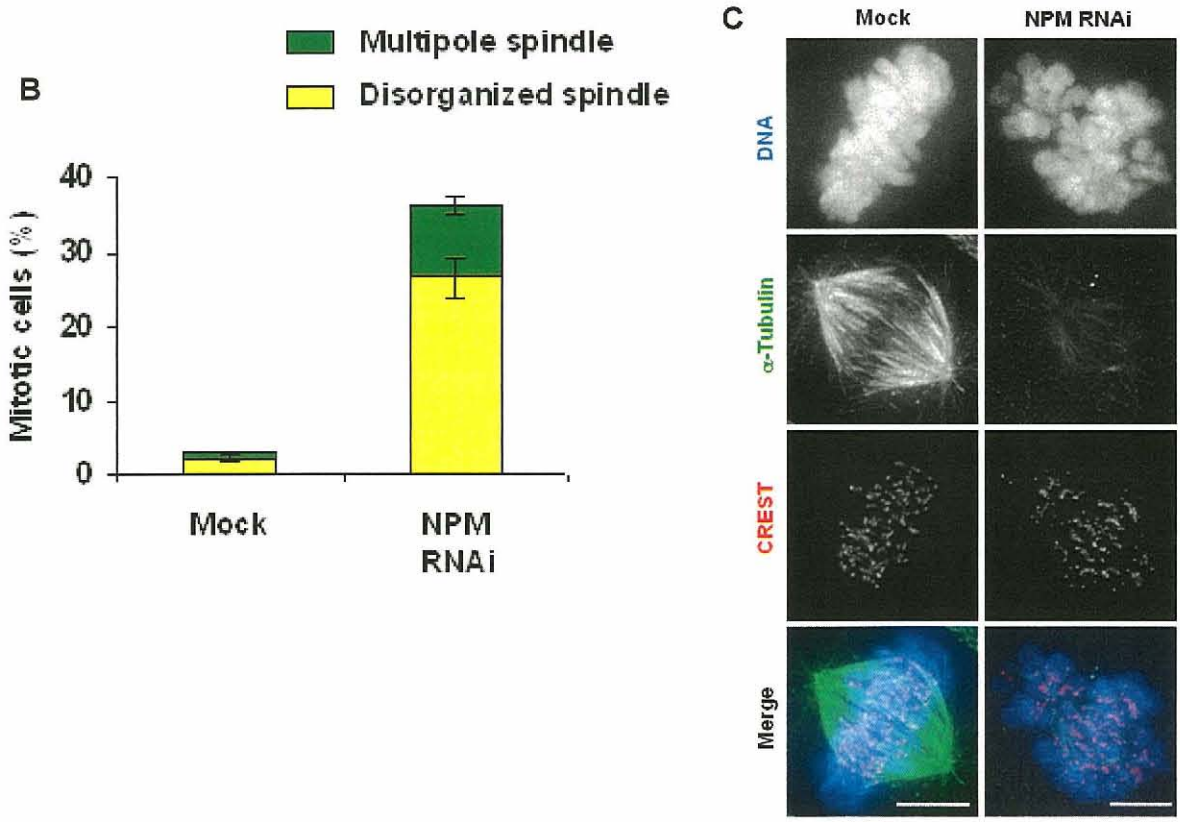

Fig. 3.3.3 NPM is required for mitotic spindle formation. (A) Both mock and NPM siRNA treated cells were immunostaining for α-tubulin (green), γ-tubulin (red) and counterstained for DNA (blue) with Hoechst 33342. Scale bars = 5 μm. (B) Percentages of cells showing disrupted mitotic spindles. Data are the mean ± s. d. of three independent experiments with at least 100 mitotic cells. (C) Mitotic HeLa cells trasfected with mock and NPM siRNAs were incubated on ice for 10 min and stained with CREST (red), α-tubulin (green) and DNA (blue). Scale bars = 5 μm.

The defective spindle phenotype was further analyzed by testing the stability of the spindle microtubules in response to cold treatment (Brinkly et al., 1975). Immunostaining showed that mitotic spindles became unstable and largely disintegrated in NPM-depleted cells, whereas the overall structure of the kinetochore-attached microtubules remained robust in mock treated cells after cold treatment (Fig. 3.3.3C). These results indicate that NPM is required for the formation of a bipolar and stable mitotic spindle with an intact centrosome.

3.3.4 NPM is required for proper kinetochore-microtubule attachment

Double immunostaining showed that NPM was localized at the attached positions of kinetochores during mitosis (Fig. 3.3.4A), indicating that NPM might be involved in kinetochore function.

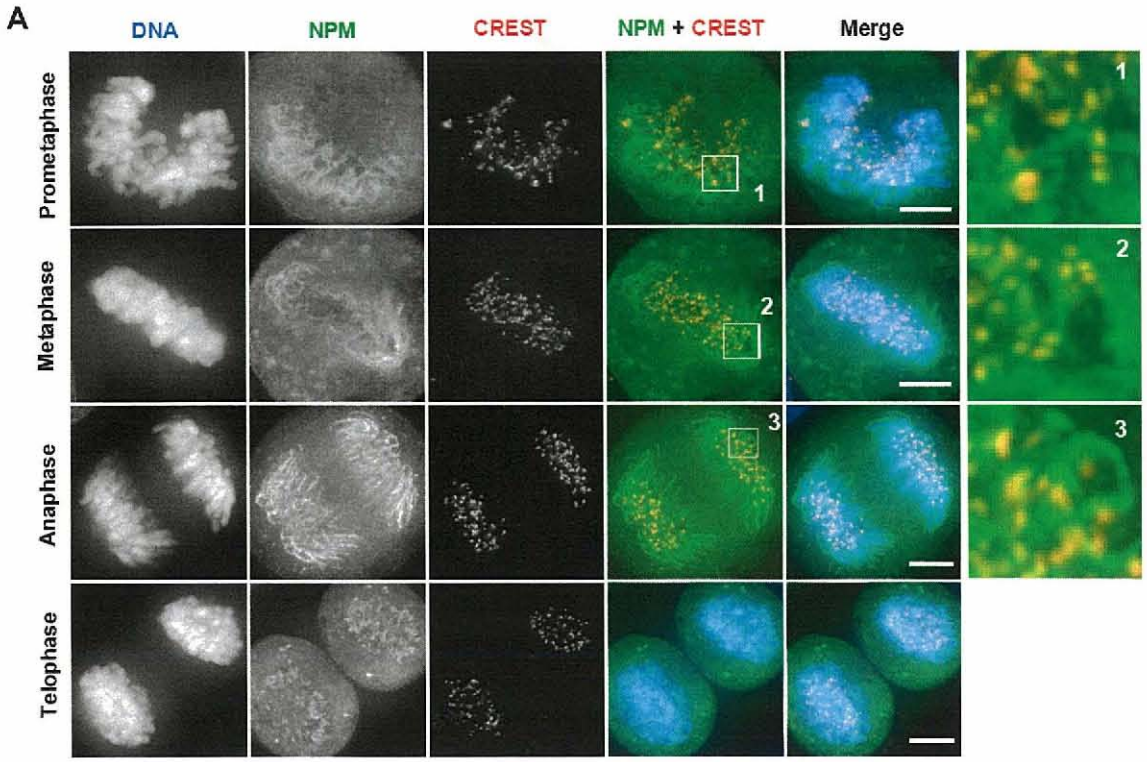

Fig. 3.3.4A Localization of NPM at the kinetochore attachment positions in mitotic cells. HeLa cells were double immunostained for NPM (green) and CREST (red). DNA was counter-stained with Hoechst 33342 (blue). Scale bars = 5 μm. The 3-fold inset magnifications show the localization of NPM at positions attached to kinetochores.

Closer inspection of the uncongressed chromosomes showed that sister kinetochores faced opposite poles (data not shown), whereas depletion of NPM led to whereas depletion of NPM led to monotelic (one kinetochore bound and one kinetochore free) or syntelic (both kinetochores attach to the same spindle poles) attachment of sister kinetochores in uncongressed chromosomes (Fig. 3.3.4C).

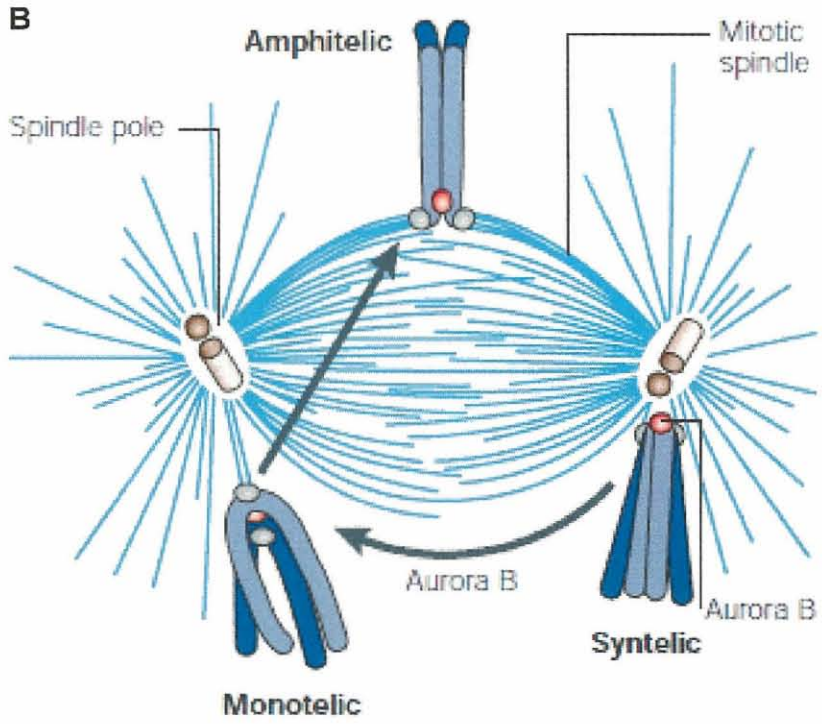

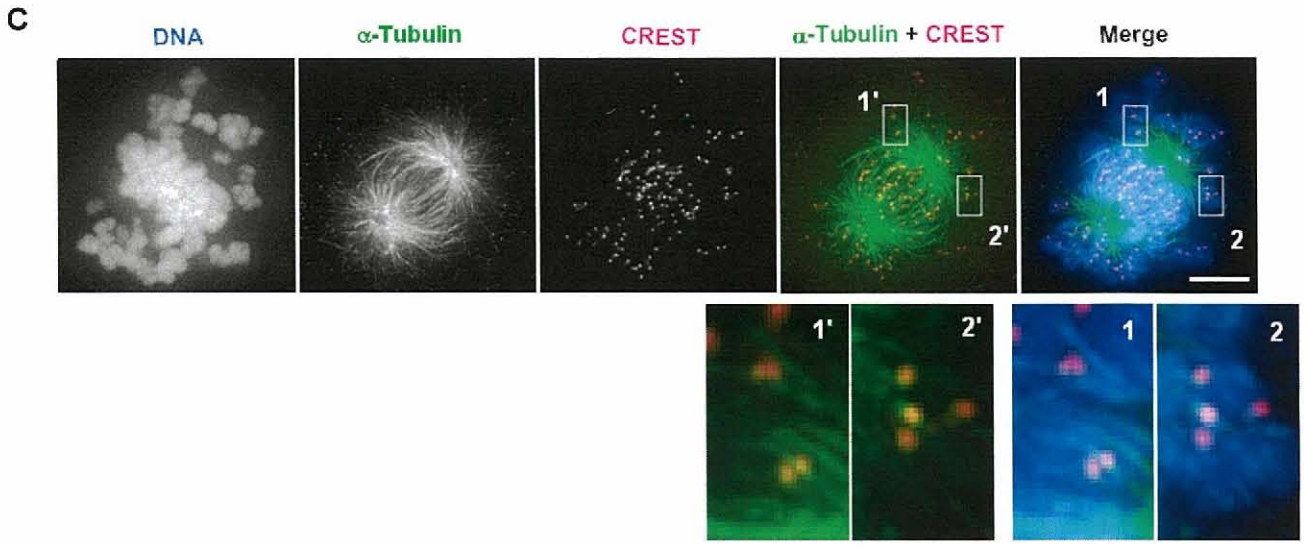

Fig. 3.3.4 (A) **Role of Aurora B in promoting chromosome biorientation on the mitotic spindle.** Normally, the first attachment of chromosomes to the spindle microtubules (blue) is monotelic (one kinetochore bound, one kinetochore free). If both kinetochores attach to the same spindle pole (syntelic attachment), Aurora B in the inner centromere (red) promotes release of the bound microtubules, which therefore promotes the formation of monotelic attachments. Eventually, chromosomes become attached to both spindle poles (amphitelic attachment) (Carmena and Earnshaw, 2003). (B) **NPM is required for kinetochore-microtubule attachment.** An NPM-depleted mitotic cell stained with α-tubulin (green), CREST to show the positions of kinetochores (red) and counterstained with Hoechst 33342 for DNA (blue). Scale bar = 5 μm. Insets, 2.8-fold magnifications of boxed regions show monotelic (insets 1′ and 1) and syntelic (insets 2′ and 2) attached sister kinetochores.

To determine whether the defect in kinetochore-microtubule attachment is due to the defective kinetochore structure, next the localization of various kinetochore proteins was investigated to assess the integrity of the kinetochore structure in NPM-depleted cells. We found that CREST (a marker of outer kinetochore), CENP-E (a kinetochore motor protein), Aurora B kinase (a key kinetechore protein), and Hec1 (a key regulator in kinetochore-microtubule attachment; (DeLuca et al., 2007) were remarkably accumulated at kinetochores in NPM-depleted cells (Fig. 3.3.4D-G). These results indicate that NPM depletion does not affect kinetochore formation. Taken together, these findings suggest that NPM is required for proper kinetochore-microtubule attachment.

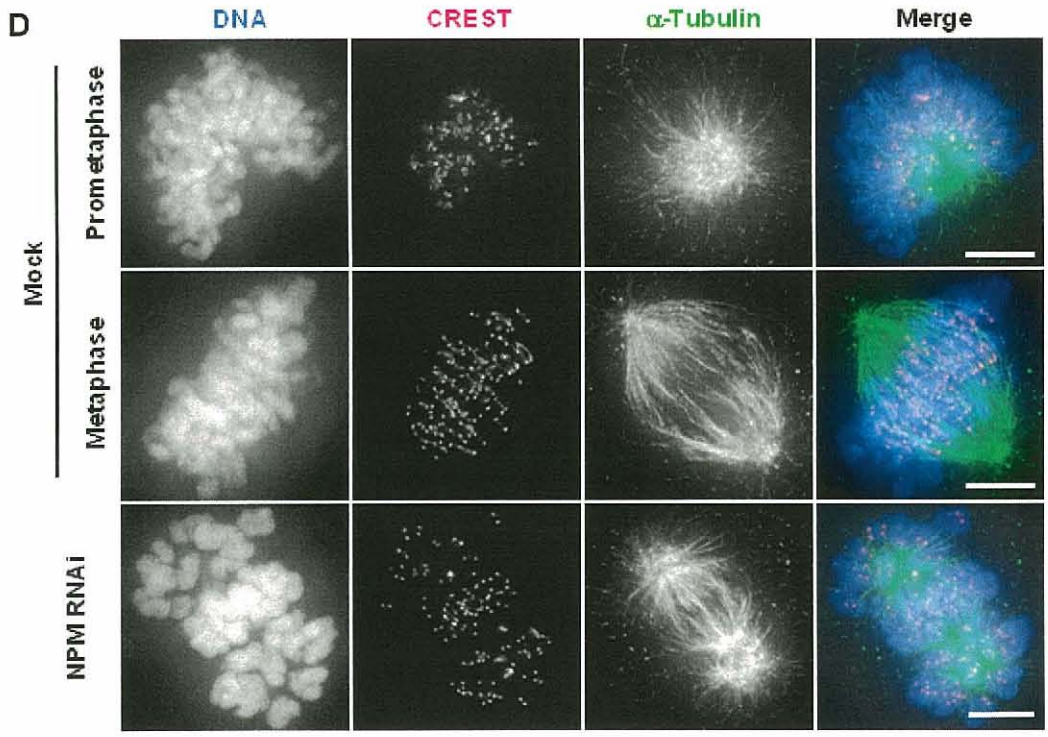

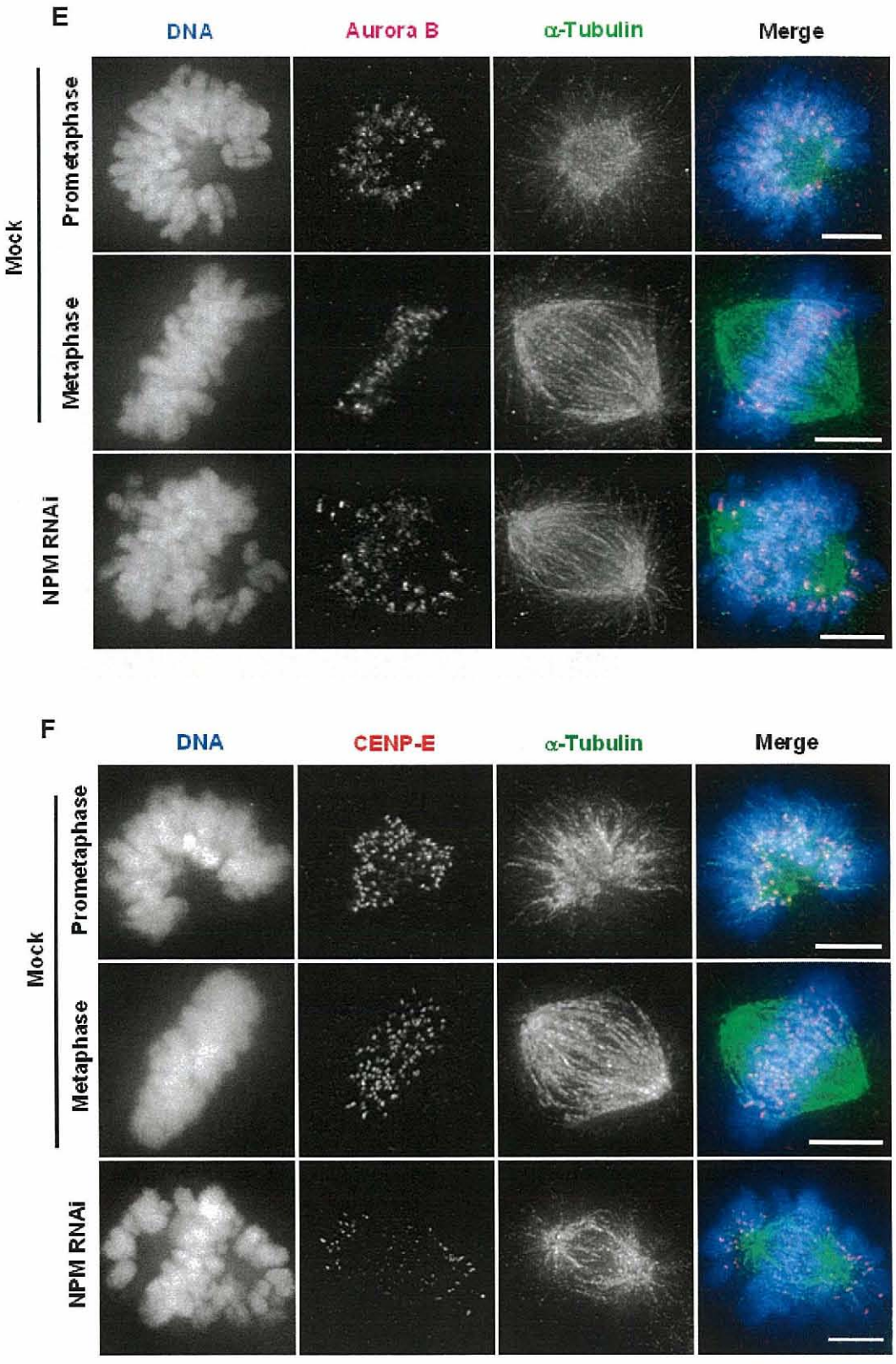
E
DNA
Aurora B
α-Tubulin
Merge
Mock
Prometaphase
Metaphase
NPM RNAi
F
DNA
CENP-E
α-Tubulin
Merge
Mock
Prometaphase
Metaphase
NPM RNAi

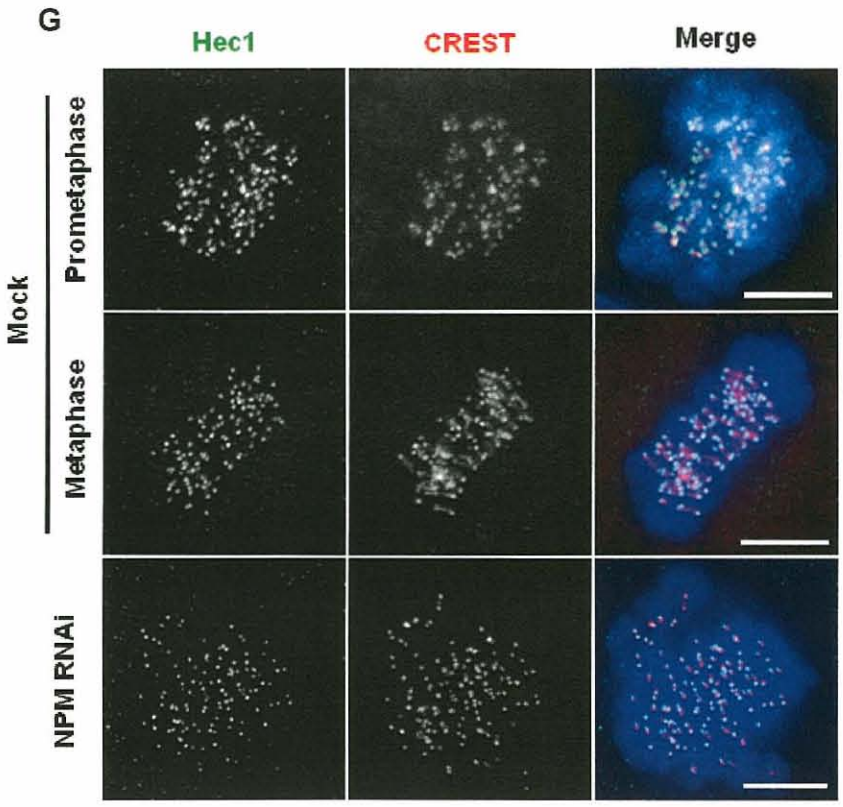

Fig. 3.3.4D-G **Kinetochore protein assembly is intact in NPM-depleted cells.** Mock and NPM siRNA-treated cells were stained with tubulin (green) for CREST (A, red), Aurora B (B, red), CENP-E (C, red) and Hec1 (D, green). DNA was counterstained with Hoechst 33342 (blue). Scale bars = 5 μm. Aurora B, CENP-E, and Hec1 all are localized at uncongressed chromosomes indicating kinetochores unattached with microtubules. CREST acts as a positive marker of kinetochores. As with NPM depletion, Hec1 knockdown results in a disorganized spindle (Deluca et al., 2006). However the staining levels of Hec1 at kinetochores are similar in control and NPM-depleted cells. Mouse anti-CENP-E (Abcam), anti-CENP-A (Abcam), anti-Hec1 (Affinity BioReagents), and rabbit anti-Aurora-B (Abcam) were used.

3.3.5 Live Cell imaging of mitotic defects and delay in NPM-depleted cells

To get insight into the proliferative inhibition, cell cycle progression was analyzed by taking the advantages of synchronization with double thymidine block and immunostaining with CENP-F. NPM-depleted cells significantly delayed in cell-cycle progression and apparently arrested in G_2/M phase, as judged by increased amounts of CENP-F expressing and mitotic cells (Table 1). Detailed analysis of cell cycle showed that more than 95% control cells had already completed mitosis at 12 h after release from the G_1/S boundary because the mitotic index at this time was only less than 1%. In contrast, NPM-depleted cells had a mitotic index of ca. 15.4% at this time point. The accumulation of mitotic cells resulted from delayed exit of mitosis. These results indicate that NPM depletion would induce G_2/M checkpoint activation.

Hours after thymidine release	8h			10h			12h			16h		
Phase (%)	G2	M	G1	G2	M	G1	G2	M	G1	G2	M	G1
Mock	42.99	19	38	1.46	5.84	92.68	4.18	0.51	95.3	2.08	0.95	96.96
NPM RNAi	65.76	12.8	21.43	24.2	16.07	59.72	17.35	12.03	70.61	10.4	17.02	72.57

Table-1 Analysis of cell cycle profile in mock and NPM siRNA-treated cells. HeLa cells treated with 2.5 mM thymidine (Sigma) for 16 h, washed and released into fresh medium for 8 h, and then treated with thymidine for another 16 h to obtain cells uniformly blocked at the G_1/S boundary. Cells were released from double thymidine block and fixed at the indicated times, and the percentage of cells in G_2, mitosis and early

G_1 was determined (Liao et al., 1995; Kao 2001). Cells were released from double thymidine block and fixed at the indicated times, and the percentage of cells in G_2, mitosis and early G_1 was determined. Cells in G_2 were identified by nuclear staining for CENP-F with anti-CENP- F antibody (Novus Biologicals). Mitotic cells were identified by the presence of condensed chromosomes. Newly divided cells that were in early G_1 were identified from a lack of CENP-F staining and from paired cells tethered together at the mid-body. For each point 800-1,000 cells were counted.

Activation of spindle checkpoint delays the anaphase onset (Chen, 2002). Live cell image analyses showed that HeLa GFP-H1.2 cells (Higashi et al, 2007) had a longer period (more than 3 h) of mitotic progression (mitotic progression was defined as the time of nuclear envelope breakdown to chromosome segregation at anaphase) than that of mock treated cells (45-60 min) following NPM depletion (Fig. 3.3.5A). Further analyses showed that over 95% control cells went through at least one round of mitosis within the course of visualization (18 h), whereas approx. 40% of NPM-depleted cells entered mitosis (consistent with growth curve) and showed four different types of mitotic progression: normal (N), division (D) after a prolonged mitotic period, death during mitosis (DM) and micronuclei formation after division (MD) (Fig. 3.3.5B and Movie 1,2). Approx. 18%, 51.9%, 12% and 14% of mitotic cells were of N, D, DM and MD type, respectively (Fig. 3.3.5C). D, DM and MD types of mitotic progression were caused by severe mitotic defects (Fig. 3.3.5B and discussed earlier). Micronuclei usually originate from acentromeric chromosome fragments or whole chromosome lagging due to mitotic defect (Fenech, 2002). Immunostaining showed that most micronuclei

contained centric chromosomes due to the presence of CENP-A (Fig. 3.3.5D) and that underwent apoptosis (Movie 2). Taken together, these observations strongly suggest that NPM is essential for proper mitotic progression.

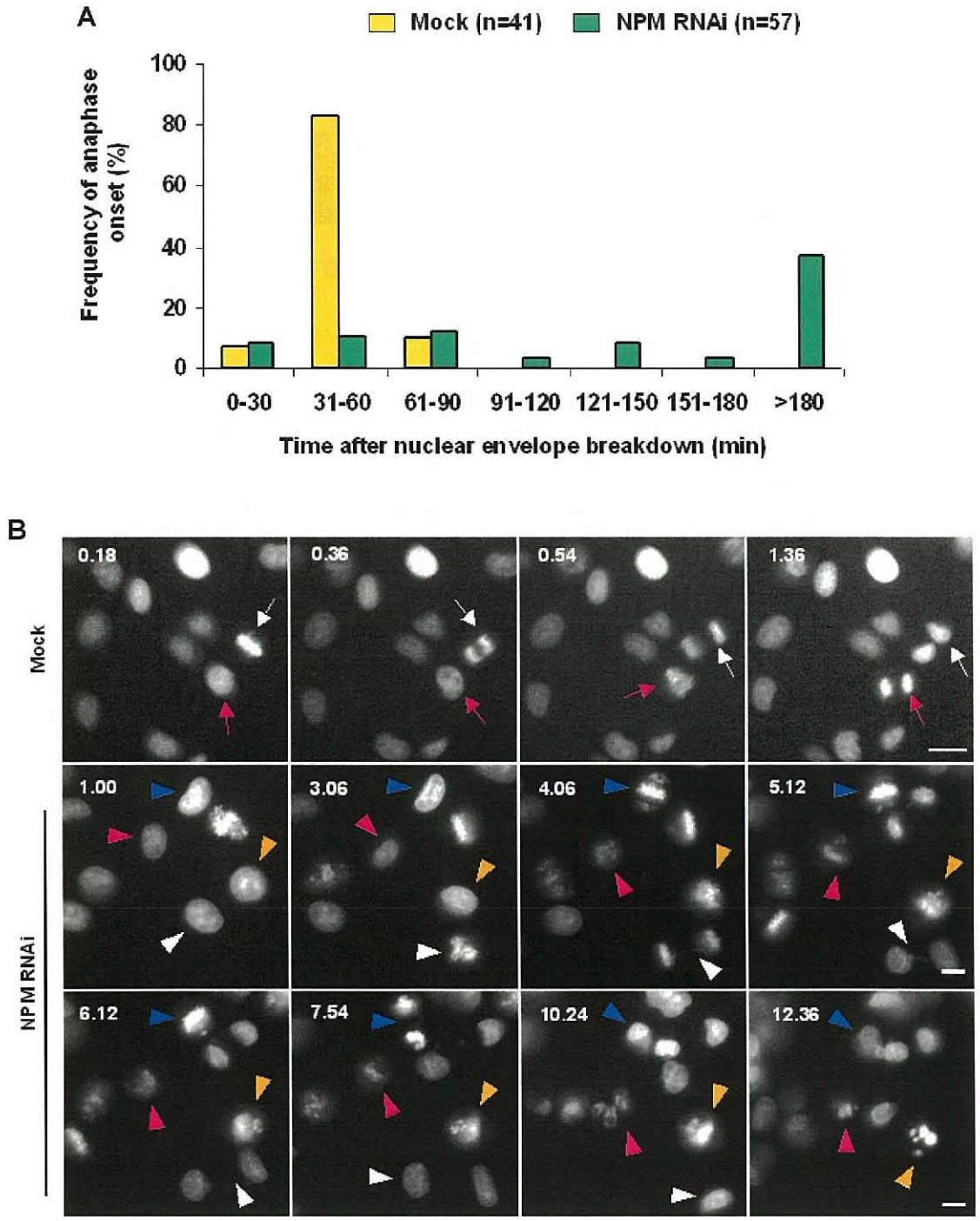

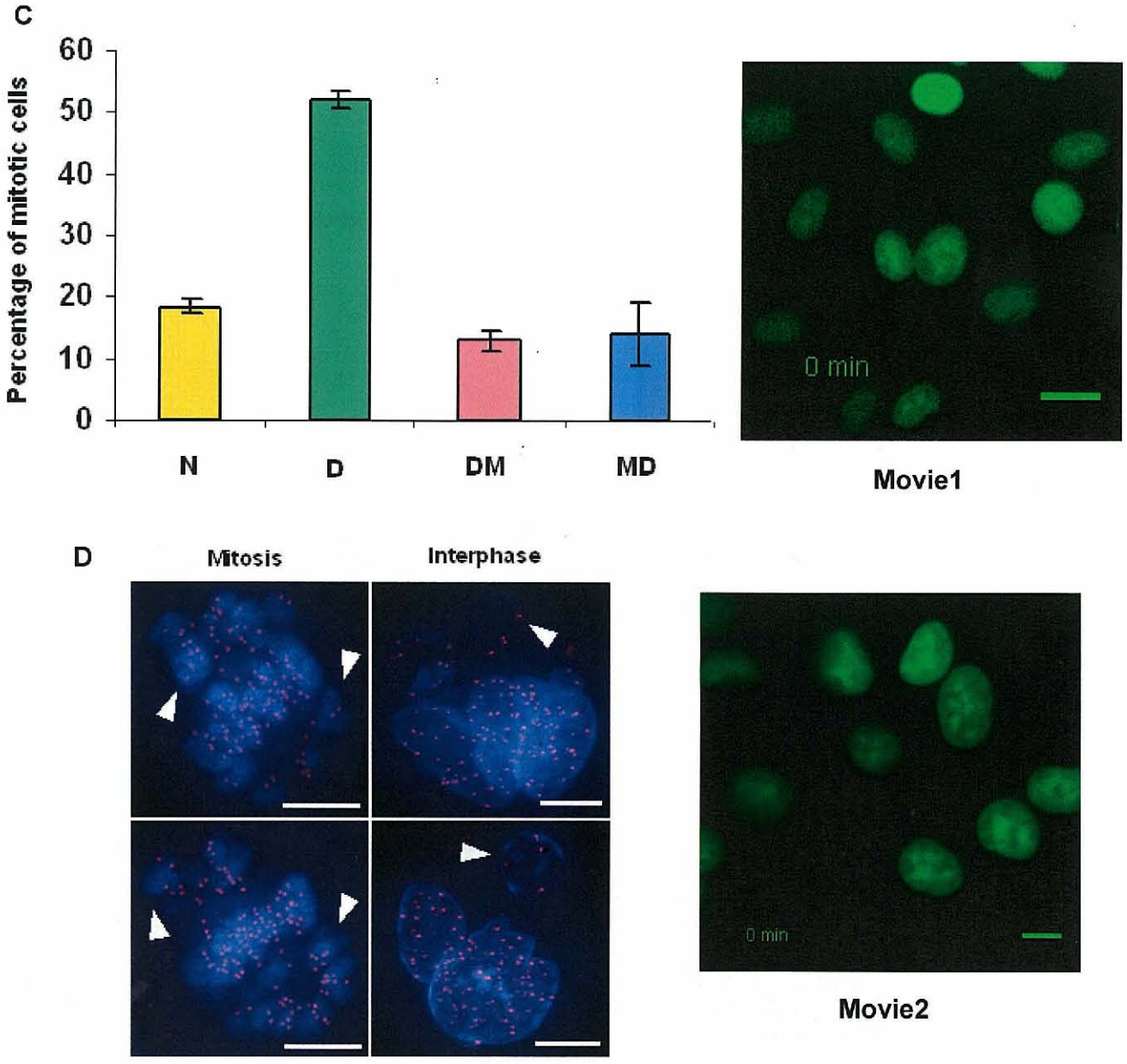

Fig. 3.3.5 Depletion of NPM causes mitotic delay in HeLa stably expressing GFP-H1.2 cells. (A) Time intervals between nuclear envelope breakdown and the anaphase onset of live cells were measured at 20 h post-transfection of mock and NPM siRNAs. (B) Live cell imaging of HeLa cells stably expressing GFP-H1.2. Cells were treated with

mock and NPM siRNAs for 20 h and then photographed at 6-min intervals for up to 18 h. Some of the mock treated cells are indicated by arrows, and some of the NPM-depleted cells by arrowheads. The cell indicated by the white arrowhead divided after normal mitosis. The cell indicated by the blue arrowhead divided after a prolonged mitosis. The cell indicated by yellow arrowhead entered mitosis, showed chromosome misalignment and finally died. The cell indicated by the red arrowhead contained uncongressed chromosomes, multiple micronuclei and eventually died of apoptosis. Scale bars = 20 μm. (C) Percentages of four different types of mitotic progression. Data are the mean ± s. d. of at least double cell counts (n= 20~50). (D) NPM depletion induces chromosome aberrations. Mitotic and interphasic NPM-depleted cells were fixed at 24 h and 48 h post-transfection, respectively and immunostained for CREST (red) and DNA (blue). Scale bars = 5 μm. Over 95% misaligned or uncongressed chromosomes contained CREST signals in NPM siRNA-treated cells (indicated by arrowheads). Strikingly, most (~95%) micronucleated NPM-depleted cells displayed CREST-positive micronuclei (indicated by arrowheads in interphasic cells). Micronuclei arising from aneugenic events (i.e., which induce aneuploidy, such as chromosome segregation errors) are typically centromere/kinetochore-positive.

Movie 1 Mitosis of mock treated cells. HeLa cells stably expressing GFP-histone H1.2 were transfected with mock siRNA for 21 h and then visualized and photographed at 6-min intervals for another 18 h. The video, which was generated by combining the first 200 images, shows normal progression of mitosis (1 s corresponds to 30 min of real time). Scale bars = 20 μm.

Movie 2 Mitotic catastrophe in NPM-depleted HeLa cells stably expressing GFP-histone H1.2 were transfected with mock siRNA for 21 h and then visualized and photographed at 6-min intervals for another 18 h. he video, which was generated by combining the first 126 images, shows various defects characteristic of mitotic catastrophe, including chromosome misalignement/missegregation, cell death during mitosis and apoptosis multinucleated cells (1 s corresponds to 30 min of real time). Scale bars = 20 μm.

3.4 Summary

The findings in the present study indicate that NPM is essential for cellular proliferation, supporting its oncogenic function. NPM-depleted cells were arrested in the G_1 state in a p53-dependent manner immediately after defective cell division and mitotic spindle damage. The loss of NPM leads to arrest of DNA synthesis. Cessation of DNA synthesis appears to be dependent on a post-mitotic checkpoint pathway involving p53. Abnormal nuclear shapes develope from defects in mitosis or cytokinesis (Yang et al., 2004). Consistent with this, NPM-depleted cells experience severe mitotic defects leading to severe morphological changes and micronuclei formation. The spindle assembly checkpoint machinery monitors defects during prometaphase, such as kinetochores unattached by microtubules or lack of tension generated on kinetochores by microtubules, to ensure the fidelity of chromosome segregation (Pinsky and Biggins, 2005). Here, in the absence of NPM, spindle checkpoint proteins are activated leading to problems in kinetochore-microtubule attachment or possibly lack of tension in the chromosome regions that fail to align properly to the equatorial planes during metaphase, and thus interrupts progression of mitosis (Cleaved et al., 2003). Moreover, both mitotic spindle and spindle-pole cannot be formed properly following NPM depletion, which together with defects in kintechore-microtubule attachment would delay mitotic progression.

In summary, these results indicate that in addition to cell proliferation, NPM is required for proper chromosome alignment on the equatorial planes during metaphase. NPM is also required for the formation of functional and stable spindles with intact centrosomes and for proper kinetochore-microtubule attachments and thus is essential

mitotic progression and cell proliferation. This study sheds new light on the functional significance of the nucleolar protein NPM in controlling cell cycle progression and/or carcinogenesis. Studies into the mechanism of how NPM regulates mitotic progression will be important for future cancer therapies considering NPM as a target.

Chapter 4

Functional analyses of a nucleolar protein, nucleophosmin in the formation of nucleolar and nuclear structure of HeLa cells

4.1 Introduction

The most active and dynamic nuclear domain, nucleolus plays a prominent role in the organization of various components of the nucleus and is considered as plurifunctional (Pederson, 1998). In addition to ribosome production, maturation, and assembly (Hadjiolov 1985), nucleolus plays important roles in the regulation of numerous cellular processes including cell-cycle regulation, apoptosis, telomerase production, RNA processing monitoring and response to cellular stress (Oslon and Dundr, 2005; Lo et a., 2006; Mayer and Grummt, 2005). NPM (nucleophosmin), a major nucleolar protein continuously shuttles between the nucleus and cytoplasm (Borer et al., 1989). NPM acts as an oncogene and is required for the development of the mouse embryo (Grisendi et al., 2005, 2006). Other reports have shown that NPM acts as a tumor suppressor (Colombo et al., 2005; Kurki et al., 2004). The role of NPM in oncogenesis thus still remains controversial. Moreover, its roles in the structure of nucleolus and nucleus are still unknown.

It is reasonable that depletion of nuclear or related proteins caused abnormal nuclear morphology (Kimura et al., 2003; Ulbert et al., 2006a). Interestingly, depletion of nucleolar protein fibrillarin also showed aberrant nuclear morphology and growth inhibition (Chapter 2). Thus the nucleolus has been reported to function in the cell survival and to contribute to the general nuclear function and architecture (Hernandez-Verdun et al., 2002).

NPM (also known as B23) is an abundantly and ubiquitously expressed multifunctional nucleolar phosphoprotein, which is involved in numerous cellular

processes including ribosome biogenesis, protein chaperoning and centrosome duplication (Okuwaki et al., 2001, 2002; Okuda et al., 2000); however, the role of NPM in the cell cycle still remains unknown. In this chapter, it was shown that NPM is dynamically localized throughout the cell cycle: during interphase at nucleolus and during mitosis at the peripheral region of chromosome, and NPM thus interacts with other major nucleolar proteins fibrillarin and nucleolin. Localization of NPM at the chromosome periphery during mitosis was confirmed by using a combination of RNA interference (RNAi) and 3-D microscopy. Depletion of NPM causes distortion of nucleolar structure as expected and leads to unexpected dramatic changes in nuclear morphology with multiple micronuclei formation. The defect in nuclear shape of NPM depleted cells, which is clearly observed by live cell imaging, is due to the distortion of cytoskeletal (α-tubulin and β-actin) structure resulting from the defects in centrosomal microtubule nucleation. These results indicate that NPM is an essential protein not only for the formation of normal nucleolar structure but also for the maintenance of regular nuclear shape in HeLa cells.

4.2 Materials and Methods

4.2.1 Cell culture, siRNA transfection and rescue assay

Please see in sections 3.2.1 and 3.2.2

4.2.2 Western blot analysis

The Western blot analysis was performed by standard methods. The mouse monoclonal anti-NPM and β-actin were used at 1:500 to detect nucleophosmin and β-actin, goat polyclonal anti-lamin A/C at 1:100 to detect nuclear membrane protein and mouse monoclonal anti-nucleolin and rabbit polyclonal anti-fibrillarin at 1:250 were used to detect other nucleolar proteins nucleolin and fibrillarin, respectively. Secondary antibodies conjugated to alkaline phosphatase (anti-mouse from Leinco Technologies; anti-rabbit and goat from Vector Laboratories) were used for immunoreactions, which were finally detected by NBT (Ntiro Blue Tetrazolium/BCIP (5-bromo-4-chloroindol-3-yl phosphate) solution (Roche) in alkaline phosphatase buffer (100 mM Tris-HCl pH 9.5, 100 mM NaCl, and 1 mM $MgCl_2$).

4.2.3 Indirect immunofluorescence microscopy

HeLa cells were grown on a glass cover slips and fixed with 4% (w/v) para-formaldehyde at 37°C or methanol at –20°C were incubated with primary antibodies. The antibodies used in the present study were as follows: goat polyclonals anti-nucleophosmin at 1:50 (Santa Cruz), goat polyclonal anti-lamin A/C at 1:50 (Santa Cruz); mouse monoclonals anti-α-tubulin (Calbiochem), anti β-actin (Sigma), anti-fibrillarin (Cytoskeleton), anti-Ki-

67 (Dako) and anti-nucleolin (Abcam) at 1:100 and anti-nucleophosmin (Santa Cruz) at 1:1000; rabbit polyclonals anti-fibrillarin (Abcam) at 1:100. Immunofluorescence staining was performed by standard methods. DNA was stained with Hoechst 33342 (Sigma). Acquisition and processing of images were explained in section 3.2.3

4.2.4 Live cell imaging

Please see in section 3.2.4

4.3 Results and discussion

4.3.1 NPM is a highly dynamic protein and interacts with fibrillarin and nucleolin in the cell cycle

A previous study by proteomic analyses with highly purified human metaphase chromosome showed that NPM is located at the chromosome periphery (Uchiyama et al., 2005). In the present study, the localization of NPM throughout the cell cycle of fixed HeLa cells was examined by double immunostaining. NPM is dynamically localized from the interphase to telophase (Fig. 4.3.1A). In interphase, NPM is mainly located in the dense fibrillar components and granular components of nucleoli and also in the necleoplasm as scattered foci. In prophase, NPM is dispersed due to nucleolar disintegration. In prometaphase, NPM moves towards the chromosome periphery where it remains until anaphase. The localization of NPM at the chromosome periphery was confirmed using an RNAi method. Chromosome-spread and immunostaining experiments showed that NPM signals were robust at the chromosome periphery of mock -treated cells, whereas those were absent in the case of NPM-depleted cells (Fig. 4.3.1B). NPM is also distributed throughout the cytoplasm during mitosis. In telophase, NPM is concentrated into pre-nucleolar bodies (PNBs) to be involved in the eventual establishment of daughter nucleoli before NE (nuclear envelope) formation. Thus NPM actively shuttles from the nucleolus to perichromosomal region and cytoplasm only after NE breakdown at the end of prophase and returns back to the PNBs and nucleoplasm at

the end of telophase. These data indicate that NPM is a highly dynamic protein throughout the cell cycle.

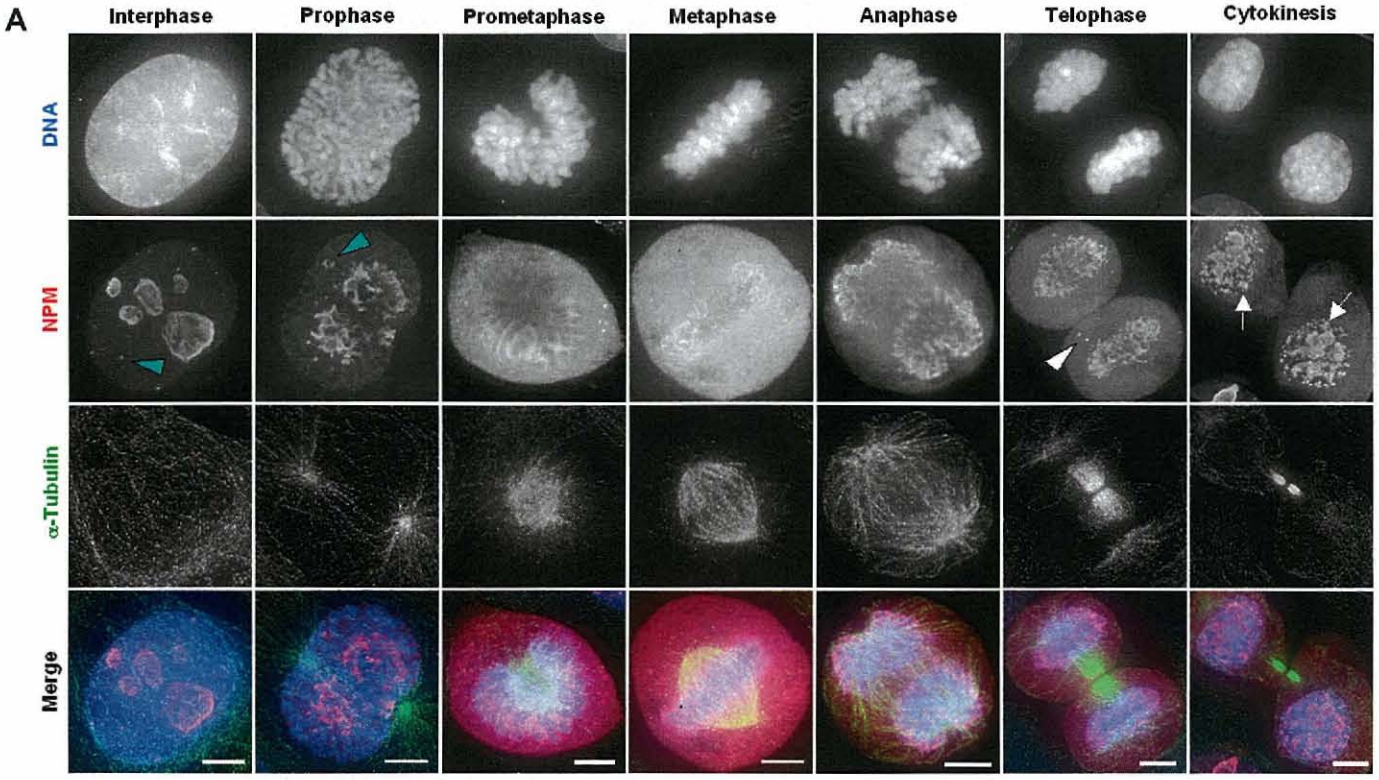

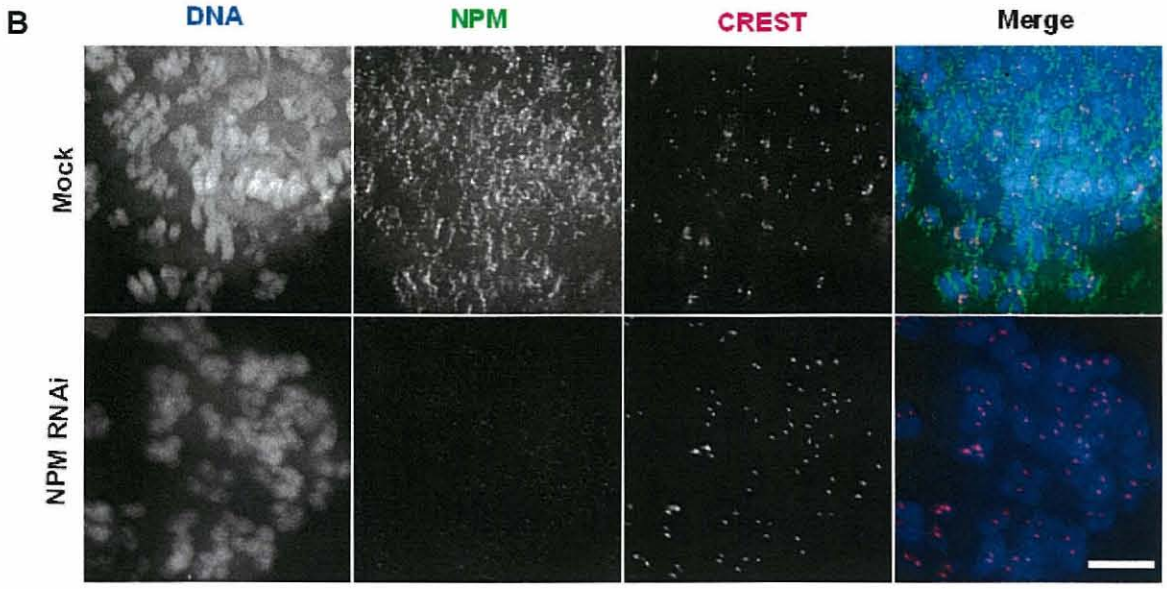

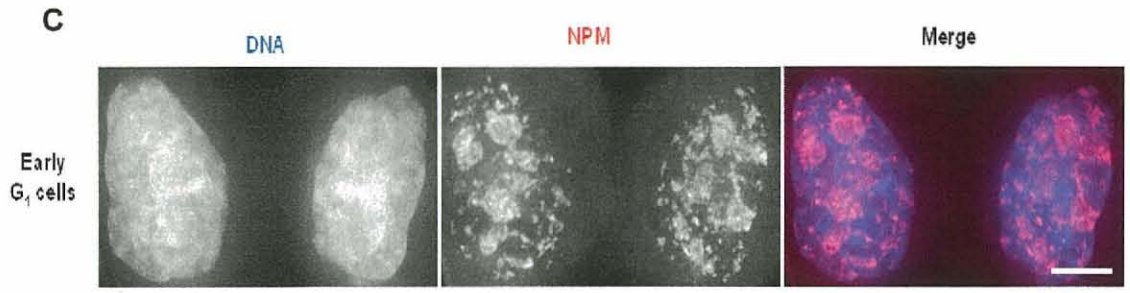

Fig. 4.3.1 NPM is a highly dynamic protein and interacts with fibrillarin and nucleolin in the cell cycle. (A) HeLa cells fixed with para-formaldehyde were stained for NPM (red) and α-tubulin (green). DNA (blue) was counter stained with Hoechst 33342. The green arrowheads indicate the foci of NPM at nucleoplasm, the white arrowhead indicate the nucleolus-derived focus in the cyctoplasm and white arrows for the pre-nucleolar bodies in the newly forming nucleus. Scale bars = 5 μm. (B) Chromosome spread and immunostaining for NPM in mock and NPM siRNAs-treated cells. Scale bar = 5 μm. (C) Immunostaining of early G_1 cells for NPM (red) and DNA (blue). Scale bar = 5 μm.

In early G_1-phase cells, NPM is found to localize at the PNBs and nucleoplasm, and inner nuclear membrane as scattered dots (Fig. 4.3.1C). Chapter 2 and previous study showed that fibrillarin and nucleolin were also localized at the chromosomal periphery and in the PNBs (Ma et al., 2007). Nucleolin interacts with fibrillarin (Ma et al., 2007) and NPM directly interacts with nucleolin (Liu and Yung, 1999). Taken together the results indicate that fibrillarin, nucleolin and NPM are co-localized at the chromosome periphery and PNBs, where they interact each other during cell cycle.

4.3.2 NPM is required for the formation of nucleolar structure in HeLa cells

To understand the functional importance of NPM in nucleolus, endogenous NPM was depleted by RNAi in HeLa cells. Western blot analysis and immunostaining of both mock and NPM siRNAs-treated cells showed significant depletion of NPM at 48 h post-transfection, whereas the expression levels of fibrillarin, nucleolin, and α-tubulin were unchaged (Fig. 4.3.2-1A-C). DIC (Differential interference contrast) imaging showed that mock-treated cells presented at best three large, spherical intranuclear masses corresponding to nucleoli (Fig. 4.3.2-1D). In contrast, the nucleolar masses appeared distorted and fragmented in several small spots in NPM-depleted cells (Fig. 4.3.2-1D). Moreover, immunofluorescence showed that nucleolar marker proteins such as fibrillarin, nucleolin and Ki-67 were associated with nucleoli in mock-treated cells (Fig. 4.3.2-1E-G), whereas they were associated with remnants of the nucleolar compartment in NPM-depleted cells, exhibiting the disorganized pattern of the nucleolar structure with a relatively reduced size (Fig. 4.3.2-1E-G). Western blot analysis showed that NPM depletion did not significantly affect the expression level of nucleolin and fibrillarin as compared with mock-treated cells (Fig. 4.3.2-1A). Moreover, single depletion of nucleolin or fibrillarin did not show any effect on the localization of each other and of NPM (Fig. 4.3.2-2A,B). NPM depletion caused distortion of the nucleolar structure in other cell lines such as HEK (Human embryonic kidney)-293T and NHDF (normal human dermal fibroblast) (Fig. 4.3.2-3A,B). These results indicate that endogenous NPM generally plays a crucial role in the maintenance of the structural integrity of the

nucleolus with an exception in the case of U2OS osteosarcoma cells (Korgaonkar et al., 2005).

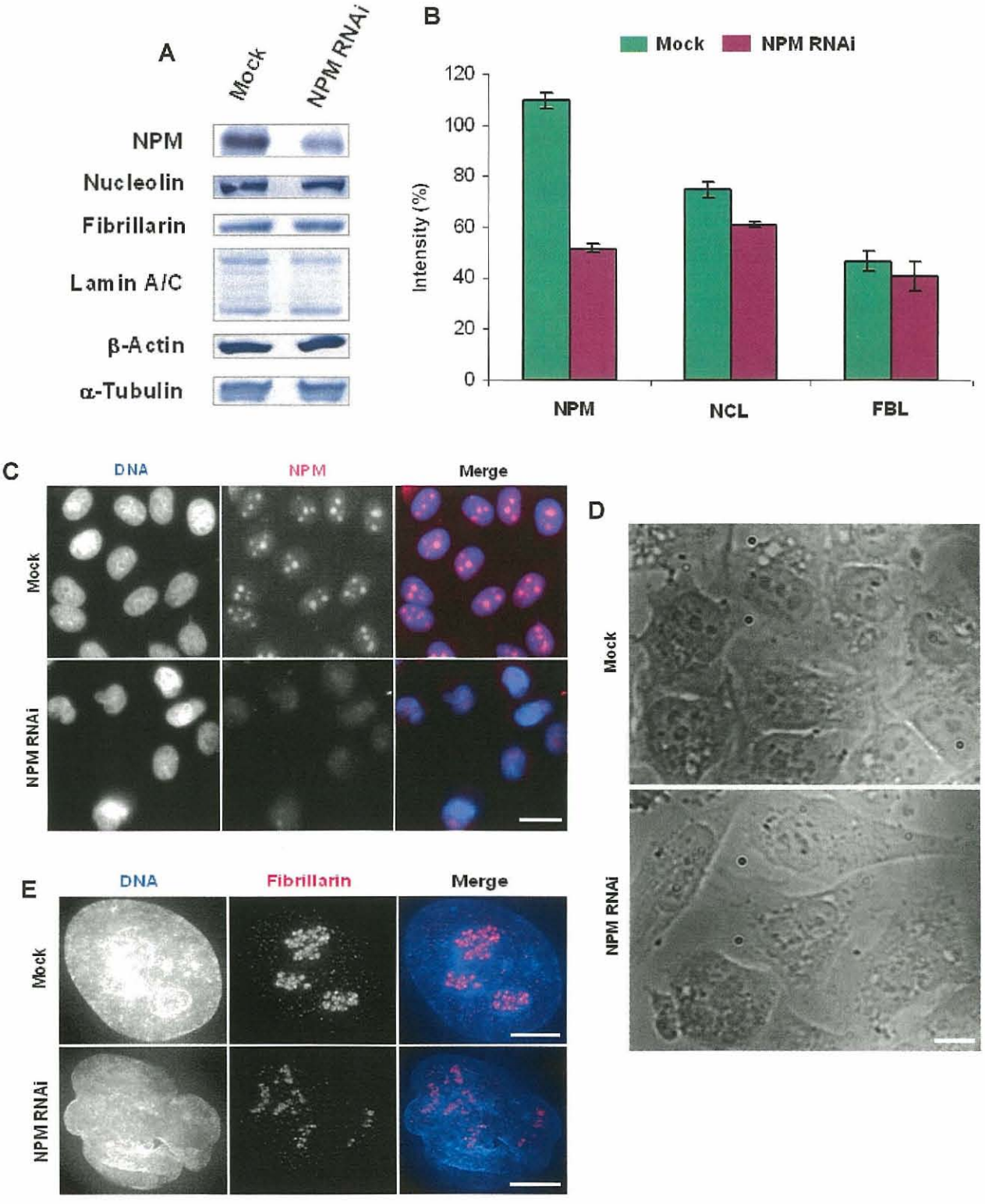

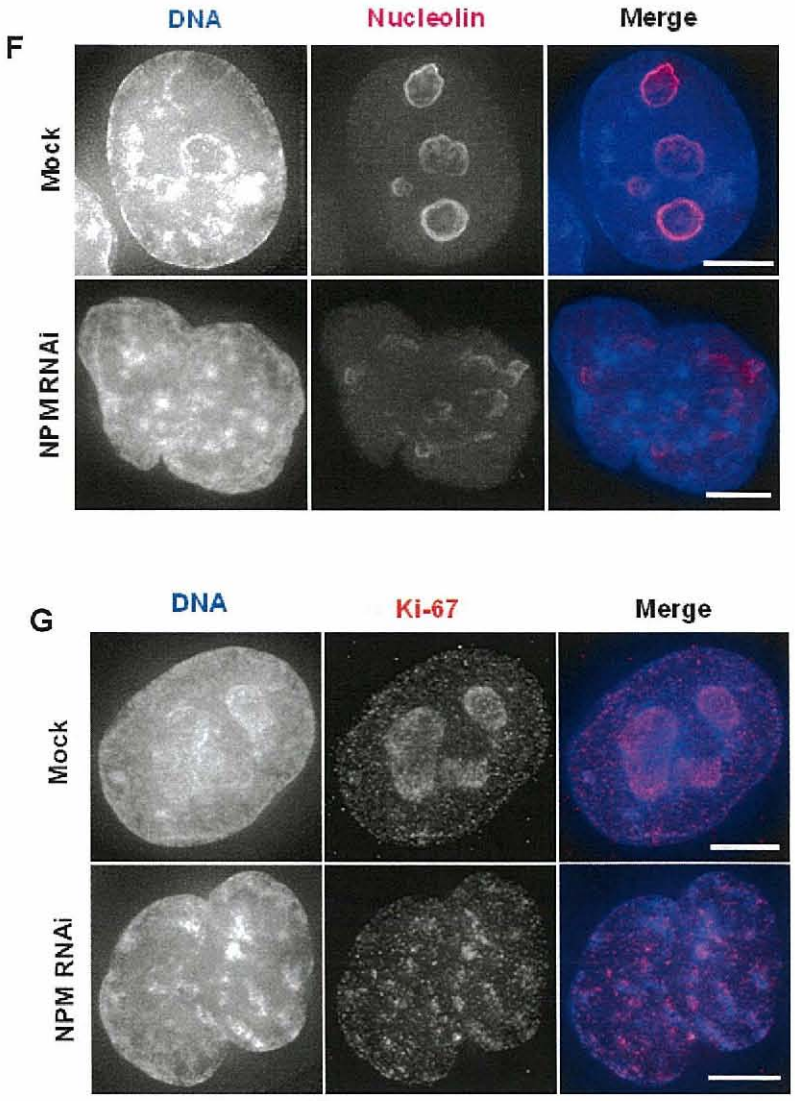

Fig. 4.3.2-1 Depletion of NPM leads to disorganized nucleolar structure in HeLa cells. (A) Western blot analysis at 48 h post-transfection of mock and NPM RNAi cells. NPM expression level was reduced to ~80% by RNAi. Other nucleolar proteins such as fibrillarin and nucleolin; a nuclear envelop protein lamin A/C and a cytoskeleton protein β-actin were also immunoblotted. Western blot analysis of α-tubulin served as loading control. (B) Qunatification of NPM, nucleolin and fibrillarin levels in mock and NPM

siRNAs-treated cells in Western blots. Data are the mean ± s. d. of three independent blots. (C) Immunostaining for NPM (red) and DNA (blue) in mock and NPM siRNA-treated cells. Scale bar = 10 μm. (D) Phase-contrast images of fixed cells showing the pattern of nucleolar organization in mock treated cells and the distortion of this pattern in NPM-depleted cells. Scale bar = 10 μm. (E-G) Immunostaining for nucleolar proteins in mock and NPM siRNA-treated cells, (E) fibrillarin (red), (F) nucleolin (red), and (G) Ki-67 (red); DNA is shown in blue. Scale bars = 5 μm.

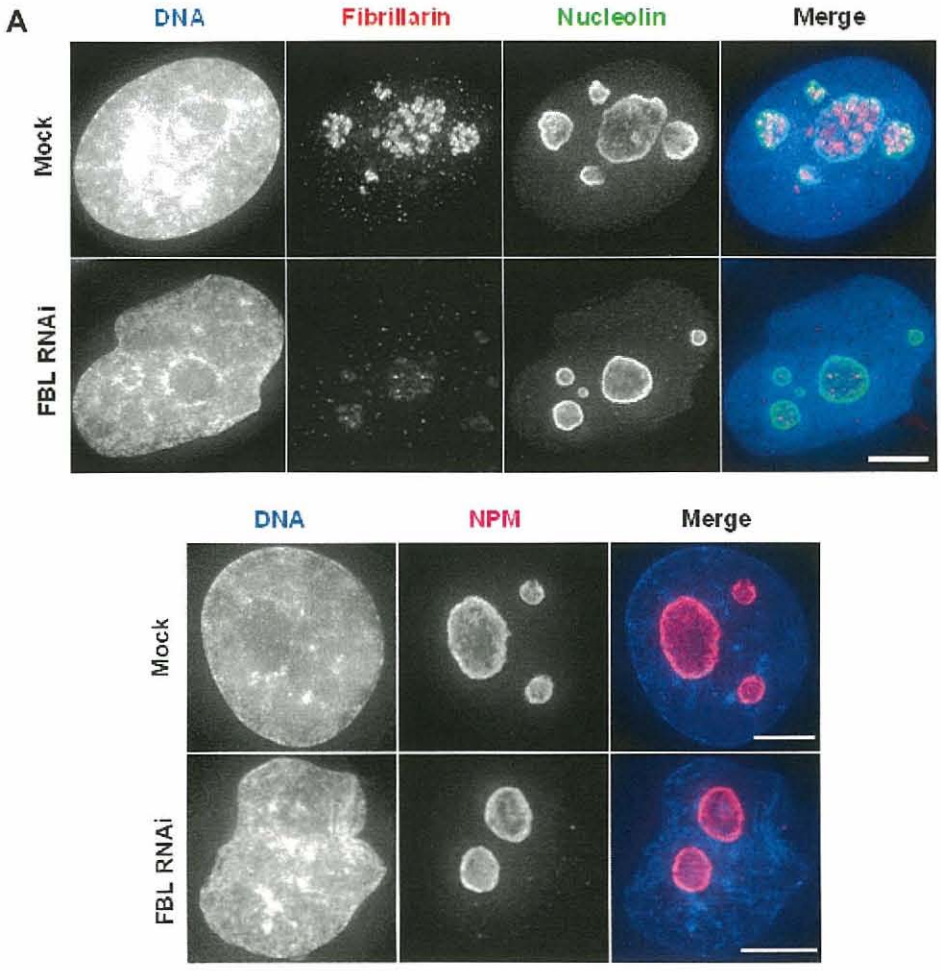

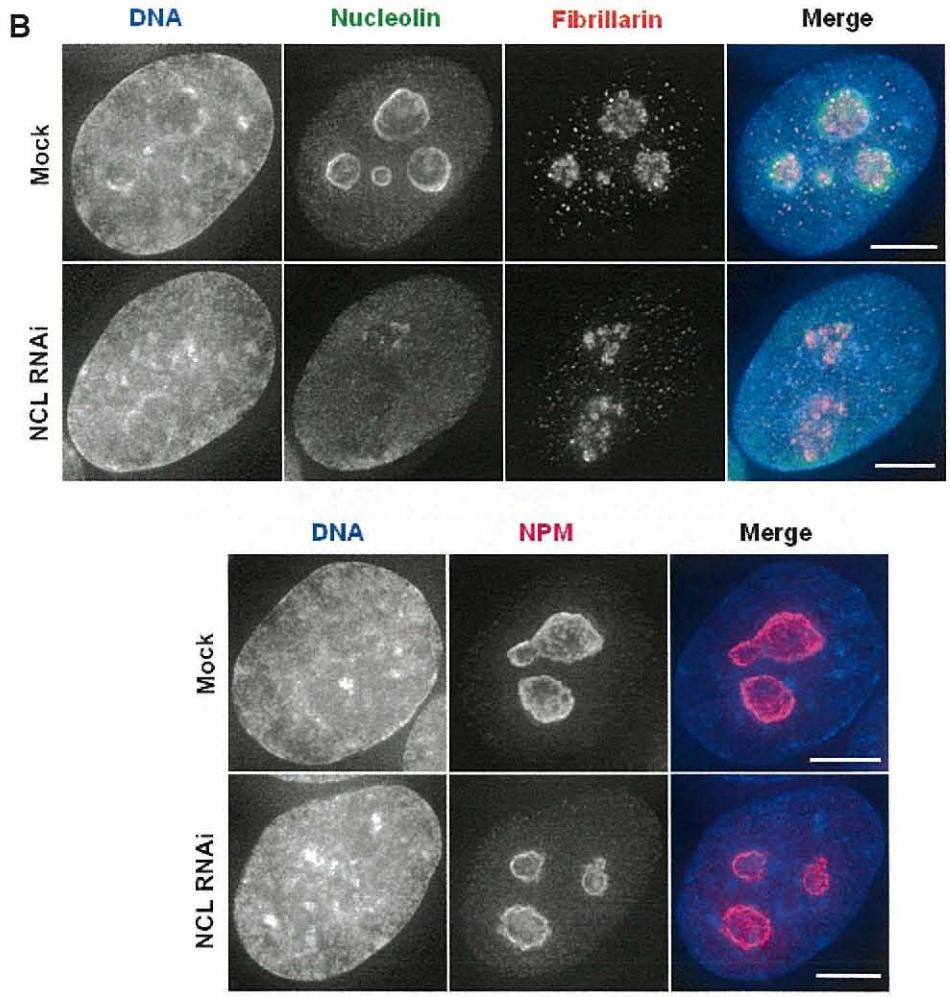

Fig. 4.3.2-2 Depletion of nucleolin or fibrillarin does not affect the localization of nucleolar proteins. (A) Mock and nucleolin siRNAs-treated interphasic cells were stained for nucleolin (green) and fibrillarin (red) (left-hand panels), and NPM (red) (right-hand panels). DNA was counter-stained with Hoechst 33342 (blue). Scale bars = 5 μm. (B) Mock and fibrillarin siRNAs-treated interphasic cells were stained for nucleolin (green) and fibrillarin (red) (left-hand panels), and NPM (red) (right-hand panels). DNA was counter-stained with Hoechst 33342 (blue). Scale bars = 5 μm.

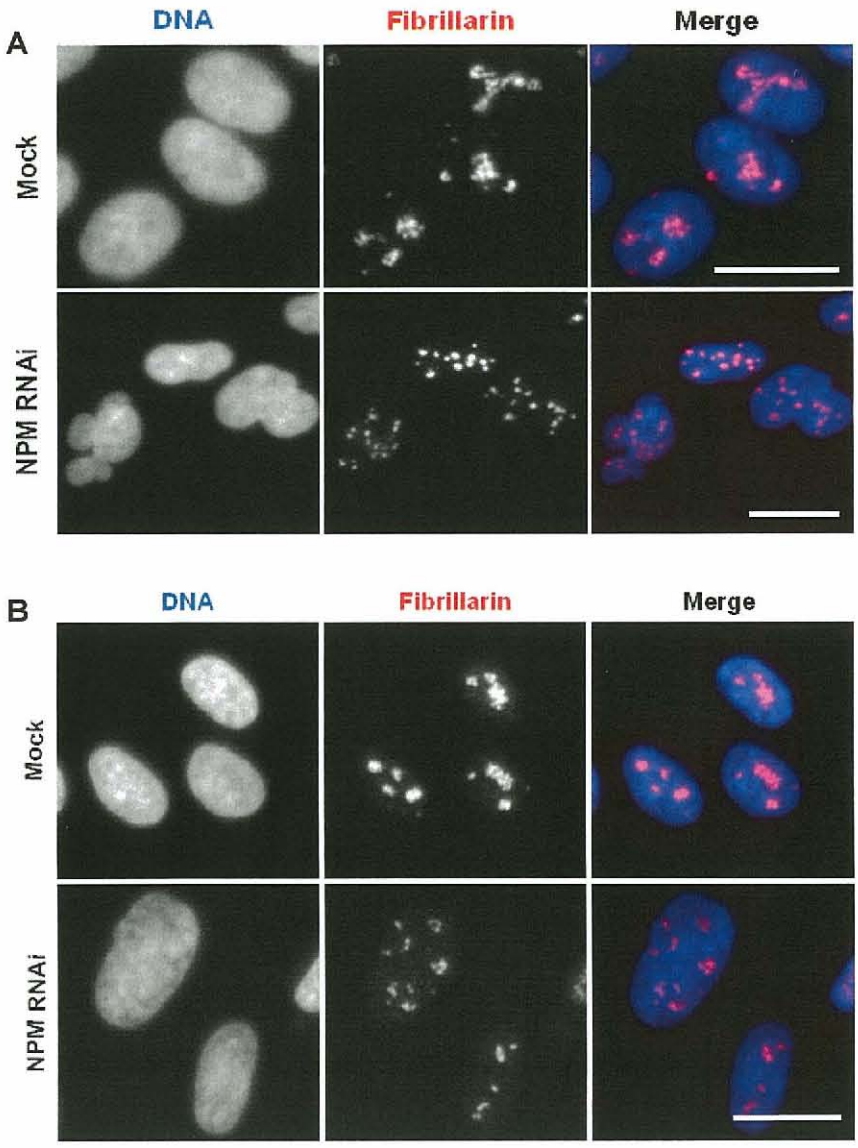

Fig. 4.3.2-3 Depletion of NPM causes distortion of nucleolar structure in HEK293T and NHDF cell lines. Both mock and NPM siRNA-treated cells were stained with fibrillarin (red) and DNA (blue) for HEK293T (A) and NHDF cells (B). Scale bar = 10 μm.

4.3.3 NPM is required for the maintenance of normal nuclear shape

NPM-depleted cells showed aberrant nuclear morphology with micronuclei formation at 48 h post-transfection (Fig. 4.3.3A,B). Approx. 50% of NPM-depleted cells had defective nuclear morphologies of various types such as irregular, ruffled, lobulated morphologies and more than 12% of cells formed multiple micronuclei (Fig. 4.3.3C), whereas more than 98% of mock-treated cells had the regular nuclear structure with rare micronuclei formation. More than a 25- and 10-fold higher number of NPM-depleted cells had the aberrant nuclear morphology and multiple micronuclei, respectively, compared with mock-treated cells. Obviously, the effect of NPM depletion at 48 h post-transfection on the nuclear structure is ~2-fold higher than that of fibrillarin depletion (approx. 35% of cells with nuclear defects at 72 h post-transfection; Chapter 2). These results indicate that NPM plays a more effective role on the nuclear morphology than fibrillarin. To rule out potential off-target effects (Echeverri et al., 2006), the rescue assay was performed, which showed that these morphological changes were significantly recovered by introducing RNAi resistant NPMr plasmid (Fig. 4.3.3C). An abnormal nuclear shape would develop from defects in mitosis or cytokinesis (Yang et al., 2004). Moreover, down-regulation of NPM delays mitotic entry (Jiang and Yung, 1999). Then the effect of NPM depletion on mitotic was checked. Depletion of NPM caused accumulation of mitotic cells when HeLa cells were synchronously released from cell-cycle arrest at the G_1-S boundary (Fig. 4.3.3D). Moreover, 24 h post-transfection of NPM siRNA caused accumulation of aberrant mitotic chromosomes in asynchronous cells, which were recovered by the rescue experiment (showed in Chapter 3). Further

transfection of NPM siRNA until 48 h resulted in micronuclei formation at cytokinesis (Fig. 4.3.3E). These results indicate that the defects in mitosis and/or cytokinesis in the absence of NPM would lead to the formation of abnormal nuclear shape and micronuclei.

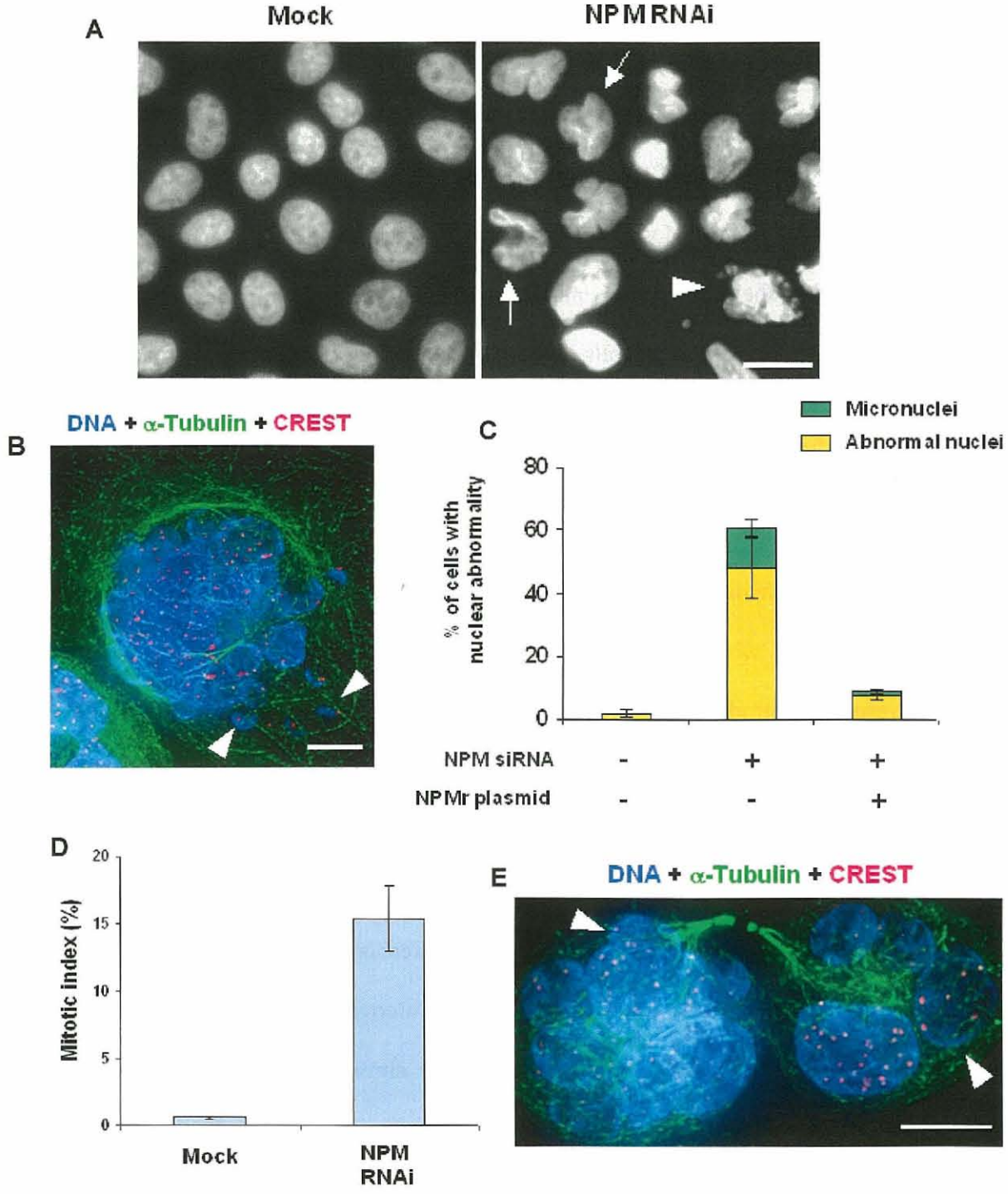

Fig. 4.3.3 Depletion of NPM causes abnormal nuclear morphology and mitotic defects in HeLa cells. (A) Representative nuclear morphologies in mock (cells treated with control siRNA) and NPM-depleted cells. Arrows indicate cells with abnormal nuclear structure and the white arrowhead indicates micronucleated cell. Scale bar = 10 μm. (B) Cell containing micronuclei was stained with α-tubulin (green), CREST (red) and DNA (blue). Scale bar = 5 μm. The arrowheads indicate the micronuclei. (C) Percentages of cells showing irregular nuclear morphology and micronuclei formation and recovering the defects in the presence of NPM RNAi resistant plasmid (NPMr). For both mock and NPM RNAi experiments, at least 400 cells were counted. Values are the means ± s. d. of at least triplicate cell counts (P <0.05). (D) HeLa cells were synchronized at the G1-S boundary by double-hymidine arrest, released into fresh media and fixed at 12 h. The mitotic index was counted for both mock and NPM RNAi cells by immunostaining with α-tubulin and DNA. Values are the means ± s. d. of at least triplicate cell counts (n=800-1000). (E) An NPM-depleted cell forming micronuclei at cytokinesis at 48 h post-transfection was stained for α-tubulin (green), CREST (red) and DNA (blue). Scale bar = 5 μm. The arrowheads indicate the micronuclei.

4.3.4 Defective nuclear structure in NPM-depleted cells is due to defects in microtubule polymerization and cytoskeletal structure in HeLa cells.

It is likely that irregular nuclear morphology may result from a defect in the post-mitotic assembly of the NE (Foisner and Gerace, 1993; Ulbert et al., 2006b); however, Western blot analysis and immunofluorescenc showed that the localization pattern and

expression level of NE protein, lamin A/C were intact in NPM-depleted cells as well as in the mock-treated cells (Figs. 4.3.2-1A and 4.3.4A). These results indicate that the nuclear defects in NPM-depleted cells were independent from the post-mitotic nuclear reassembly. Alternatively, nuclear abnormalities were reported to form independently from mitosis (Chapter 2; Ulbert et al., 2006a). Live cell imaging of HeLa GFP-H1.2 cells (Higashi et al., 2007) clearly showed that approx. 50% of cells dramatically changed their nuclear morphology (Fig. 4.3.4B and Movie 3, 4). Cells without entering mitosis showed defects in the nuclear shape. These observations indicate that nuclear abnormality also occurs independently from mitosis. Thus nuclear shape defects in NPM-depleted cells are dependent and or independent of mitosis.

Since nuclear morphology is strongly influenced by the cytoskeletal structure (Olin and Olins, 2004) the status of α-tubulin and β-actin was examined by immunosfluorescence and Western blot analysis. More than 66% of NPM-depleted cells had defects in the cytoskeletal structure (α-tubulin and β-actin elements became shrunken; Fig. 4.3.4C, D); however, the expression levels of both cytoskeleton elements remained unaffected by NPM depletion compared with mock treatment (Fig. 4.3.2-1A). The defects in cytoskeletal structure were markedly recovered by the rescue experiments (Fig. 4.3.4D). Although treatment with the microtubule-modifying agent nocodazole did not affect nuclear morphology in a way similar to NPM depletion (data not shown), a marked defect in centrosomal microtubule re-polymerization was observed after recovery from cold treatment in NPM-depleted cells (Fig. 4.3.4E). Taken together, these observations indicate that aberrant nuclear morphology induced by NPM depletion is due to defects in microtubule polymerization and thus in cytoskeletal structure.

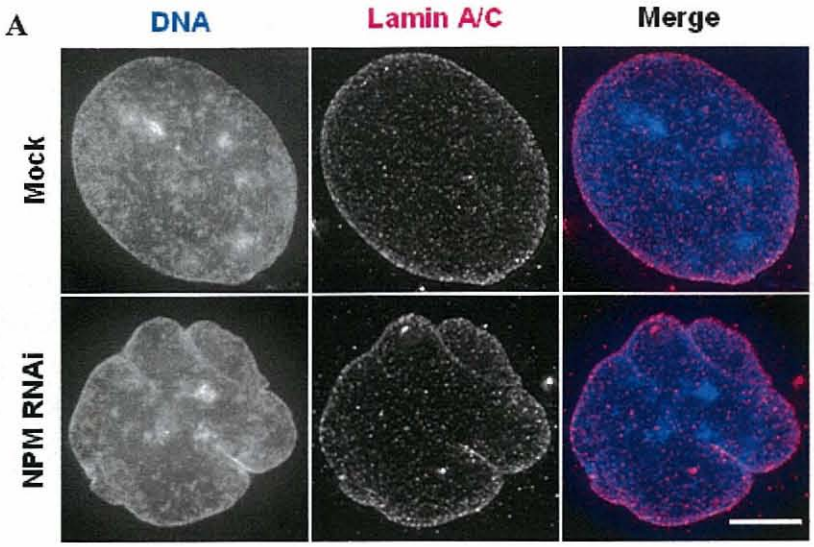

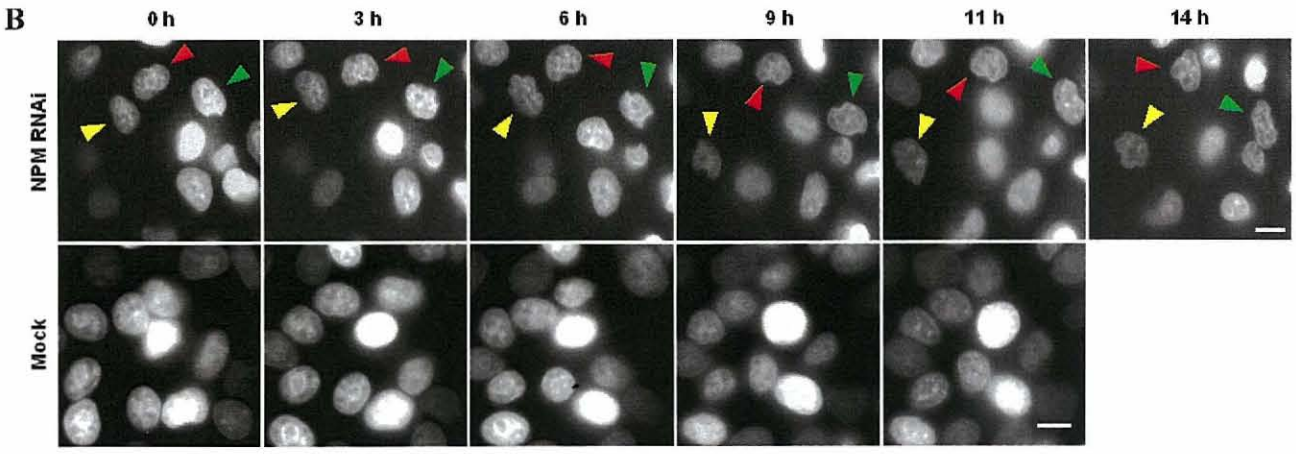

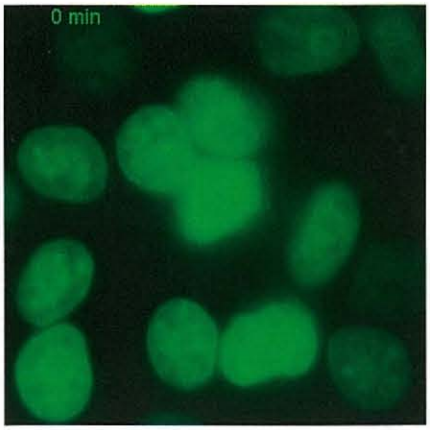

Movie 3

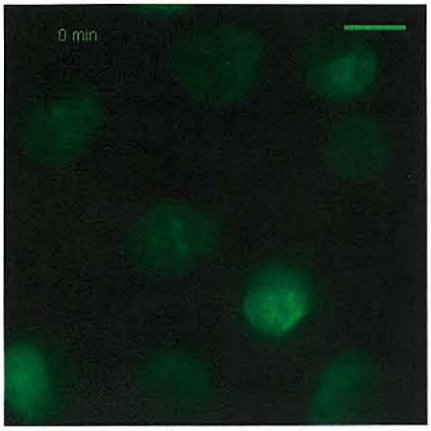

Movie 4

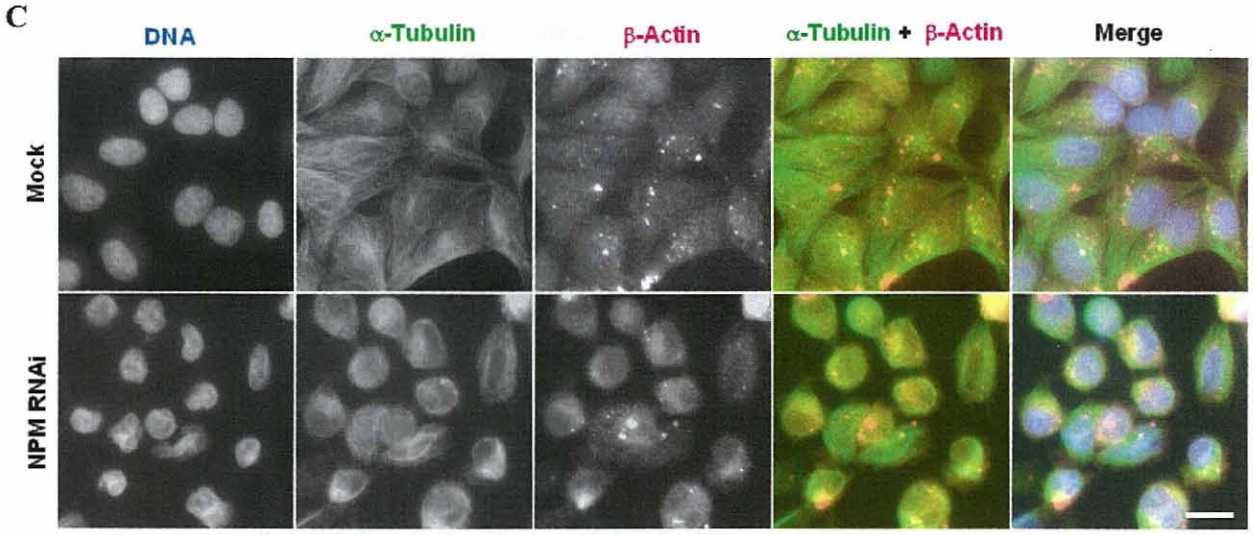
C
DNA
α-Tubulin
β-Actin
α-Tubulin + β-Actin
Merge
Mock
NPM RNAi

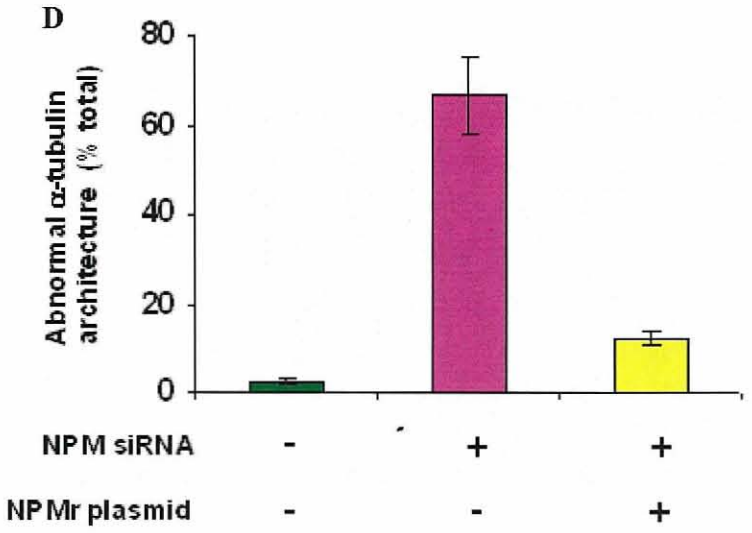
D
Abnormal α-tubulin architecture (% total)
80
60
40
20
0
NPM siRNA - + +
NPMr plasmid - - +

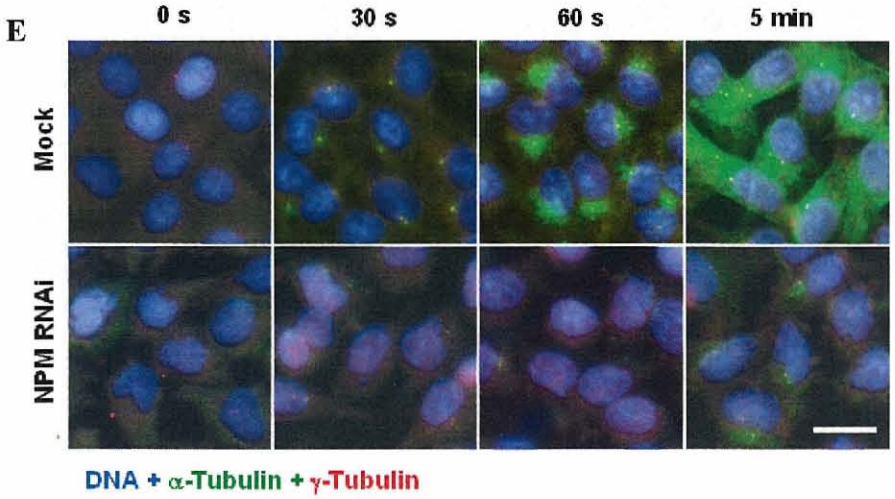
E
0 s
30 s
60 s
5 min
Mock
NPM RNAi
DNA + α-Tubulin + γ-Tubulin

Fig. 4.3.4 The defective nuclear structure in NPM-depleted cells is due to defects in microtubule polymerization and cytoskeletal structure in HeLa cells. (A) Mock and NPM siRNA-treated cells were immunostained for lamin A/C (red) and DNA (blue). Scale bar= 5 μm. (**B**) Live cell imaging of HeLa cells stably expressing GFP-histone H1.2. Cells were treated with NPM (top panels) and mock (lower panels) siRNAs for 21 h and then photographed at 6-min intervals for additional 10-14 h. Representative photographs for both mock and NPM-depleted cells were shown. Cells indicated by yellow, red and white arrowheads in the top panels dramatically change their nuclear shape with time. Scale bars = 10 μm. (**C**) Mock and NPM siRNA-treated cells were stained for α-tubulin (green), β-actin (red), and DNA (blue). Scale bar = 10 μm. (**D**) Percentages of cells showing shrinked cytoskeletal structure. The defect in tubulin skeleton is recovered in the rescue assay. Values are the mean ± s. d. of at least triplicate cell counts (n= at least 300) ($P < 0.05$). (**E**) Re-plymerization of mock (left-hand panels) and NPM siRNAs-treated cells (right-hand panels). Cells were fixed and stained for γ-tubulin (red), microtubules (green), and DNA (blue) at 0, 30, 60 s and 5 min after recovery from cold treatment. Scale bar = 10 μm.

Movie 3 Normal nuclear shape of mock treated cells. HeLa cells stably expressing GFP-histone H1.2 were transfected with mock siRNA for 21 h and then visualized and photographed at 6-min intervals for another 18 h. The video, which was generated by combining the first 100 images, shows the normal nuclear shape (1 s corresponds to 30 min of real time). Scale bar = 20 μm.

Movie 4 NPM-depleted cells with abnormal nuclear shape and two cells undergo apoptosis. HeLa cells stably expressing GFP-histone H1.2 were transfected with mock siRNA for 21 h and then visualized and photographed at 6-min intervals for another 18 h. The video, which was generated by combining the first 139 images, shows dramatic changes in the nuclear shape (1 s corresponds to 30 min of real time).

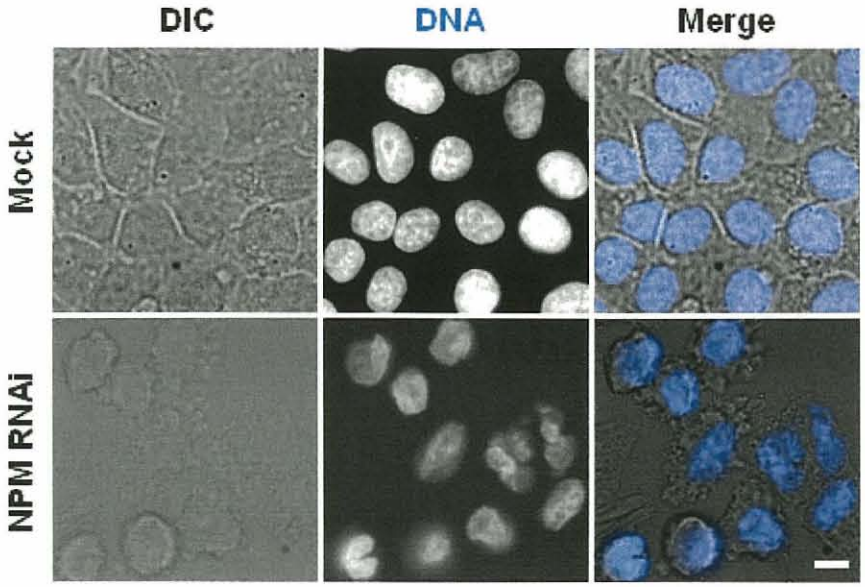

Fig. 4.4 Image of cells under phase contrast microscopy. The whole cellular structure is distorted by NPM depletion. Scale bar = 10 μm.

4.4 Summary

In summary, in the present study, the functional importance of NPM in the structural integrity of nucleolus and nucleus in HeLa cells was explored. It was observed that depletion of NPM, rather than nucleolin or fibrillarin, results in disorganized localization of the major nucleolar proteins. Although NPM, nucleolin, and fibrillarin interact with each other during the cell cycle, among them only NPM would play a crucial role in maintaining the nucleolar integrity by keeping nucleolar proteins compact at the nucleoli. Moreover, it was observed that cells have aberrant nuclear structure in the absence of NPM. Although the exact reason why fibrillarin depletion causes nuclear abnormal shape is still unknown, NPM depletion leads to defective centrosomal microtubule nucleation and cytoskeletal structure, which may result in aberrant nuclear shape. NPM thus would maintain the normal nuclear structure by maintaining the cytoskeletal structure through tubulin/actin fibers. NPM can bind nucleic acids (Wang et al., 1994) and appears to be involved in different aspects of DNA metabolism and chromatin regulation (Frehlick et al., 2007). Although the exact mechanism how NPM maintains nuclear structure is unknown, it can be speculated that the interactions of NPM with either chromatin/DNA or with the inner membrane in early G_1-phase are involved in providing the structural basis for a normal shaped nucleus. Moreover, DIC imaging showed that cells with distorted nuclear shape also had distorted cellular structure (Fig. 4.4) suggesting that cells with aberrant nuclear morphology eventually underwent apoptosis. Studies into the mechanism of how the changes in nuclear and cytoskeleton

structures are connected with apoptosis will be important to understand the carsinogenic role of NPM.

Chapter 5

General conclusion

In this study, the dynamic localization and novel functions of the nucleolar proteins, fibrillarin and nucleophosmin were immensely studied by using RNA interference (RNAi) method, fluorescence microscopy, 3-D microscopy and live imaging.

Fibrillarin (FBL) is dynamically localized throughout the cell cycle in HeLa cells. In the mitosis, FBL is localized at the chromosome periphery and at end of anaphase it is concentrated as dot like structure in pre-nucleolar bodies, which eventually establish the newly formed nucleolus in daughter cells. In interphasic cells, FBL is mainly localized at nucleolus and Cajal bodies, and in early G_1 cells it is localized in nucloplasm as dot like structures, which represent condensed chromosomes.

Previously FBL was known to play a role mainly in ribosome biogenesis; however, the results of the present study conclude that FBL has multifunctional activities. FBL maintains the normal nuclear structure of cells; however, the exact mechanism how FBL maintains the nuclear structure is still unknown. Depletion of FBL causes reduction of cellular proliferation, which is probably due to cessation of cell cycle, rather than, reduction of DNA replication. FBL thus plays a role in the cellular growth. This finding is consistent with the previous report that FBL is essential for the early development of the mouse embryo (Newton et al., 2003). Although FBL is one of the major nucleolar proteins, it does not play role in the structural integrity of the nucleolus. In conclusion, FBL plays important roles in maintaining the normal nuclear structure to sustain cellular

growth. These novel functions suggest that FBL is thus acts as multifunctional protein during cell cycle. Studies in the mechanism of how the changes in nuclear structure are connected to cell proliferation will be important to understand the tumorigenic roles of FBL.

Nucleophosmin (NPM), a nucleolar protein, is also a highly dynamic in its localization throughout the cell cycle. In interphasic cells, NPM is mainly localized in the nucleolus. During mitosis, NPM is localized at the perichromosomal regions as well as in the nucleoplasm. At the end of mitosis NPM concentrated at PNBs, which eventually establish newly formed nucleoli.

The loss of NPM leads to proliferative inhibition due to cell division defects followed by an arrest of DNA synthesis due to activation of p53-dependent checkpoint response. Loss of NPM leads to increased levels of p53, which results in the up-regulation of downstream factor p21 and thus induces cell growth arrest and apoptosis (Levine, 1997). NPM is required for the cellular proliferation and survival of HeLa cells and these results thus support the oncogenic function of NPM (Grisendi et al., 2005, 2006). Moreover, depletion of NPM leads to mitotic arrest with defects in chromosome congression. Loss of NPM also leads to defects in the formation of proper mitotic spindle and centrosomes keeping consistency with the phenotypes observed in NPM knockout MEFs (mouse embryonic fibroblasts) (Grisendi et al., 2005). Moreover, depletion of NPM causes defects in kinetochore-microtubule attachment in mitotic cells. NPM-depleted cells thus have severe mitotic defects, and show delayed mitotic process. The disorganiozed and multiple mitotic spindles, and fragmented centrosome and/or defective kinetochore-microtubule attachment would result in delayed mitotic process. The results

of the present study thus conclude that NPM is required for chromosome congression, mitotic spindle formation, and proper kinetochore-microtubule attachment to progress mitosis as well as cell cycle.

Moreover, depletion of NPM leads to distorted nucleolar and nuclear structure in HeLa cells. The distortion of nucleolus by NPM depletion would induce post-mitotic p53-dependent checkpoint. The remarkable changes in nuclear shape of NPM-depleted cells would be due to defects in mitosis and/or independent of mitosis, centrosomal microtubule nucleation, and cytoskeletal structures. From the results of the present study, it can be concluded that NPM is essential for the formation and structural integrity of nucleolus and also for the maintenance of normal nuclear structure through the cytoskeletal fibers (α-tubulin and β-actin). The novel functions of NPM obtained from the present study lead to conclude that NPM also acts plurifunctional protein during the cell cycle. Studies in the mechanism of how the changes in nuclear and cytoskeletal structures are connected to cell proliferation will be important to understand the tumorigenic roles of NPM.

A previous study showed that nucleolin (NCL) plays roles in chromosome congression and spindle formation (Ma et al., 2007). Together with the existing evidences (Liu and Yung, 1999; Ma et al., 2007), this study showed that FBL, NCL and NPM interact with each other during the cell cycle. Studies in the mechanism of how these proteins interrelated in their function will be provide more insights into their function in controlling cell cycle.

Inactivation of p53 functions has been well known as a common mechanism for tumorigenesis (Vogelstein et al., 2000). Therefore, reactivation of p53 functions or

inactivation of p53 negative regulators has long been considered as an effective therapy for cancers. For example, because DNA damage up-regulates p53 mainly through attenuation of it negative regulator Mdm2 (Maya et al., 2001), DNA damage-inducing drugs such as etoposide have been shown to be effective anti-cancer drugs in clinical application (Chresta and Hickman, 1996; Lutzker and Leivine, 1996). The present study shows that suppression of NPM induces cell cycle defects and eventually apoptosis, thus providing a proof of conceptive evidence that the pathological elevations of NPM found in cancer cells are important for maintaining their survival and resistance to apoptosis. Thus, NPM antagonists could be used as novel therapeutic agents or adjuvant in combination with DNA damage drugs for cancer prevention and treatments.

References

Andersen, J.S., Lyon, C.E., Fox, A.H., Leung, A.K., Lam, Y.W., Steen, H., Mann, M. and Lamond, A.I. (2002) Direct proteomic analysis of the human nucleolus. Curr. Biol. **12**, 1-11.

Andersen, J.S., Lam, Y.W., Leung, A.K., Ong, S.E., Lyon, C.E., Lamond, A.I.and Mann, M. (2005) Nucleolar proteome dynamics. Nature **433**, 77-83.

Andreassen, P.R., Lohez, O.D., Lacroix, F.B. and Margolis, R.L. (2001) Tetraploid state induces p53-dependent arrest of nontransformed mammalian cells in G_1. Mol. Biol. Cell **12**, 1315-1328.

Angelier, N., Tramier, M., Louvet, E., Coppey-Miosan, M., Savino, T.M., De Mey, J.R. and Hernandez-Verdun, D. (2005) Tracking the interactions of rRNA processing proteins during nucleolar assembly in living cells. Mol Biol. Cell, **16**, 2862-2871.

Aris, J.P. and Blobel, G. (1991) CDNA cloning and sequencing of human fibrillarin, a conserved nucleolar protein recognized by autoimmune antisera. Proc. Natl. Acad. Sci. **88**, 931-935.

Azum-Gelade, M.C., Noaillac-Depeyre, J., Caizergues-Ferrer, M. and Gas, N. (1994) Cell cycle redistribution of U3 snRNA and fibrillarin. Presence in the cytoplasmic nucleolus remnant and in the prenucleolar bodies at telophase. J Cell Sci. **107**, 463-475.

Bacco, A.D., Ouyang, J., Lee, H.Y., Catic, A., Ploegh, H. and Gill, G. (2006) The SUMO-specific protease SENP5 is required for cell division. Mol. Cell. Biol. **26**, 4489-4498.

Bertwistle, D. Sugimoto, M. and Sherr, C.J. (2004) Physical and functional interactions of the Arf tumor suppressor protein with nucleophosmin/B23. Mol Cell Biol. **24**, 985-96.

Boisvert, F.M., van Koningsbruggen, S., Navascues, J. and Lamond, A.I. (2007) The multifunctional nucleolus. Nat. Rev. Mol. Cell Biol. **8**, 574-85.

Borer, R.A., Lehner, C.F., Eppenberger, H.M. and Nigg, E.A. (1989) Major nucleolar proteins shuttle between nucleus and cytoplasm. Cell **56**, 379-390.

Brinkly, B.R. and Cartwright, J.Jr. (1975) Cold-labile and cold-stable microtubules in the mitotic spindle of mammalian cells. Ann. NY Acad. Sci. **253**, 428-439.

Bunz, F., Dutriaux, A., Lengauer, C., Waldman, T., Zhou, S., Brown, J.P., Sedivy, J.M., Kinzler, K.W. and Vogelstein, B. (1998) Requirement for p53 and p21 to sustain G_2 arrest after DNA damage. Science. **282**, 1497-501.

Busch, H. and Smetana, K. (1970) The Nucleolus. New York: Academic Press.

Carmena, M. and Earnshaw, W.C. (2003) The cellular geography of Aurora kinases. Nat. Cell Biol. **4**, 842-854.

Carmo-Fonseca, M., Mendes-Soares, L. and Campos, I. (2000) To be or not to be in the nucleolus. Nat. Cell. Biol. **2**, E107-112.

Castedo, M., Perfettini, J.L., Roumier, T., Andreau, K., Medema, R. and Kroemer, G. (2004) Cell death by mitotic catastrophe: a molecular definition. Oncogene **23**, 2825-2837.

Chang, J.H. and Olson, M.O. (1989) A single gene codes for two forms of rat nucleolar protein B23 mRNA. J. Biol. Chem. **264**, 11732-11737.

Chen, R.H. (2002) BubR1 is essential for kinetochore localization of other spindle

checkpoint proteins and its phosphorylation requires Mad1. J Cell Biol. **158**, 487-496.

Chresta, C.M. and Hickman, J.A. (1996) Oddball p53 in testicular tumors. Nat. Med. **2**, 745-746

Christensen, M.E., Bayer, A.L., Walker, B. and LeStourgeon, W.M. (1977) Identification of NG, NG-dimethylarginine in a nuclear protein from the lower eukaryote physarum polycephalum homologous to the major proteins of mammalian 40S ribonucleoprotein particles. Biochem. Biophys. Res. Commun. **74**, 621-9.

Cleaved, D.W., Mao, Y. and Sullivan, K.F. (2003) Centromeres and kinetochores: from epigenetics to mitotic checkpoint signaling. Cell **112**, 407-421.

Colombo, E., Marine, J.C., Danovi, D., Falini, B. and Pelicci, P.G. (2002) Nucleophosmin regulates the stability and transcriptional activity of p53. Nat Cell Biol. **4**, 529-33.

Coute, Y., Burgess, J.A., Diaz, J.J., Chichester, C., Lisacek, F., Greco, A. and Sanchez, J.C. (2006) Deciphering the human nucleolar proteome. Mass Spectrum. Rev. **25**, 215-234.

DeLuca, J.G., Gall, W.E., Ciferri, C., Cimini, D., Musacchio, and A. and Salmon, E.D. (2006) Kinetochore microtubule dynamics and attachment stability are regulated by Hec1. Cell **127**, 969-982.

Derenzini, M., Sirri, V., Trere, D. and Ochs, R.L. (1995) The quantity of nucleolar proteins nucleolin and protein B23 is related to cell doubling time in human cancer cells. Lab. Invest. **73**, 97-502.

Dousset, T., Wang, C., Verheggen, C., Chen, D., Hernandez-Verdun, D. and Huang, S. (2000) Initiation of nucleolar assembly is independent of RNA polymerase I

transcription. Mol. Biol. Cell. **11**, 2705-2717.

Du, Y.C. and Stillman, B. (2002) Yph1p, an ORC-interacting protein: potential links between cell proliferation control, DNA replication, and ribosome biogenesis. Cell. **109**, 835-848.

Dundr, M., Hebert, M.D., Karpova, T.S., Stanek, D., Xu, H., Shpargel, K.B., Meier, U.T., Neugebauer, K.M., Matera, A.G. and Misteli, T. (2004) In vivo kinetics of Cajal body components. J Cell Biol. **164**, 831-842.

Echeverri, C.J., Beachy, P.A., Baum, B., Boutros, M., Buchholz, F., Chanda, S.K., Downward, J., Ellenberg, J., Fraser, A.G., Hacohen, N. et al. (2006) Minimizing the risk of reporting false positives in large-scale RNAi screens. Nat. Methods **3**, 777-779.

Espada, J., Ballestar, E., Santoror, R., Fraga, M.F., Villar-Garea, A., Nemeth, A., Lopez-Serra, L., Ropero, S., Aranda, A., et al. (2007) Epigenetic disruption of ribosomal RNA genes and nucleolar architecture in DNA methyltransferase 1 (Dnmt1) deficient cells. Nucl. Acids Res. **35**, 2191-2198.

Fenech, M. (2002) Chromosomal biomarkers of genomic instability relevant to cancer. Drug Discov. Today **7**, 1128-1137.

Foisner, R., and Gerace, L. (1993) Integral membrane proteins of the nuclear envelope interact with lamins and chromosomes, and binding is modulated by mitotic phosphorylation. Cell **73**, 1267-1279.

Fomproix, N., Gebrane-Younes, J. and Hernandez-Verdun, D. (1989) Effects of anti-fibrillarin antibodies on building of functional nucleoli at the end of mitosis. J Cell Sci. **111**, 359-372.

Frehlick, L.J., Eirin-Lopez, J.M. and Ausio, J. (2007) New insights into the

nucleophosmin/nucleoplasmin family of nuclear chaperons. *Bioessays* **29**, 49-59.

Gall, J.G. (2000) Cajal bodies: the first 100 years. Annu. Rev. Cell Dev. Biol. **16**, 273 -300.

Gall, J.G. (2003). The centennial of the Cajal body. Annu. Rev. Cell Dev. Biol. **4**, 975-980.

Grisendi, S., Bernardi, R., Rossi, M. Cheng, K., Khandker, L., Manova, K. and Pandolfi, P.P. (2005) Role of nucleophosmin in embryonic development and tumorigenesis. Nature **437**, 147-153.

Grisendi, S., Mecucci, C., Falini, B. and Pandolfi, P.P. (2006) Nucleophosmin and cancer. *Nat. Rev. Cancer* 6:493-505.

Gruber, J., Lampe, T. Osborn, M. and Weber, K. (2004) RNAi of FACE1 protease results in growth inhibition of human cells expressing lamin A: implications for Hutchinson-Gilford progeria syndrome. J. Cell Sci. **118**, 689-696.

Hadjiolov, A.A. (1985) The nucleolus and ribosome biogenesis. Alfert, M., Bergman, W., Goldstein, L., Porter, K.R. and Site, P. editors. Springer Verlag, Wein. 1-268.

Henriquez, R., Blobel G., and Aris, J.P (1990). Isolation and sequencing of Nop1. A yeast gene encoding a nucleolar protein homologous to a human autoimmune antigen. J. Biol. Chem. **265**, 2209-2215.

Hernandez-Verduz, D. and Gautier, T. (1994). The chromosome periphery during mitosis. *Bioessays* **16**, 179-185.

Hernandez-Verduz, D., Roussel, P. and Gebrane-Younes, J. (2002) Emerging concepts of nucleolar assembly. J. Cell Sci. **115**, 2265-2270.

Higashi, T., Matsunaga, S., Isobe, K., Morimoto, A., Shimada, T., Kataoka, S., Watabnabe, W., Uchiyama, S., Itoh, K. and Fukui, K. (2007) Histone H2A mobility is regulated by its tails and acetylation of core histone tails. Biochem. Biophys. Res. Commun. **357**, 627-632.

Ishii, S., Kurasawa, Y., Wong, J. and Yu-Lee, L (2007). Histone deacetylase 3 localizes to the mitotic spindle and is required for kinetochore-microtubule attachment. Proc. Natl. Acad. Sci. **105**, 4179-4184.

Itahana, K., Bhat, K.P., Jin, A., Itahana, Y., Hawke, D., Kobayashi, R., and Zhang Y. (2003). Tumor suppressor ARF degrades B23, a nucleolar protein involved in ribosome biogenesis and cell proliferation. Mol. Cell **12**, 1151-1164.

Jansen, R.P., Hurt, E.C., Kern, H., Lehtonen, H., Carmo-Fonseca, M., Lapeyre, B. and Tollervey, D. (1991) Evolutionary conservation of the human nucleolar protein fibrillarin and its functional expression in yeast. J. Cell Biol. **113**, 715-729.

Jiang, P.S. and Yung B.Y.M. (1999) Down-regulation of Nucleophosmin/B23 mRNA delays the entry of cells into mitosis. Biochem. Biophys. Res. Commun. **257**, 865-870.

Kametaka, A., Takagi, M., Hayakawa, T., Haraguchi, T., Hiraoka, Y. and Yoneda, Y. (2002) Interaction of the chromatin compaction-inducing domain (LR domain) of Ki-67 antigen with HP1 proteins. Genes Cells **7**, 1231-1242.

Kao, G.D., McKenna, W.G. and Yen, T.J. (2001) Detection of repair activity during the DNA damage induced G2 delay in human cancer cells. Oncogene **20**, 3486-3496.

Kastan, M.B., Onyekwere, O., Sidransky, D., Vogelstein, B. and Craig R.W. (1991) Participation of p53 protein in the cellular response to DNA damage. Cancer Res. **51**, 6304-11.

Kimura, T., Ito, C., Watanabe, S., Takahashi, T., Ikawa, M., Yomogida, K., Fujita, Y., Ikeuchi, M., Asada, N., Matsumiya, K. Okuyama, A. Okabe, M., Toshimori, K. and Nakano, T. (2003) Mouse germ cell-less as an essential component for nuclear integrity. Mol Cell Biol. **23**, 1304-1315.

Korgaonkar, C., Hagen, J., Tompkins, V., Frazier, A.A., Allamargot, C., Quelle, F.W. and Quelle, D.E. (2005) Nucleophosmin (B23) targets ARF to nucleoli and inhibits its function. *Mol Cell Biol.* **25**, 1258-71.

Kurki, S., Peltonen, K., Latonen, L., Kiviharju, T.M., Ojala, P.M., Meek, D. and Laiho, M. (2004). Nucleolar protein NPM interacts with HDM2 and protects tumor suppressor protein p53 from HDM2-mediated degradation. *Cancer Cell.* **5**, 465-75.

Lanni, J.S. and Jackes, T. (1998). Characterization of the p53-dependent postmitotic checkpoint following spindle disruption. Mol. Cell Biol. **18**, 1055-1064.

Leung, A.K., Gerlich, D., Miller, G., Lyon, C., Lam, Y.W., Lleres, D., Daigle, N., Zomerdijk, J., Ellenberg, J. and Lamond, A.I. (2004) Quantitative kinetic analysis of nucleolar breakdown and reassembly during mitosis in live human cells. J. Cell. Biol. **166**, 787-800.

Levine, A.J. (1997) p53, the cellular gatekeeper for growth and division. Cell. **88**, 323-331.

Li, J., Zhang, X., Sejas, D.P. and Pang, Q. (2005) Negative regulation of p53 by nucleophosminantagonizes stress-induced apoptosis in human normal and malignant hematopoietic cells. Leukemia Res. **29**, 1415-1423.

Liao, H., Winkfein, R.J., Mack, G., Rattner, J.B. and Yen, T.J. (1995) CENP-F is a protein of the nuclear matrix that assembles onto kinetochores at late G_2 and is rapidly

degraded after mitosis. J. Cell Biol. **130**, 507-518.

Liu, H.T. and Yung, B.Y. (1999) In vivo interaction of nucleophosmin/B23 and protein C23 during cell cycle progression in HeLa cells. Cancer Lett. **144**, 45-54.

Lo, S.J., Lee, C.C. and Lai, H.J. (2006) The nucleolus: reviewing oldies to have new understandings. Cell Res. **16**, 530-538.

Lutzker, S.G. and Levine, A.J. (1996) A functionally inactive p53 protein in teratocarcinoma cells is activated by either DNA damage or cellular differentiation. Nat. Med. **2**, 804-810.

Ma, N., Matsunaga, S., Takata, H., Ono-Maniwa, R., Uchiyama, S. and Fukui, K. (2007) Nucleolin functions in nucleolus formation and chromosome congression, J. Cell Sci. **120**, 2091-2105.

Manilal, S., Nguyen, T.M., Sewry, C.A. and Morris, G.E. (1996) The Emery-Dreifuss muscular dystrophy protein, emerin, is a nuclear membrane protein. Hum. Mol. Genet. **5**, 801-808.

Maggi, L.B.Jr and Weber, J.D. (2005) Nucleolar adaptation in human cancer. Cancer Investig. **23**, 599-608.

Maya, R., Balass, M., Kim, S.T., Shkendy, D., Leal, J.F., Shifman, O. et al. (2001) ATM-dependent phosphorylation of Mdm2 on serine 395: role in p53 activation by DNA damage. Genes Dev. **15**, 1067-1077.

Mayer, C. and I. Grummt. (2005) Cellular stress and nucleolar function. Cell Cycle **4**, 1036-1038.

Medina, F.J., Cerdido, A. and Fernandez-Gomez, M.E. (1995) Components of the nucleolar processing complex (Pre-rRNA, Fibrillarin, and nucleolin) colocalize during

mitosis and are incorporated to daughter cell nucleoli. Exp. Cell Res. **221**, 111-125.

Mehes, G. and Pajor, L. (1995) Nucleolin and fibrillarin expression in stimulated lymphocytes and differentiating HL-60 cells. A flow cytometric assay. Cell Prolif. **28**, 329-336.

Michael, D. and Oren, M. (2002) The p53 and Mdm2 families in cancer. Curr. Opin. Gent. Dev. **12**, 53-59.

Minn, A.J., Boise, L.H. and Thompson, C.B. (1996) Expression of Bcl-x_L and loss of p53 can cooperate to overcome a cell cycle checkpoint induced by mitotic spindle damage. Genes Dev. **10**, 2621-2631.

Musacchio, A. and Salmon, E.D. (2007) The spindle-assembly checkpoint in space and time. Nat. Rev. Mol. Cell Biol. **8**, 379-393.

Newton, K., Petfalski, E., Tollervey, D. and Caceres, J.F. (2003) Fibrillarin is essential for early development and required for accumulation of an intron-encoded small nucleolar RNA in the mouse. Mol Cell Biol. **23**, 8519-8527.

Ochs, R.L, Lischwe, M.A., Spohn, W.H. and Busch, H. (1985) Fibrillarin: a new protein of the nucleolus identified by autoimmune sera. Biol Cell. **54**, 123-33.

Ochs, R.L. and Smetana, K. (1991) Detection of fibrillarin in nucleolar remnants and the nucleolar matrix, Exp. Cell Res. **197**, 183-190.

Okuda, M., Horn, H.F., Tarapore, P., Tokuyama, Y., Smulian, A.G., Chan, P.K., Knudsen, E.S., Hofmann, I.A., Snyder, J.D., Bove, K.E. and Fukasawa, K. (2000) Nucleophosmin/B23 is a target of CDK2/cyclin E in centrosome duplication. Cell **103**, 127-140.

Okuwaki, M., Matsumoto, K., Tsujimoto, M. and Nagata, K. (2001). Function of

nucleophosmin/B23, nucleolar acidic protein, as a histone chaperone. FEBS Lett. **506**, 272-276.

Okuwaki, M., Tsujimoto, M. and Nagata, K. (2002) The RNA binding activity of a ribosome biogenesis factor, nucleophosmin/B23, is modulated by phosphorylation with a cell cycle-dependent kinase and by association with its subtype. Mol. Biol. Cell **13**, 2016-2030.

Olins, A.L. and Olins, D.E. (2004) Cytoskeletal influences on nuclear shape in granulocytic HL-60 cells. BMC Cell Biol. **5**, 30.

Olson, M.O.J., Dundr, M. and Szebeni, A. (2000) The nucleolus: an old factory with unexpected capabilities. Trends Cell Biol. **10**, 189-196.

Olson, M.O. and Dundr, M. (2005) The moving parts of the nucleolus. Histochem. Cell Biol. **123**, 203-216.

Pederson, T. (1998) The plurifunctional nucleolus. Nucleic Acids Res. **26**, 3871-3876.

Pendle, A.F., Clark, G.P., Boon, R., Lewandowska, D., Lam, Y.W., Andersen, J., Mann, M., Lamond, A.I., Brown, J.W. and Shaw, P.J. (2005) Proteomic analysis of the Arabidopsis nucleolus suggests novel nucleolar functions. Mol. Biol. Cell **16**, 260-269.

Rubbi, C.P. and Milner, J. (2003) Disruption of the nucleolus mediates stabilization of p53 in response to DNA damage and other stresses. EMBO J. **22**, 6068-6077.

Saiwaki, T., Kotera, I., Sasaki, M., Takagi, M. and Yoneda, Y. (2005). In vivo dynamics and kinetics of pKi-67: transition from a mobile to an immobile form at the onset of anaphase. Exp. Cell. Res. **308**, 123-134.

Sandeep, S.N. and Oslon, M.O.J. (2006) Effects of interphase and mitotic phosphorylation on the mobility and location nucleolar protein B23. J. Cell Sci. **119**,

3676-3685.

Savino, T.M., Bastos, R., Jansen, R. and Hernandez-Verdun, D. (1999) The nucleolar antigen Nop52, the human homologue of the yeast ribosomal RNA processing RRP1, is recruited at late stages of nucleologenesis, J. Cell. Sci. **122**, 1889-1900.

Savkur, R.S. and Olson, M.O. (1998) Preferential cleavage in pre-ribosomal RNA by protein B23 endoribonuclease. Nucleic Acids Res. **26**, 4508-4515.

Scherl, A., Coute, Y., Deon, C., Calle, A., Kindbeiter, K., Sanchez, J.C., Greco, A., Hochstrasser, D. and Diaz, J.J. (2002) Functional proteomic analysis of human nucleolus. Mol. Biol. Cell **13**, 4100-4109.

Schimmang, T., Tollervey, D., Kern, H., Frank, R. and Hurt, E.C. (1989) A yeast nucleolar protein related to mammalian fibrillarin is associated with small nucleolar RNA and is essential for viability. EMBO J. **8**, 4015-4024.

Scholzen, T., Endl, E., Wohlenberg, C., van dar Sar, S., Cowell, I.G., Gerdes, J. and Singh, P.B. (2002) The Ki-67 protein interacts with members of the heterochromatin protein 1 (HP1) family: a potential role in the regulation of higher-order chromatin structure. J. Pathol. **196**, 135-144.

Schrank, B., Gotz, R., Gunnersen, J.M., Ure, J.M., Toyka, K.V., Smith, A.G. and Sendtner, M. (1997) Inactivation of the survival motor neuron gene, a candidate gene for human spinal muscular atrophy, leads to massive cell death in early mouse embryos. Proc. Natl. Acad. Sci. USA **94**, 9920-9925.

Schluter, C., Duchrow, M., Wohlenberg, C., Becker, M.H., Key, G., Flad, H.D. and Gerdes, J. (1993) The cell proliferation-associated antigen of antibody Ki-67: a very large ubiquitous nuclear protein with numerous repeated elements, representing a new

kind of cell cycle-maintaining proteins. J. Cell Biol. **123**, 513-522.

Takagi, M., Absalon, M.J., McLure, K.G. and Kastan, M.B. (1999) Regulation of p53 translation and induction after DNA damage b ribosomal protein L26 and nucleolin. Cell **123**, 49-63.

Taylor, W.R. and Stark, G.R. (2001) Regulation of the G2/M transition by p53. Oncogene **20**, 1803-1815.

Tollervey, D., Lehtonen, H., Jansen, R., Kern, H. and Hurt, E.C. (1993) Temperature sensitive mutations demonstrate roles of yeast fibrillarin in pre-rRNA processing, pre-rRNA methylation, and ribosome assembly. Cell **72**, 443-457.

Tsai, R.Y. and McKay, R.D. (2002) A nucleolar mechanism controlling cell proliferation in stem cells and cancer cells, Genes and Dev. **16**, 2991-3003.

Tucker, K.E., Berciano, M.T., Jacobs, E.Y., LePage, D.F., Shpargel, K.B., Rossire, J.J., Chan, E.K., Lafarga, M., Conlon, R.A. and Matera, A.G. (2001) Residual Cajal bodies in coilin knockout mice fail to recruit Sm snRNPs and SMN, the spinal muscular atrophy gene product. J. Cell. Biol. **154**, 293-307.

Uchiyama, S., Kobayashi, S., Takata, H., Ishihara, T., Hori, N., Higashi, T., Hayashihara, K., Sone, T., Higo, D., Nirasawa, T., Takao, T., Matsunaga, S. and Fukui, K. (2005) Proteome analysis of human metaphase chromosomes. J. Biol. Chem. **17**, 16994-17004.

Ulbert, S., Antonin, W., Platani, M., Mattaj, I.W. (2006a) The inner nuclear membrane protein Lem2 is a critical for normal nuclear envelope morphology. FEBS Letters. **580**, 6435-6441.

Ulbert, S., Platani, M., Boue, S., and Mattaj, I.W. (2006b) Direct membrane protein-DNA interactions required early in nuclear envelope assembly. J. Cell Biol. **173**, 469-

476.

Umekawa, H., Chang, J.H., Correia, J.J., Wang, W., Wingfield, P.T. and Olson, MO. (1993) Nucleolar protein B23: bacterial expression, purification, oligomerization and secondary structures of two isomers. Cell. Mol. Biol. Res. **39**, 635-645.

Wang, D., Umekawa, H. and Olson, M.O. (1993) Expression and subcellular locations of two forms of nucleolar protein B23 in rat tissues and cells. Cell. Mol. Biol. Res. **39**, 33-42.

Wang, D., Baumann, A., Szebini, A. and Olson, M.O.J. (1994) The nucleic acid binding activity of nucleolar protein B23.1 resides in its carboxyl-terminal end. J. Biol. Chem. **269**, 30994-30998.

Wang, H., Boisvert, D., Kim, K.K., Kim, R. and Kim, S.H. (2000) Crystal structure of a fibrillarin homologue from Methanococcus jannaschii, a hyperthermophile, at 1.6 A resolution. EMBO J. **19**, 317-323.

Yang, D., Welm, A. and Bishop, J.M. (2004) Cell division and cell survival in the absence of surviving. Proc. Natl. Acad. Sci. **101**, 15100-15105.

Yasuda, Y. and Maul, G.G. (1990) A nucleolar auto-antigen is part of a major chromosomal surface component, Chromosoma. **99**, 152-160.

List of Publications

Related articles

Mohammed Abdullahel Amin, Matsunaga, S., Ma, N., Takata, H., Yokoyama, M., Uchiyama, S., and Fukui K. (2007). Fibrillarin, a nucleolar protein is required for normal nuclear morphology and cellular growth in HeLa cells. *Biochem. Biophys. Res. Commun.* **360**, 320-326.

Mohammed Abdullahel Amin, Matsunaga, S., Uchiyama, S., and Fukui K. (2008). Nucleophosmin is required for chromosome congression, spindle formation, kinetochore-microtubule attachment in HeLa cells. (Minor revision by *FEBS Lett*).

Mohammed Abdullahel Amin, Matsunaga, S., Uchiyama, S., and Fukui K. (2008). Depletion of nucleophosmin leads to nucleolar and nuclear structures in HeLa cells. *Biochemical J.* (in press).

Other articles

Okazawa, A., **Mohammed Abdullahel Amin**, Izumi, Y., Wakabayashi, T., Onishi, R., Fujiwara, R., Fukusaki, E., and Kobayashi, A. (2008). Deuterium Oxide Delays Seed Germination of *Arabidopsis thaliana* by alteration of expression profiles of genes involved in hormone metabolism. (Submitted).

Acknowledgments

First of all, I express my heartiest gratitude to God, the sustainer of the Universe, the most Gracious and the most Merciful for His miracle and kind help in conducting my studies.

I feel greatly honored in expressing gratitude and indebtness to my supervisor Professor Kiichi Fukui for his dynamic and intellectual guidance, and constructive instruction. I am also happy and thankful to him for his kindness, caring and loving.

I would also like to express my heartfelt thanks to Professor Dr. Satoshi Harashima and Professor Dr. Shigenori Kanaya for their great suggestions and comments.

I am particularly grateful to Dr. Shachihiro Matsunaga, associate professor of Biotechnology Department for his dynamic leadership, continuous supervision, co-operation and caring during my studies.

I am thankful to Dr Susumu Uchiyama, assistant professor of Biotechnology Department for his prudent critiques and kind co-operation during my work.

I am also extremely grateful to all professors of the Department of Biotechnology, Graduate school of Engineering, Osaka University.

I would like to convey my special thanks to all members of Fukui laboratory. Especially, thanks for the members of Dynamic Mapping Group. I am particularly thankful to Mr. Akihiro Morimoto for his technical and logistic supports during my research work.

Special thanks are for administrative staffs Mr. Tomoyuki Doi, Mrs. Sachiko Kurihara, Mrs. Reiko Isobe and Mrs. Keiko Ueda-Sarson for their kind helps.

I am thankful to Mrs. Mayumi Shigehiro for her technical assistance to carry out sequencing.

My utmost thanks and gratitude to my parents who always prayed for me and encouraged me over cellular phone.

Finally, I am so grateful and thankful to Ministry of culture, sports, science and technology (MEXT), Japan for the financial assistance.